

Lecture Notes
Gauge Theories of the Standard Model
Part II

Jorge Casalderrey-Solana

Departament de Física Quàntica i Astrofísica
Universitat de Barcelona

(Last version update: May 6, 2021)

These are lecture notes for the second part of the course *Gauge Theories for the Standard Model*, which is part of the Master in *Astrophysics, Particle Physics and Cosmology* offered by University of Barcelona. None of the material presented in these notes is original and it has been collected by me from different sources as a guide for the students taking the course. These notes should not be used as a substitution of books and original articles. The notes have not been checked or proofread, so the students should be aware of possible typos and use them with care. A list of books and useful reviews, from which most of the material of this lecture notes has been taken is below.

References:

1. G. Sterman, An introduction to Quantum Field Theory, Cambridge, UK: Cambridge Univ. Press (1994)
2. M. E. Peskin and D. V. Schroeder, An introduction to quantum field theory, Reading, USA: Addison- Wesley (1995).
3. R. K. Ellis, W. J. Stirling and B. R. Webber, QCD and collider physics, Camb. Monogr. Part. Phys. Nucl. Phys. Cosmol. 8, 1 (1996).
4. John C. Collins, Foundations of Perturbative QCD, Cambridge Monographs on Particle Physics, 2011
5. P. Nason, Introduction to QCD, lecture notes available online at <http://moby.mib.infn.it/~nason/misc/QCD-intro.ps.gz>
6. J. Rojo, The Strong Interactions and LHC phenomenology, lecture notes available online at <http://juanrojo.com/teaching>

Contents

1	Renormalisation of Gauge Theories	5
1.1	Divergent Structure of Gauge Theories	5
1.1.1	Dimensional regularisation	7
1.2	Renormalisation and counter-terms in QCD	9
1.2.1	Renormalisation schemes	13
1.3	The renormalised QCD Lagrangian and the meaning of renormalisation	14
1.4	The renormalization Group	15
1.5	The QCD β -function	17
1.5.1	Asymptotic freedom	18
1.6	Fixed points	19
1.7	Running coupling	21
1.8	The Running Mass and Infrared safety	25
1.9	The R parameter	27
1.10	Heavy Quark Decoupling	29
1.10.1	Going beyond $\mathcal{O}(1/M^0)$	34
2	The limits of perturbation theory	40
2.1	Infrared divergences. Inclusive and Exclusive processes	40
2.1.1	Jets in e^+e^-	44
2.1.1.1	IR&Coll divergences in dimensional regularisation	46
2.1.1.2	Infrared and Collinear Safety	49
2.1.1.3	The anti- k_t jet reconstruction algorithm	50
2.1.2	Deep Inelastic Scattering	52
2.1.2.1	The parton model	54
2.1.2.2	Radiative corrections in DIS	57
2.1.2.3	Scaling violation	60
2.1.2.4	DGLAP evolution	62
2.1.3	Parton Showers and MonteCarlo Simulations	64
2.2	The Operator Product Expansion	71
2.2.1	OPE analysis of $e^+ - e^-$	73
2.2.2	Sum-rules and power corrections to the R parameter	76
2.3	Confinement	79

2.3.1	Regge Trajectories and QCD strings	79
2.3.2	Heavy Quarks and confinement	80
2.3.2.1	The Area Law	85
2.3.3	Confinement/deconfinement transition	85
2.3.3.1	\mathcal{Z} -symmetry and confinement	88
2.3.3.2	Dynamical light quarks and confinement	89
A	Basic facts about SU(N)	91
B	Feynman Rules	94

Renormalisation of Gauge Theories

1.1 Divergent Structure of Gauge Theories

UV divergences appear in loop diagrams. A typical example of a diagram with a UV divergence is a self-energy diagram, with a generic form

Taking the large k limit we can infer from the behaviour of the momentum powers in the integrand associated to the loop that this diagram possess a logarithmic divergence. Certainly, the analysis here is sloppy, since it is not quite clear what $k \rightarrow \infty$ means for a four-momentum in Minkowski space, although it gives the correct degree of divergences. To actually compute the integral and analyse its divergence we need to perform a Wick rotation and introduce Feynman parameters. We will not review this procedure in this notes, which you can find in

any textbook in QFT (Peskin and Schöeder, for example).

An important thing to remember is that not all loop diagrams diverge in the UV. By simply inspecting a given diagram, we can assign to it a *superficial degree of divergence* by simply counting the number of loops and lines that appear in the diagram. Since each loop leads to a four-momentum integration, they contribute by a factor of $4L$, with L the number of loops, to the potential divergence of the diagram. Since each line introduces inverse powers of the loop momentum, they contribute to reducing the divergence; bosons reduce the apparent divergence of the diagram by a factor $-2N_b$, since the propagator is quadratic in momentum, while fermion lines contribute by $-N_f$, with N_b and N_f the number of boson and fermion propagators¹. In QED, this is the only information we need to determine the superficial degree of divergence, since the coupling between fermions and photons do not introduce additional powers of momentum. However, in QCD the triple gluon vertex is proportional to a power of momentum, which increases the apparent divergence of a diagram by a power of g_3 , with g_3 the number of this type of vertices. Putting everything together, the superficial degree of divergence of a given diagram is given by

$$w = 4L - 2N_b - N_f + g_3. \quad (1.1)$$

if $w < 0$, then the number of powers of momentum in the denominator is larger than those in the numerator of the integrand and that particular diagram is UV convergent. If $w \geq 0$ then the diagram is potentially divergent, with $w = 0, 1, 2 \dots$ signalling logarithmic, linear, quadratic... divergence. Note, however, that even if a diagram possesses a positive superficial degree of divergence, symmetries can make the corresponding divergence less severe or even make the diagram convergent altogether.

Using the fact that in QCD there are only three type of vertices, those connecting two fermions and a boson (ψ), three-gluon and four gluon vertices (g_3 and g_4) we can relate the superficial degree of divergence to the number of external boson (E_b) and fermions (E_f) in the diagram. Using the identities $L = N_b + N_f - \psi - g_3 - g_4 + 1$ and $2N_b + E_b = 3g_3 + 4g_4 + \psi$ and $2N_f + E_f = 2\psi$

$$w = 4 - E_b - \frac{3}{2}E_f. \quad (1.2)$$

This identity means that only a few number of diagrams, those with few external particles, are potentially divergent, which allows us to classify all possible divergences. Since all diagrams may be constructed from one-particle irreducible diagrams, we focus on those. The list of all possible n-point functions (not including tadpoles or vacuum-bubble diagrams) with superficial degree of divergence $w \geq 0$ is shown in Fig. 1.1. These are the gluon/photon (a), fermion (b) and ghost (c) self energies, the gluon/photon-fermion (d) and gluon/photon-ghost (e) and triple gluon/photon (f) three point functions and the four gluon/photon (g), two gluon/photon two ghost (h) and four ghost (i) four-point functions. Note that all these n-point functions have a superficial degree of divergence independently of the particular order

¹Ghost fields are treated as boson in this counting, since, while they are anti-commuting variables, their propagator is quadratic in momentum.

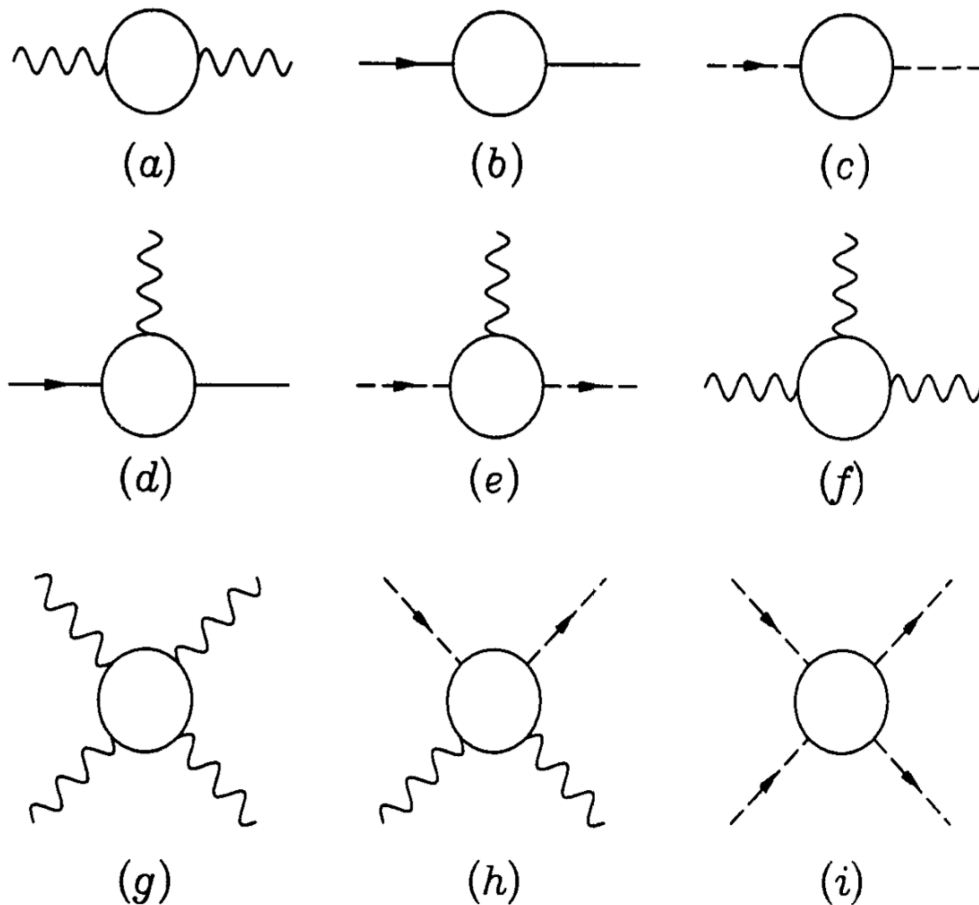


Figure 1.1: One particle irreducible n -point functions with $w \geq 0$ (not including tad-pole or vacuum diagrams). Figure taken from G. Sterman's book.

in perturbation theory at which they are evaluated. Note also that since the ghost couplings always involve a power of the outgoing momentum, while the four-point functions involving ghost have $w = 0$ they are actually UV-convergent and we will not refer to these any longer.

To proceed further we need to evaluate those point n -point functions to the desired order. In this notes, we will only address the evaluation of the different diagrams to one-loop order. To do so, we need to discuss how we will regularise the different divergent diagrams. We will use dimensional regularisation, which we shortly describe to set conventions and notation.

1.1.1 Dimensional regularisation

A regularisation procedure is any method that can be used to consistently remove the divergent contributions that appear in the evaluation of Feynman diagrams. While there are many possible methods, the most useful and popular to evaluate gauge theory amplitudes is dimensional regularisation. One of the main advantages of this method is that it preserves gauge invariance, which is essential to prove the renormalisability and unitarity of the regularised

theory.

The method of dimensional regularisation is based on the observation that the superficial degree of UV-divergence of any given diagram decreases with the number of space-time dimensions in which the quantum field theory lives. This is easy to see, since integration of the loop momentum becomes

$$d^4k \rightarrow d^n k, \quad (1.3)$$

and by reducing the number of dimensions, the powers of momentum in the numerator decreases.

The procedure of dimensional regularisation is based on treating the number of dimensions as a continuous variable and studying the different divergent integrals as $n \rightarrow 4$ from below. For convenience, we define

$$\epsilon = \frac{4 - n}{2} \quad (1.4)$$

which is positive for $n < 4$. The limit to analyse UV-divergence is, therefore, $\epsilon \rightarrow 0^+$.

Extending the theory to arbitrary number of dimensions introduces some conceptual problems. One of them is the dimensionality of the couplings. Both for QED and QCD in $n=4$ space-time dimensions, the gauge coupling constant g is dimensionless. However, at any other space-time dimension this is no longer the case. Demanding that the action has zero mass-dimension, so that it can be taken as a probability weight for any space-time dimension, it is easy to see that the dimension of the n -dimensional coupling constant is

$$[g_n] = [M]^{(4-n)/2} \quad (1.5)$$

Therefore, to take into account this non-trivial change in the dimensionality of the coupling constant, when extending the theory to arbitrary space-time dimension we must introduce a mass scale μ to be able to relate the dimensionless coupling constant of the regularised theory in $n=4$ dimensions to that of the theory in a smaller number of dimension as

$$g \rightarrow g_R \mu^\epsilon \quad (1.6)$$

where g_R is the (regularised) coupling of the regularised theory. As we will see, this is an arbitrary scale introduced by the process of renormalisation, which is therefore called renormalisation scale.

The details of dimensional regularisation can be found in many textbooks. The crucial step to remember is that, after reducing the denominators associated to propagators via the introduction of Feynman parameters and a Wick rotation, the typical integral to be evaluated for a one loop diagram is given by

$$I_{n,s}(M) = i(-1)^s \Omega_{n-1} \int_0^\infty d\kappa \frac{\kappa^{n-1}}{(\kappa^2 + M^2)^s}, \quad (1.7)$$

where $\Omega_d = 2^d \pi^{d/2} \frac{\Gamma(d/2)}{\Gamma(d)}$ is the angular volume of the d -sphere, can be easily evaluated to be

$$I_{n,s}(M) = i(-1)^s \pi^{n/2} \frac{\Gamma(s - n/2)}{\Gamma(s)} (M^2)^{n/2-s} \quad (1.8)$$

This expression provides an analytic continuation for the integral to all values of n , which is analytic in all the n -plane up to a discrete set of poles whenever the argument $s - 1/2n$ becomes a negative integer. A particularly relevant example is $s = 2$, which is divergent for $n = 4$. However, infinitesimally away from $n = 4$ the integral is finite and possesses a simple pole in ϵ as defined in equation 1.4. Expanding around in $\epsilon = 0$ we find

$$I_{n,2}(M) = i\pi^{2-\epsilon} (M^2)^{-\epsilon} \Gamma(\epsilon) = i\pi^2 \left(\frac{1}{\epsilon} - \gamma_E - \log(\pi M^2) + \mathcal{O}(\epsilon^2) \right). \quad (1.9)$$

with γ_E the Euler-Mascheroni constant.

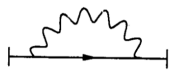
1.2 Renormalisation and counter-terms in QCD

Armed with this technology, we can analyse the divergent n -point functions displayed in Figure 1.1 at one loop order. For concreteness, we will focus on Feynman gauge, i. e., the covariant gauge with $\lambda = 1$. Many of the contributions are identical to QED, up to trivial pre-factors. We will nevertheless review the result of the calculation for some of them. As usual we will define the hyperfine-constant as

$$\alpha = \frac{g_R^2}{4\pi}. \quad (1.10)$$

Since self-energy corrections lead to non-trivial contribution to the poles of propagators, we will denote the mass parameter of each of the quarks in the QCD Lagrangian as m_R . Therefore, all the diagrams we will discuss below will be function of m_R .

The first diagram we analyse is the **fermion self energy**. After the standard steps and taking the $\epsilon \rightarrow 0$ limit, the analytically continued amplitude is²



$$\Sigma^{1\text{ Loop}} = -\frac{\alpha}{2\pi} C_F \left\{ \left(\frac{1}{2} \not{p} - 2m_R \right) \left[\frac{1}{\epsilon} + \log \left(\frac{4\pi\mu^2}{p^2} \right) - \gamma_E \right] \right. \\ \left. - \frac{1}{2} \not{p} + m_R - \int_0^1 dx \left[\not{p}(1-x) - 2m_R \right] \log \left[-x(1-x) + x \frac{m_R^2}{p^2} - i\epsilon \right] \right\}, \quad (1.11)$$

where C_F is the weight of the Casimir operator of the $SU(N)$ group in the fundamental representation

$$C_F I = \sum_{A=1}^{N^2-1} t^A t^A, \quad C_F = \frac{N^2 - 1}{2N}. \quad (1.12)$$

This contribution is identical to the QED one, up to replacing $C_F \rightarrow 1$. As in that case, the UV divergence is codified by the ϵ^{-1} term in equation (1.11). As in that case, the divergence is cured by introducing two counter-terms in the Lagrangian, associated to the two different

²The expression for $\Sigma^{1\text{ Loop}}$ in Sterman's book has a typo in the sign in front of the x -integral

momentum structures of the divergences of the self energies. These are given by

$$\delta_\psi^{1\text{Loop}} \bar{\psi} i \not{\partial} \psi \quad \text{with} \quad \delta_\psi^{1\text{Loop}} \equiv -\frac{\alpha}{4\pi} C_F \left(\frac{1}{\epsilon} + c_{\psi 1} \right) \quad (1.13)$$

$$-\left(\delta_m^{1\text{Loop}} + \delta_\psi^{1\text{Loop}} \right) m_R \bar{\psi} \psi \quad \text{with} \quad \delta_m^{1\text{Loop}} \equiv -\frac{3\alpha}{4\pi} C_F \left(\frac{1}{\epsilon} + c_{m1} \right) \quad (1.14)$$

Where $c_{\psi 1}$ and c_{m1} are two arbitrary constants, which we will discuss later. These constants indicate some arbitrariness in regularising the amplitude, since we may choose to remove not only the divergent piece, but also some finite piece.

Before continuing evaluating more divergent diagrams, let us note one interesting observation. After introducing the counter-term specified above, the regularised self energy becomes finite. However, it also becomes explicitly dependent on the arbitrary scale μ , which we introduced as a way to fix the dimensionality in the dimensionally-continued theory. The renormalisation procedure has indeed succeed in making this diagram finite but we have payed the prize of making the self energy arbitrary. This is not just a problem of this diagram; similar μ dependence occur in all of the divergent 1PI diagrams. We will elaborate on this observation bellow.

We now turn to the **gluon self energy**. In QCD in Feynman gauge and at one loop, this is given by four diagrams



The first diagram is identical to the QED correction. The other three diagrams are intrinsically non-abelian. And all of them are divergent and require renormalisation. The analysis of the different contributions leads to

$$\text{Feynman diagram 1} \equiv -i\pi_{AB,\mu\nu}^{1\text{Loop (a)}}(q) = -i(q^2 g_{\mu\nu} - q_\mu q_\nu) T_F \delta_{AB} \frac{\alpha}{3\pi} \frac{1}{\epsilon} + \mathcal{O}(\epsilon^0) \quad (1.15)$$

$$\text{Feynman diagram 2} \equiv -i\pi_{AB,\mu\nu}^{1\text{Loop (b)}}(q) = i \left(\frac{19}{6} q^2 g_{\mu\nu} - \frac{11}{3} q_\mu q_\nu \right) N \delta_{AB} \frac{\alpha}{8\pi} \frac{1}{\epsilon} + \mathcal{O}(\epsilon^0) \quad (1.16)$$

$$\text{Feynman diagram 3} \equiv -i\pi_{AB,\mu\nu}^{1\text{Loop (c)}}(q) = i \left(\frac{1}{6} q^2 g_{\mu\nu} + \frac{1}{3} q_\mu q_\nu \right) N \delta_{AB} \frac{\alpha}{8\pi} \frac{1}{\epsilon} + \mathcal{O}(\epsilon^0) \quad (1.17)$$

$$\text{Feynman diagram 4} \equiv -i\pi_{AB,\mu\nu}^{1\text{Loop (d)}}(q) = 0$$

The first contribution to the self gluon energy, $-i\pi_{AB,\mu\nu}^{1\text{Loop (a)}}(q)$ is analogous to the to the QED one, if one were to set $T_F \rightarrow 1$. In QCD, however, this is a property of the fundamental representation of the $SU(N)$ algebra

$$\text{Tr} [t^A t^B] = T_F \delta^{AB} \quad \text{with} \quad T_F = \frac{1}{2}, \quad (1.18)$$

This contribution is also transverse ($q^\mu \pi_{\mu\nu} = 0$), as we expect from current conservation. However, the individual contributions non-abelian contributions $-i\pi_{AB,\mu\nu}^{1\text{Loop}^{(b)}}(q)$ and $-i\pi_{AB,\mu\nu}^{1\text{Loop}^{(c)}}(q)$, i. e., the contributions from the triple gluon vertex and the ghost fields, are not. Nevertheless, their sum is indeed transverse, since

$$-i\pi_{AB,\mu\nu}^{1\text{Loop}^{(b)}}(q) + -i\pi_{AB,\mu\nu}^{1\text{Loop}^{(c)}}(q) = i(q^2 g_{\mu\nu} - q_\mu q_\nu) N \delta_{AB} \frac{5\alpha}{12\pi} \frac{1}{\epsilon} + \mathcal{O}(\epsilon^0) \quad (1.19)$$

This result illustrates that including the effect of ghosts it is crucial to preserve gauge invariance in the quantum computation.

Finally, the fact that the last contribution $-i\pi_{AB,\mu\nu}^{1\text{Loop}^{(d)}}(q) = 0$ is the result of a cancelation between an UV divergence and another type of divergence which we will analyse in then next chapter, called infrared divergence. We will return to this in the next chapter. A characteristic feature of this diagram is that it posses a divergent scale-less integrals. In general, this type of scaleless integrals always vanish in dimensional regularisation.

Putting everything together, and assuming that there are n_f different families of fermions (or quarks), the divergent part of the gluon self-energy at one loop is given by

$$-i\pi_{AB,\mu\nu}^{1\text{Loop}}(q) = i(q^2 g_{\mu\nu} - q_\mu q_\nu) \delta_{AB} \left(\frac{5}{4}N - T_F n_f \right) \frac{\alpha}{3\pi} \frac{1}{\epsilon} + \mathcal{O}(\epsilon^0), \quad (1.20)$$

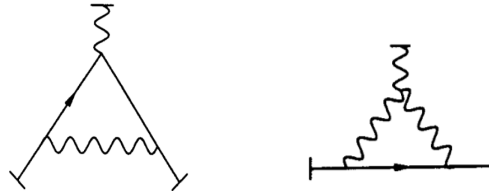
which, as expected from gauge invariance, it is transverse. The QED self energy can be immediately deduced from this equation, by setting $N \rightarrow 0$ and $T_F \rightarrow 1$.

The Lorentz and colour structure of the divergence of this 2-point function also suggest the form of the counter-term that needs to be added to the QCD Lagrangian to cancel this divergence. Since this is basically proportional to the numerator of the propagator, it is easy to check that a contribution proportional to the kinetic part of the gluon gauge field will cancel this divergence, if we the proportionality factor is divergent as

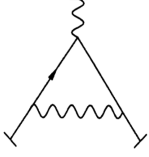
$$-\delta_A^{1\text{Loop}} \frac{1}{4} (\partial_\mu A_\nu - \partial_\nu A_\mu) (\partial^\mu A^\nu - \partial^\nu A^\mu) \quad \text{with} \quad \delta_A^{1\text{Loop}} = \left(\frac{5}{4}N - T_F n_f \right) \frac{\alpha}{3\pi} \left(\frac{1}{\epsilon} + c_{A1} \right) \quad (1.21)$$

with c_{A1} an arbitrary constant.

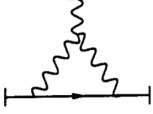
The next 1PI contribution to consider is the gluon-fermion coupling. The diagrams that contribute to this 3-point function are



The left diagram is identical to the QED contribution, while the right diagram is a non-abelian term. The divergent parts of each diagram are



$$\equiv \Gamma_{\mu}^{A \text{ 1Loop (a)}} = -g\gamma_{\mu} \left(C_F - \frac{1}{2}N \right) t^A \frac{\alpha}{4\pi} \frac{1}{\epsilon} + \mathcal{O}(\epsilon^0) \quad (1.22)$$



$$\equiv \Gamma_{\mu}^{A \text{ 1Loop (b)}} = -g\gamma_{\mu} N t^A \frac{3\alpha}{8\pi} \frac{1}{\epsilon} + \mathcal{O}(\epsilon^0) \quad (1.23)$$

where we have used the colour identities

$$t^B t^A t^B = i f^{ABC} t^C t^B + t^A C_F = -\frac{1}{2} f^{ABC} f^{CBD} t^D + t^A C_F = \left(C_F - \frac{1}{2}N \right) t^A \quad (1.24)$$

Putting those two contribution together, we obtain

$$\Gamma_{\mu}^{A \text{ 1Loop}} = -g\gamma_{\mu} (C_F + N) t^A \frac{\alpha}{4\pi} \frac{1}{\epsilon} \quad (1.25)$$

As in the previous cases, the QED expression for the divergent part of this diagram may be obtained by setting $C_F \rightarrow 1$ and $N \rightarrow 0$.

The Lorentz structure of this divergent contribution is identical to the gluon-fermion vertex that appears in the Lagrangian. Therefore we can cancel this contribution in the computation by adding a counter-term in the Lagrangian of the form

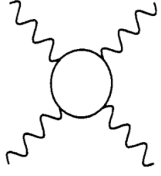
$$- \delta_1^{\text{1Loop}} g \mu^{\epsilon} \bar{\psi} \not{A}^A t^A \psi \quad \text{with} \quad \delta_1^{\text{1Loop}} = - (C_F + N) \frac{\alpha}{4\pi} \left(\frac{1}{\epsilon} + c_{11} \right) \quad (1.26)$$

where again c_{11} is an arbitrary constant from the renormalisation procedure.

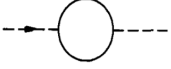
Let us pause for a second and analyse the results we have obtained. We have computed three out of the seven divergent 1PI diagrams of Figure 1.1 and for all of them we have found the same pattern: for each of these n-point functions the divergence is proportional to the Lorentz and colour structure of the contribution of one of terms of the gauge fixed QCD Lagrangian to that n-point function. Remarkably, the number of 1PI diagrams we have not yet computed (3-gluon, 4-gluon, ghost-self energy and ghost-gluon interaction) coincide with the number of terms in the gauge-fixed Lagrangian left without counter-term modification. We may now guess (or compute explicitly) that the divergences introduced by the remaining divergent 1PI diagrams possess the same structure as one of the remaining vertices and can therefore be cancelled by adding new counter-terms to the Lagrangian. To set the notation, let us associate to each of the diagrams its counter-term as



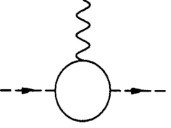
$$\delta_1^{\prime \text{1Loop}} \frac{1}{2} g_R \mu^{\epsilon} f^{ABC} A_R^{\mu B} A_R^{\nu C} (\partial_{\mu} A_{R\nu}^A - \partial_{\nu} A_{R\mu}^A) \quad (1.27)$$



$$-\delta_4^{1\text{Loop}} \frac{1}{4} g_R^2 \mu^{2\epsilon} f^{ABC} f^{AB'C'} A_{R\mu}^B A_{R\nu}^C A_R^{B'\mu} A_R^{C'\nu} \quad (1.28)$$



$$-\delta_c'^{1\text{Loop}} \bar{c}_R^A \partial^2 c_R^A \quad (1.29)$$



$$\delta_1''^{1\text{Loop}} g_R \mu^\epsilon f^{ABC} \bar{c}_R^A \partial_\mu A_R^{\mu B} c_{Rc} \quad (1.30)$$

The structure we have discussed, i. e., the fact that the divergences of the 1PI diagrams correspond to the different terms in the QCD Lagrangian and can be cancelled by a finite number of counter-terms persists to all orders and it is essential for proving the renormalisability of QCD. Furthermore, as we will see, not all the constants are independent; in fact, we will be able to determine the value of the four undetermined counter-terms from those we have already computed.

1.2.1 Renormalisation schemes

Before closing this section we would like to discuss the undetermined constants

$$c_{\psi 1} \quad c_{m 1} \quad c_{A 1} \quad c_{1 1} . \quad (1.31)$$

As already stated, these constants arise from an arbitrariness in the renormalisation procedure. To be able to perform reliable computation, the counter-terms must remove the divergent contributions to the different 1PI. But they can also remove arbitrary amounts of the finite part of those contributions. And as long as these constants are always the same, any choice (up to some restrictions that will become apparent in the next section) are equally good. Each of these choices is called a **renormalisation scheme**.

In QED it is customary to fix those constants by demanding different physical conditions, such as that the parameter m that appears in the Lagrangian corresponds to the pole mass of the propagating particle. This is the so called mass-shell renormalisation scheme. But this is not the only choice. In fact, this is not a good choice for QCD, where the pole mass of the different quarks is unknown, since quarks are not asymptotic states.

Other popular and useful set of schemes are the so called minimal subtraction schemes (MS) and the modified minimal subtraction scheme ($\overline{\text{MS}}$). These amount to choose those constant as either zero or a fixed number

$$c_{\psi 1} = c_{m 1} = c_{A 1} = c_{1 1} = 0 \quad \text{in MS scheme} \quad (1.32)$$

$$c_{\psi 1} = c_{m 1} = c_{A 1} = c_{1 1} = -\gamma_E + \log(4\pi) \quad \text{in } \overline{\text{MS}} \text{ scheme} \quad (1.33)$$

The advantage of this choice is that in this scheme, counter-terms δ_i depend explicitly only on the coupling constant g_R . The disadvantage is that now the parameter m_R on the Lagrangian does not correspond to the pole mass of the different particles; it may still be related to it via a perturbative expansion in g_R . This arbitrariness highlights that the parameters in the Lagrangian may not be directly related to physical quantities, as we will explore shortly.

1.3 The renormalised QCD Lagrangian and the meaning of renormalisation

Let us now collect the results of the previous section and put them in perspective by looking into the QCD Lagrangian. The diagrammatic contributions to each of the 1PI diagrams that gives divergent contribution are determined from the tree level Lagrangian

$$\begin{aligned} \mathcal{L}_{t.l.}(g_R\mu^\epsilon, m_R) &= \bar{\psi}_R \left(i\not{\partial} - g_R\mu^\epsilon \not{A}_R^A t^A - m_R \right) \psi_R - \frac{1}{4} F_{\mu\nu}^A(A_R, g_R\mu^\epsilon) F^{\mu\nu A}(A_R, g_R\mu^\epsilon) \\ &\quad - \frac{1}{2} \lambda_R (\partial \cdot A_R)^2 + \bar{c}_R^A \left[\partial^2 \delta^{AB} - g_R\mu^\epsilon f^{ABC} \partial_\mu A_R^{\mu B} \right] c_R^C. \end{aligned} \quad (1.34)$$

where we have specified that this is a function of the parameters g_R , m_R and the arbitrary scale μ . For completeness, the non-abelian field strength is given by.

$$F_{\mu\nu}^A(A_R, g_R\mu^\epsilon) = \partial_\mu A_{R\nu}^A - \partial_\nu A_{R\mu}^A - g_R\mu^\epsilon f^{ABC} A_{R\mu}^B A_{R\nu}^C. \quad (1.35)$$

The observation that each of the divergent 1PI can be made finite by introducing a number of divergent counter-terms in the Lagrangian, means that if instead of the tree-level Lagrangian we consider the renormalised Lagrangian

$$\begin{aligned} \mathcal{L}_R(g_R, m_R, \mu) &= \mathcal{L}_{t.l.}(g_R\mu^\epsilon, m_R) \\ &\quad + \delta_\psi^{1\text{Loop}} \bar{\psi}_R i\not{\partial} \psi_R - \left(\delta_m^{1\text{Loop}} + \delta_\psi^{1\text{Loop}} \right) m_R \bar{\psi}_R \psi_R - \delta_1^{1\text{Loop}} g_R\mu^\epsilon \bar{\psi} \not{A}_R^A t^A \psi \\ &\quad - \delta_A^{1\text{Loop}} \frac{1}{4} (\partial_\mu A_{R\nu} - \partial_\nu A_{R\mu}) (\partial^\mu A_R^\nu - \partial^\nu A_R^\mu) \\ &\quad + \delta_1'^{1\text{Loop}} \frac{1}{2} g_R\mu^\epsilon f^{ABC} A_R^{\mu B} A_R^{\nu C} (\partial_\mu A_{R\nu}^A - \partial_\nu A_{R\mu}^A) \\ &\quad - \delta_4^{1\text{Loop}} \frac{1}{4} g_R^2 \mu^{2\epsilon} f^{ABC} f^{AB'C'} A_{R\mu}^B A_{R\nu}^C A_R^{B'\mu} A_R^{C'\nu} \\ &\quad - \delta_c'^{1\text{Loop}} \bar{c}_R^A \partial^2 c_R^A + \delta_1''^{1\text{Loop}} g_R\mu^\epsilon f^{ABC} \bar{c}_R^A \partial_\mu A_R^{\mu B} c_{Rc} \end{aligned} \quad (1.36)$$

then all correlation functions are finite, for finite values of the parameters g_R , m_R and μ .

Since the counter-terms that we have introduced are proportional to the different vertexes of the tree level Lagrangian, it is easy to see that we can better understand the renormalised Lagrangian if we treat the fields it depends upon as renormalised with respect to a set of bare fields and constants

$$\psi_{(0)} = \sqrt{Z_\psi} \psi_R \quad A_{(0)} = \sqrt{Z_A} A_R \quad c_{(0)} = \sqrt{Z_c} c_R \quad (1.37)$$

$$g_{(0)} = Z_g g_R \mu^\epsilon \quad m_{(0)} = Z_m m_R \quad (1.38)$$

where we relate a generic renormalisation constant Z_i to the one loop counter-term as

$$Z_i = 1 + \delta_i^{1\text{Loop}} + \mathcal{O}(\alpha^2) \quad (1.39)$$

for $i = \{\psi, A, c, m, \dots\}$. All the required renormalisation constants but Z_g can be determined immediately at one loop from the computations in the previous section. To determine this last constant we simply demand that the tree level Lagrangian written in terms of the bare fields $\{\phi_{(0)}\}$ is identical to the renormalised Lagrangian written in terms of the renormalised fields $\{\phi_R\}$

$$\mathcal{L}_{\text{t.l.}}(g_{(0)}, m_{(0)}; \{\phi_{(0)}\}) = \mathcal{L}_R(g_R, m_R, \mu; \{\phi_R\}) \quad (1.40)$$

By looking into the interaction terms, for this equality between Lagrangians to be true the renormalization constant Z_g must be given by

$$Z_g = \frac{Z_1}{Z_\psi Z_A^{1/2}} = \frac{Z'_1}{Z_A^{3/2}} = \frac{Z_4^{1/2}}{Z_A} = \frac{Z''_1}{Z_c Z_A^{1/2}} \quad (1.41)$$

where the different equalities arise from the uniqueness of the bare coupling constant, as imposed by gauge symmetry in the bare theory. Therefore as a consequence of gauge symmetry, there is a non-trivial relation between the counter-terms in the gauge theory known as the Taylor-Slavnov identities

$$\frac{Z_1}{Z_\psi} = \frac{Z'_1}{Z_A} = \left(\frac{Z_4}{Z_A} \right)^{1/2} = \frac{Z''_1}{Z_c} \quad (1.42)$$

To conclude this section, let us discuss the gauge fixing parameter λ_R . As any other parameter in the Lagrangian we could have included an renormalisation constant

$$\lambda_0 = Z_\Lambda \lambda_R. \quad (1.43)$$

However, since after renormalization the gluon self energy is still transverse, with $\lambda = 1$, this means that the gauge fixing term does not renormalise, which implies $Z_\Lambda = 1/\sqrt{Z_A}$.

1.4 The renormalization Group

The procedure we have described above is apparently pleasing: we have managed to absorb all the infinities that appear in the perturbative evaluation of correlation functions into a finite number of (divergent) constants, which we can get rid off by changing the normalisation of the different fields. However, there a number of nuances that we still have to get in terms with.

The first problem that we observe is that we have introduced an arbitrary parameter into the microscopic description of the theory. From a classical point of view, the two parameter of the Lagrangian g_R and m_R specify the $SU(N)+1$ flavour theory. If one fixes the value of these parameters, the theory should become predictive and we should be able to determine all possible correlation functions. However, after renormalization this is no longer the case.

As we have seen, the renormalization procedure introduces an arbitrary scale μ which appear explicitly in the Lagrangian. And, at first sight, there is no apparent way to fix this parameter. We have therefore introduced arbitrariness in the microscopic description of the theory and we seem to have lost predictive power.

However, after renormalising the fields, we can relate the renormalised Lagrangian to a bare Lagrangian which is independent on μ , as expressed in equation (1.40). This relation implies that in the space of all possible theories, parametrised by g_R , m_R and μ there is a group of theories, those that satisfy equation (1.40) that are equivalent, since they all relate to the same bare theory. This group of theories may be parametrised by trajectories in the the parameter space

$$(g_R, m_R, \mu) \rightarrow (g_R(\mu), m_R(\mu)) \quad (1.44)$$

which relate equivalent gauge theories.

So, why should we talk about this group of theories and not just about the bare theory? This is in fact the second complication. Since the parameters Z_i are divergent in the $\epsilon \rightarrow 0$ ($n \rightarrow 4$) limit, the fact that g_R and m_R are finite implies that the bare parameters are divergent, and therefore unobservable. We therefore cannot determine them and we cannot use the bare theory for explicit computations. Nevertheless, the relation between the bare and renormalised theory is enough to determine the trajectory in theory space that make Lagrangians with different values of g_R and m_R equivalent to one another. We will do so by specifying how the parameters of the theory change along the trajectory as μ changes and determine

$$\beta = \left. \frac{dg_R(\mu)}{d \log \mu} \right|_{\{g_0, m_0\} \text{ fixed}} \quad \gamma_m = - \left. \frac{d \log m_R(\mu)}{d \log \mu} \right|_{\{g_0, m_0\} \text{ fixed}} \quad (1.45)$$

To make this discussion more explicit, let us focus on mass independent schemes, such as the $\overline{\text{MS}}$ or $\overline{\text{MS}}$ schemes, in which counter-terms are solely explicitly dependent on the coupling constant.

$$Z_i = Z_i(g_R(\mu)) \quad (1.46)$$

where we have made explicit that we are evaluating the parameter over of the trajectories in theory space. By taking a derivative with respect to the scale μ of the relation between g_0 and g_R , equation (1.38) we obtain

$$0 = \beta + g_R \frac{d \log Z_g}{d \log \mu} + \epsilon g_R \quad (1.47)$$

Since we have only determined the one-loop contribution to the different renormalization constants, we only know them up to quadratic order in the coupling. We may then parametrise

$$Z_g = 1 + \frac{g_R^2}{(4\pi)^2} \frac{b_0}{2} \left(\frac{1}{\epsilon} + c_g \right) + \mathcal{O}(g_R^4) \rightarrow \log Z_g = \frac{g_R^2}{(4\pi)^2} \frac{b_0}{2} \left(\frac{1}{\epsilon} + c_g \right) + \mathcal{O}(g_R^4) \quad (1.48)$$

we may then solve equation (1.47) as

$$\beta = - \frac{g_R \epsilon}{1 + b_0 \frac{g_R^2}{(4\pi)^2} \left(\frac{1}{\epsilon} + c_g \right)} \quad (1.49)$$

Since, once again, our one loop computation is only valid up to quadratic order, we can expand the denominator to leading order in g_R and obtain

$$\beta = -g_R \left(\epsilon - b_0 \frac{g_R^2}{(4\pi)^2} (1 + c_g \epsilon) + \mathcal{O}(g_R^4) \right) \quad (1.50)$$

We may now take the $\epsilon \rightarrow 0$ limit to obtain the β function in four dimension³, which yields

$$\beta^{\text{1 Loop}} = b_0 \frac{g_R^3}{(4\pi)^2} \quad (1.51)$$

where we have specified that our computation is only valid at one loop

Equation (1.51) may be now transformed into a differential equation for the coupling constant, remembering the definition of β

$$\mu \frac{dg_R}{d\mu} = b_0 \frac{g_R^3}{(4\pi)^2} \quad (1.52)$$

which, as promised, represents a trajectory in theory space for the coupling constant. Solving the one-loop β function equation is easy, and we may express the solution as

$$\frac{1}{g_R^2(\mu)} = \frac{1}{g_R^2(\mu_0)} - \frac{b_0}{(4\pi)^2} \log(\mu^2/\mu_0^2) \rightarrow g_R^2(\mu) = \frac{g_R^2(\mu_0)}{1 - g_R^2(\mu_0) \frac{b_0}{(4\pi)^2} \log(\mu^2/\mu_0^2)} \quad (1.53)$$

where $g_R(\mu_0)$ is the value of the coupling constant at a reference scale μ_0 , which we need to specify since the differential equation (1.51) is of first order.

Let us here re-state the meaning of this trajectory. What the renormalisation group tells us is that the renormalised Lagrangian of a $SU(N)$ gauge theory with renormalised coupling constant $g_R(\mu)$ at scale μ is equivalent to the renormalised theory with coupling constant $g_R(\mu_0)$ at scale μ_0 since all these Lagrangians arise from the same bare parameters. While any single calculation we perform may appear different, since it depends on the corresponding value of g_R and μ , as long as we compare calculations performed with parameters in the trajectory given by equation (1.53) those two theories are equivalent and must lead to the same physical predictions. We will see below how this fact may be used to best determine the value of μ .

1.5 The QCD β -function

Let us now particularise the discussion for QCD. Taking advantage of the previous work, we only need to determine the parameter b_0 for a $SU(N)$ gauge theory with n_f fundamental fermions. Using the relation in equation (1.41) and the computation of the counter-terms, equations (1.13), (1.21) and (1.26) and expanding up to quadratic order in g_R we obtain

$$\delta_g^{\text{1 Loop}} = \delta_1^{\text{1 Loop}} - \delta_\psi^{\text{1 Loop}} - \frac{1}{2} \delta_A^{\text{1 Loop}} = -\frac{g_R^2}{(4\pi)^2} \left(\frac{11}{3} N - \frac{4}{3} T_F n_f \right) \frac{1}{2} \left(\frac{1}{\epsilon} + c_g \right) \quad (1.54)$$

³The careful reader will realise that at order g_R^4 and beyond, negative powers of ϵ appear, which make the $\epsilon \rightarrow 0$ ill defined. These are in fact cancelled by higher order terms in the g_R expansion, since higher order loop counter-terms possess additional inverse powers of $1/\epsilon$.

and using equation (1.48)

$$b_0 = - \left(\frac{11}{3}N - \frac{4}{3}T_F n_f \right) \quad \text{with} \quad T_F = \frac{1}{2} \quad (1.55)$$

Together with the general expression in equation (1.53), we can write an explicit expression for the strong coupling constant α

$$\alpha(\mu) = \frac{\alpha(\mu_0)}{1 + \frac{\alpha(\mu_0)}{4\pi} \left(\frac{11}{3}N - \frac{4}{3}T_F n_f \right) \log \mu^2 / \mu_0^2} \quad (1.56)$$

We may now express this in a simpler and more familiar form by reorganising the coupling constant $g_R(\mu_0)$ at the reference scale μ_0 into a single scale. By a trivial manipulation we can express the scale-dependent coupling constant as

$$\alpha(\mu) = \frac{4\pi}{-b_0 \log \mu^2 / \Lambda^2} \quad (1.57)$$

where we may identify $\Lambda = \mu_0 e^{\frac{2\pi}{b_0 \alpha(\mu_0)}}$. In this way, we can express the scale-dependent coupling in terms of an emergent scale, Λ which may be interpreted as the scale at which the (one loop) coupling constant diverges. This scale appears even for $SU(N)$ with no flavours, which has no mass-scales in the tree level Lagrangian and is therefore conformal at classical (not quantum) level. This is in fact an example of an anomaly in quantum field theory, since a symmetry of the classical field theory (namely conformal symmetry) is absent at quantum level. As we will see later, this scale has consequences for physical observables. Note that this scale has emerged as a consequence of the renormalization process and has no analogue at classical (not quantum) level.

1.5.1 Asymptotic freedom

Another important feature of the scale-dependent coupling constant is how it changes as the scale μ increases or decreases. This is mainly controlled by the sign of the parameter b_0 ,

As it is clear from equation (1.57) if b_0 is negative, the coupling constant decreases as the scale grows, becoming smaller and smaller as $\mu \gg \Lambda$. This is precisely the case for QCD, in which $N = 3$ and $n_f = 6$. Since in the asymptotic region $\mu \rightarrow \infty$ the coupling vanishes, this theory is said to be asymptotically free. Therefore, the calculations performed at any finite scale and a corresponding finite coupling yield the same results that we would have obtained by choosing $g_R \rightarrow 0$ at arbitrarily high scales. In the sections below we will see that the dynamics of processes with very large momentum exchanges behave as approximately free.

This behaviour is in contrast with that of QED, which may be obtained by setting $N = 0$ and $T_F = 1$ in equation (1.55) (or with a $SU(N)$ gauge theory with $n_f > 11N/2$). In this case $b_0 > 0$ and, unlike QCD, the coupling decreases as the scale decreases. This feature is in fact important for the success of perturbation theory to describe QED processes. Because of this dependence the coupling constant diverges at some large scale, known as Landau pole.

These two different behaviours may be also inferred directly from the one-loop β -function, equation (1.51). As it is obvious from that expression, for asymptotically free theories ($b_0 < 0$) the one-loop β function is always negative, which means that, at least while the coupling is small, the derivative of the coupling with respect to the scale along the renormalization group trajectory is always negative, and therefore the coupling decreases at large scales. And the opposite is true for $b_0 > 0$.

Finally, and for completeness, let us discuss the special case in which $b_0 = 0$, as have for example for $N = 2$ and $n_f = 11$. In this case the one-loop vanishes and, at least at one loop the coupling constant does not depend on the scale. To establish whether the coupling changes or not one must go beyond one loop order. But if at all orders one can show that the β -function vanishes, then the coupling is constant at all scales and the quantisation procedure does not introduce a new scale. In this case, if the theory was classically scale invariant so will it be its quantised version. One example in which this happens is the so called $\mathcal{N} = 4$ Super Symmetric Yang Mills. Since this is not part of the standard model, we will not discuss this theory in these notes.

1.6 Fixed points

We will now digress from the analysis of perturbative QCD and discuss some important features of the renormalisation group flow equation (1.45). Let us assume we know the expression for the β -function of a given theory for all couplings. We may then formally solve the flow equation as

$$\int_{g_R(\mu_1)}^{g_R(\mu_2)} \frac{dg}{\beta(g)} = t \quad \text{with} \quad t = \log \mu_1 / \mu_2 \quad (1.58)$$

We may now concentrate on the special values of $g_R = g^*$ in which the β -function vanishes. In the vicinity of these points the derivative with respect to the scale of the coupling constant in the flow trajectory vanishes and we may call this point a fixed point. Around this region, we may expand the β -function and find

$$\int \frac{dg}{\beta(g)} \sim \int \frac{dg}{(g - g^*)} \sim \log |g - g^*| \quad (1.59)$$

which diverges as $g \rightarrow g^*$. This means that to reach this special value of the renormalised coupling the parameter t must asymptote to $\pm\infty$. Therefore, in the parameter space of theories, those points are asymptotically away from any fixed renormalization scale.

Fixed points are usually classified as ultra-violet (UV) fixed point and infra-red (IR) fixed points. UV fixed points are reached when the scale $\mu \rightarrow 0$; while IR fixed points are reached when $\mu \rightarrow \infty$. These two situations are depicted in figure (1.2). The free limits, $g_R = 0$ of QCD and QED are examples of UV and IR fixed points respectively. In general, the quantum field theory of a classical theory with a coupling constant λ possesses a fixed point at $\lambda = 0$, which we may call the perturbative fixed point. Also, since independently of initial conditions, the coupling constant approaches zero in the vicinity of the perturbative fixed point, these values

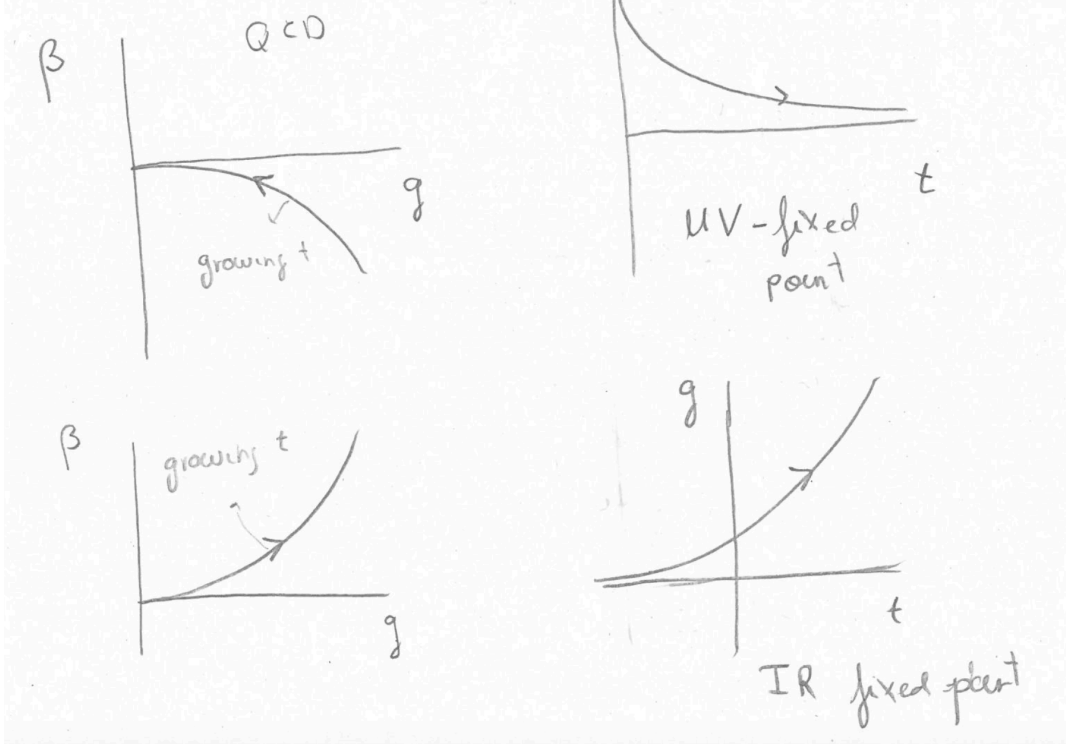
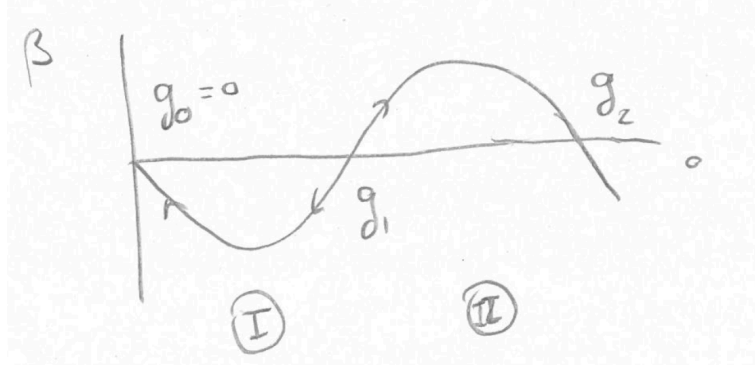


Figure 1.2: Depiction of UV and IR fixed points. For UV-fixed points the β function as function of the coupling approaches zero from below, which implies that the coupling decreases as the scale increases. For IR fixed point the opposite is true.

of the parameters are reached by more than one possible trajectory in theory space. Or, in other words, many different trajectories $g(\mu)$ flow toward the same fix point.

In perturbation theory is very hard to identify fixed points, other than the perturbative ones. It is however instructive to analyse the hypothetical β function of a theory with more than one fixed point, similar to the one depicted in figure (1.3). In this theory there are three fixed points $g_0 = 0$, g_1 and g_2 with $g_0 < g_1 < g_2$. By examining the behaviour of the β -function we can identify several properties of the theory:

- Since $\beta < 0$ between g_0 and g_1 , as the scale increases, the coupling constant flows towards g_0 and away g_1 . Therefore, in this region, denoted by I in the figure, g_0 is a UV fixed point while g_1 is IR fixed point.
- In region II the $\beta > 0$ and therefore, as the scale increases the constant flows towards g_2 and away from g_1 . As in region I, g_1 is a IR fixed point and g_2 is a UV fixed point.
- The theory described by the this β -function possesses regions of parameter space that are disconnected from each other. Since to reach either of the fixed points we must evolve the flow variable t by an infinite amount, the set of parameters that describe realisations of the theory in region I cannot describe the same physics as those of region II, since there is no renormalisation trajectory that connects them.

Figure 1.3: An interesting β function.

1.7 Running coupling

Until now, the discussion of the renormalisation group has remain rather abstract. As we have discussed, the renormalisation group allows us to use apparently different descriptions of the same physics by varying the parameters of the theory we use to compute along specified trajectories. In this section we want to show how this technology can be used to simplify the calculation of observable processes.

For simplicity, let us consider some cross section which depends only on one kinematic variable Q . An example of this is the total cross section of electron-positron annihilation to hadrons, where $Q = \sqrt{s}$, which we will analyse in the next section. After computing a calculation with our renormalised Lagrangian, and using dimensional analysis, we can express the cross section as

$$\sigma(Q) = \frac{1}{Q^2} f\left(\frac{Q^2}{\mu^2}, g_R(\mu), \frac{m_R^2}{\mu^2}\right) \quad (1.60)$$

where we have introduced the dimensionless function $f = Q^2 \sigma(Q)$. We will take the $m_R = 0$ limit for the moment and come back to this point later. In this limit, in a classical calculation f should be a constant, independent of the energy Q , since in this limit the classical theory possesses no mass scales. However, after renormalisation, any calculation will depend explicitly on the renormalisation scale μ , which introduces a momentum dependence in f via ratios of Q/μ . While we may think of this scale as a calculational artefact, we will see that this need will lead to the breaking of conformal invariance in the cross section.

Since a cross section is an observable that can be measured, it cannot depend of the arbitrary renormalisation scale μ which we must introduce to performed the regularised computation. Therefore, the computed function f must satisfy

$$\mu \frac{d}{d\mu} f = 0 = \mu \frac{\partial}{\partial \mu} f + \beta \frac{\partial}{\partial g_R} f. \quad (1.61)$$

This equation allows us to determine the function f for different equivalent theories (different μ and g_R) for a fixed kinematical value Q . However, we can use the fact that f is dimensionless

by construction to relate changes of μ to changes of Q

$$\mu \frac{\partial}{\partial \mu} f = -Q \frac{\partial}{\partial Q} f, \quad \rightarrow \quad 0 = -Q \frac{\partial}{\partial Q} f + \beta \frac{\partial}{\partial g_R} f. \quad (1.62)$$

This relation allow us to transform the equation (1.61) into a evolution equation for the cross section which determines the cross section at different Q values for a fixed μ . After changing the μ and Q derivatives, the renormalization group equation (1.61) implies that the cross section does not depend independently on Q an the coupling g_R , but rather

$$f\left(\frac{Q}{\mu}, g_R(\mu)\right) = F(\bar{g}(Q/\mu)), \quad \text{with} \quad F(g) = f(1, g) \quad (1.63)$$

i. e. the cross section becomes a function only of a *running coupling* \bar{g} , which satisfies

$$\frac{\partial}{\partial \log(Q/\mu)} \bar{g} = \beta(\bar{g}), \quad \bar{g}(Q = \mu) = g_R(\mu) \quad (1.64)$$

The equation for the running coupling is nothing else that the equation for the trajectory of the renormalised coupling in theory space that we solved in subsection (1.4). In that subsection, we solved this equation with the one-loop β -function in equation (1.56). Therefore, we can immediately find the solution of equation (1.64), which is given by

$$\bar{\alpha}(Q^2) = \frac{\alpha(\mu^2)}{1 - \frac{b_0}{4\pi} \alpha(\mu^2) \log \frac{Q^2}{\mu^2}}, \quad (1.65)$$

where, we have introduced $\bar{\alpha}(Q^2) \equiv \bar{g}(Q^2)/4\pi$.

Here we can extract a first non-trivial conclusion that arises from asymptotic freedom. Independently of the value of the renormalization scale μ we choose and independently of the value of the coupling constant $g_R(\mu)$ at that scale, as the physical energy scale Q grows, running coupling constant becomes smaller and smaller. Since the cross section becomes solely a function of the running coupling, this fact shows that asymptotic freedom implies that high-energy processes become almost free and perturbative techniques always apply for sufficiently high momentum transfer. On the contrary, as Q decreases the coupling grows and non-perturbative dynamics become important. Expressing the running coupling in terms of Λ as in equation (1.57)

$$\bar{\alpha}(Q) = \frac{4\pi}{-b_0 \log Q^2/\Lambda^2}, \quad (1.66)$$

it is then clear that for momentum transfers of order $Q \sim \Lambda$ the theory becomes non-perturbative. This dependence on the running coupling on the dynamically generated scale is a manifestation of the breaking of classical conformal invariance in the quantised theory.

From the equations above it is clear that the running coupling constant for a process at scale Q coincides with the coupling constant of a theory with $\mu' = Q$ on the renormalisation group trajectory connected to the scale μ . Therefore, we may describe the set of steps above as an indication on how to best select the scale for a given calculation. The running coupling

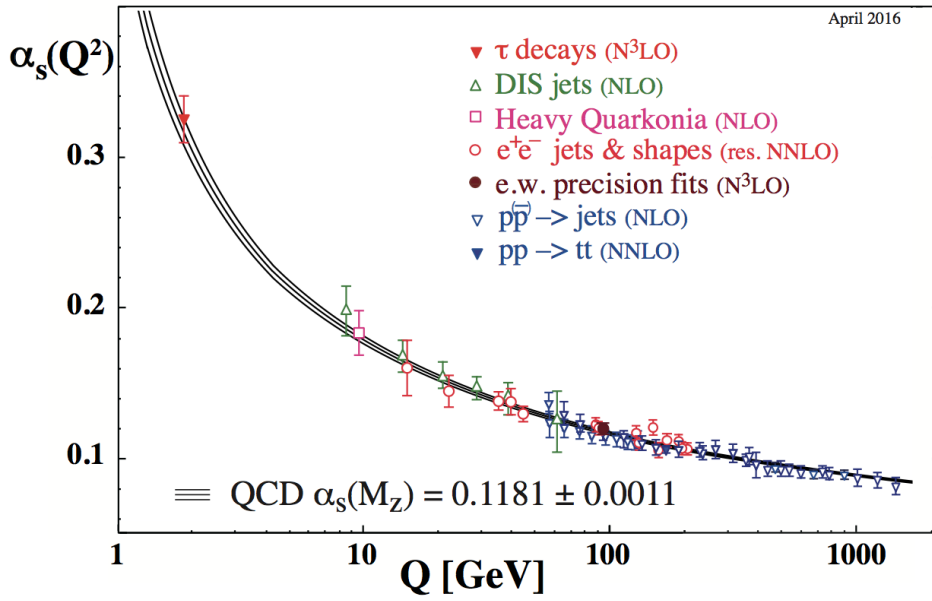


Figure 1.4: Experimental extraction of the strong coupling constant. Figure taken from the the particle data group review on Quantum Chromodynamics.

tells us that, instead of choosing a fixed value of the renormalisation scale μ for describing the cross section at all Q , it is better to change the renormalisation scale every value of the external momentum Q , such that $\mu = Q$. We will elaborate on this below interpretation below.

Since Q is a physical scale, the dependence of cross section on Λ allows us to extract it from experiments. Note, however, that Λ is scheme dependent, so whenever quoting an extraction of Λ we must specify the scheme in which the extraction has been performed. A compilation of data-based determinations of the running coupling constant is shown in figure (1.4). Therefore, instead of quoting the value of Λ the value of the coupling constant at the Z mass is quoted, from which the value of Λ may be inferred. While Λ depends of the extraction, we can use $\Lambda \sim 200\text{MeV}$ as a representative value.

Before continuing discussing how to use the running coupling to compute relevant QCD processes we would like to remark a subtlety on the way we fix the parameters of QCD. At classical level, in the massless limit, QCD is fixed by specifying the value of the coupling constant, since this is the only parameter that is not fixed in the Lagrangian. However, at quantum level, the coupling constant is no longer a constant and effectively becomes process dependent via the running coupling constant. To fix now the theory we must determine a scale, either the value of Λ or the scale at which the coupling attains a given value. Therefore, to fix now the theory we must determine a dimension-full quantity. As already stressed, in doing so we are breaking conformal invariance, and we may now expressed all physical quantities in units of this scale. The phenomenon by which the theory is no-longer fixed by the value of a coupling constant but rather the selection of a scale is called dimensional transmutation.

For $Q \gg \Lambda$ we can use the fact that the running coupling is small to evaluate the cross section of interest perturbatively. This tantamount to determining the function of the coupling $F(g)$ appearing in the right hand side of Eq. (1.63). To perform this computation we must specify a value of μ to evaluate the different Feynman diagrams that appear in the computation. Instructed by the analysis above, we can set $\mu = Q$ and evaluate the cross section, from where we can determine the value of F as

$$F_{\text{pert}}(g) = Q^2 \sigma_{\text{pert}}(Q, g, \mu = Q). \quad (1.67)$$

Since we are in the perturbative regime, we may expand F_{pert} in powers of α

$$F_{\text{pert}}(g) = \sum_{n=0} (\alpha)^n F^{(n)}, \quad (1.68)$$

where the coefficients $F^{(n)}$ as just number that are determined from the perturbative calculation.

To better understand what we are doing, let us now consider what would have happened in we would have chosen a scale $\mu \gg \Lambda$ different than Q . We want to examine how the answer we have obtained using Q as a renormalization scale would look like should we have done this different choice. Since, as we have seen, F only depends on the running coupling, the computation perturbative computation in equation (1.68) may be expressed as

$$F_{\text{pert}} = F^{(0)} + \bar{\alpha}(Q; \mu) F^{(1)} + \dots, \quad (1.69)$$

where we have made the μ dependence explicit. Let us stress once again that the coefficient $F^{(n)}$ are numbers, and not functions of the scale. This result is different to what we would have obtained by doing a perturbative computation at scale μ

$$F_{\text{fixed } \mu} = F_{\text{fixed } \mu}^{(0)} + \alpha(\mu) F_{\text{fixed } \mu}^{(1)} + \dots, \quad (1.70)$$

since the running coupling contains an infinite series in $\alpha(\mu)$. Indeed, expanding equation (1.65) in powers of $\alpha(\mu)$ we obtain

$$\bar{\alpha}(Q^2) = \alpha(\mu^2) \left[1 + \sum_{n=1}^{\infty} \left(\frac{b_0}{4\pi} \alpha_s(\mu) \log \frac{Q^2}{\mu^2} \right)^n \right]. \quad (1.71)$$

It is interesting to note that the higher order corrections in this expansion are of the form $\alpha(\mu) \log Q^2/\mu^2$, which are, in principle sub-leading and seem to be negligible in a fixed order calculation. However, if we choose $Q \gg \mu$ we can find a large logarithm that counteracts the smallness of $\alpha(\mu)$. The running coupling re-sums this type corrections into a single function of the scale.

Another way to see what is happening is that if we would have done the fixed- μ computation, at second $\alpha(\mu)$ -order we would have obtained

$$F_{\text{fixed } \mu}^{(2)} = F^{(2)} + F^{(1)} \frac{b_0}{4\pi} \log(Q^2/\mu^2) \quad (1.72)$$

To cancel this potentially dangerous log, it is therefore convenient to choose $\mu = Q$

The corollary of this discussion is that if we have a single scale process, it is necessary to choose $\mu \sim Q$ to avoid potentially large logs which can spoil perturbative computations. If the process has more than one relevant scale, there may be several relevant couplings, but we will not discuss this now. However, we started this discussion by stating that the cross section should be independent of the scale μ and we now argue that there are some choices better than others. The solution to this apparent puzzle is that independence of scale is only true at all orders; at any fixed order the cross section is indeed dependent on the scale, but the dependence is of at least one additional order than the accuracy of the calculation. This also means that we do not always have to choose $\mu = Q$, but just of the same order $\mu = \zeta Q$. As long as ζ is of order one the difference between different scales does not accumulate large logs and we can relate the coupling constants computed at different scales via one higher order term

$$\alpha_s(\zeta Q) = \alpha(Q) \left(1 + \frac{b_0}{4\pi} \alpha(Q) \log \frac{1}{\zeta^2} + \mathcal{O}(\alpha^2) \right) \quad (1.73)$$

Since by varying ζ we include a subset of next-order correction to a fixed order calculation, it is common practice in phenomenology to vary the renormalization scale around $\mu = Q$ to gauge the uncertainty of an fixed order prediction.

1.8 The Running Mass and Infrared safety

We now turn back to the issue of the mass of the quarks, which in the previous analysis we have set to zero. We will assume for simplicity that there is a single mass parameter in the Lagrangian m_R , which, via renormalization, becomes scale dependent. The generalisation to several mass parameters is straight-forward. Taking into account this parameter, we may express the cross section as

$$\sigma(Q^2) = \frac{1}{Q^2} f \left(\frac{Q^2}{\mu^2}, g_R, \frac{m_R}{\mu} \right) \quad (1.74)$$

As in the massless case, the independence of the cross section on μ for a fixed Q may be transformed into an evolution equation in Q for a fixed μ . The additional mass scale implies a change in the relation between μ and Q derivatives as

$$\mu \frac{\partial f}{\partial \mu} = -Q \frac{\partial f}{\partial Q} - m_R \frac{\partial f}{\partial m_R} \quad (1.75)$$

which leads to the equation

$$\left(Q \frac{\partial}{\partial Q} - \beta \frac{\partial}{\partial g_R} + (1 + \gamma_m) m_R \frac{\partial}{\partial m_R} \right) f = 0 \quad (1.76)$$

where the mass anomalous dimension was defined in equation (1.45). In any momentum subtraction scheme, such as $\overline{\text{MS}}$, since the mass renormalisation constant Z_m solely depends

on g_R , γ_m is an explicit function of g_R only and not on m_R nor μ . For concreteness, the one-loop anomalous dimension in $\overline{\text{MS}}$ -scheme can be determined from our computation of the mass counter-term in equation (1.13)

$$\gamma_m = \frac{d \log Z_m}{d \log \mu} = -\frac{6g_R}{(4\pi)^2} \beta C_F \left(\frac{1}{\epsilon} + c_m \right) = \frac{3\alpha}{2\pi} C_F + \mathcal{O}(\alpha^2) \quad (1.77)$$

where we have used the expression for the β -function at finite ϵ , equation (1.50).

As in the massless case, equation (1.76) implies that f becomes a function of the running coupling and the running mass

$$f\left(\frac{Q^2}{\mu^2}, g_R, \frac{m_R}{\mu}\right) = F\left(\bar{g}\left(\frac{Q}{\mu}; g_R(\mu)\right), \frac{\bar{m}\left(\frac{Q}{\mu}; g_R(\mu), m_R(\mu)\right)}{\mu}\right) \quad (1.78)$$

where the running mass is a solution of the differential equation

$$\frac{\partial \log(\bar{m}/m_R)}{\partial \log(Q/\mu)} = -(1 + \gamma_m(\bar{g})) \quad \text{with} \quad \bar{m}(Q = \mu) = m_R \quad (1.79)$$

where $\gamma_m(\bar{g})$ is the anomalous dimension evaluated at the running coupling. The solution to this equation is which is given by

$$\frac{\bar{m}(Q)}{\mu} = \frac{m_R(\mu)}{Q} \exp \left\{ - \int_0^{\log(Q/\mu)} dt \gamma_m(\bar{g}(t)) \right\}. \quad (1.80)$$

Since in an asymptotically free theory, at high scale g is small, γ_m can be treated perturbatively and it is therefore small. This implies that at large momentum the effect of a finite quark mass is small and the cross section is better and better approximated by the massless limit⁴.

In addition to the "classical" suppression expected at large Q , m/Q there is an additional logarithmic suppression as a result of the running of m_R . Although the relation between m_R and the pole mass m_p depends on the scheme, in general we expect $m_R(m_p) \sim m_p$. However, as discuss before, to avoid large logs we must choose $\mu \sim Q$. If $Q \gg \mu$ we can integrate the renormalisation equation for m_R using equation (1.77) we have

$$m_R(Q) = m_R(m_p) e^{-\int_0^{\log(Q/m_p)} \frac{3\alpha(t)}{2\pi} C_F dt} = \frac{m_R(m_p)}{\left(1 + \frac{-b_0}{2\pi} \alpha(m_p) \log \frac{Q}{m_p}\right)^{-3C_F/b_0}}. \quad (1.81)$$

For an asymptotically free theory, such that $b_0 < 0$, the renormalised mass itself at large scales decreases, making the quarks effectively massless.

This observation leads to a potential problem, since not all cross sections are well defined in the $m \rightarrow 0$. As we will see in the below, in this limit *collinear* singularities appear if the observable is not carefully defined, which makes the massless limit ill-defined. The set of observables which are well defined in this limit are generically called *infrared safe* and are particularly important in QCD, since they do not show sensitivity to the non-perturbative small values of the light quark masses.

⁴Note that should the theory not be asymptotically free, then γ_m could grow at large energies and it would be not guaranteed that the mass parameter decouples.

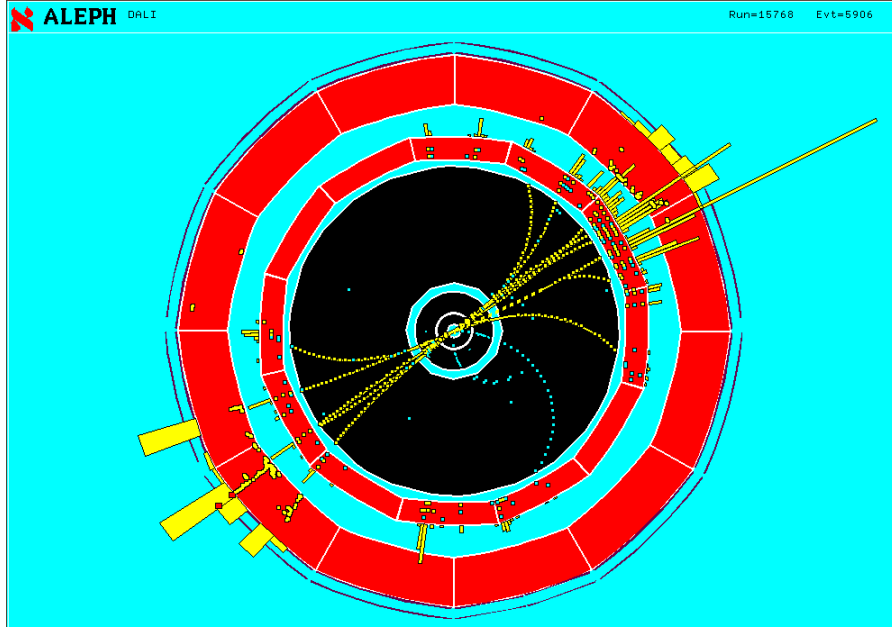


Figure 1.5: An event display of an e^+e^- annihilation into hadrons at $Q = M_Z$.

1.9 The R parameter

Let's make the discussion in the previous sections more concrete, by analysing a particularly clean and important QCD process: the annihilation of electro-positron pairs into hadrons. We will focus on fully inclusive measurements, that is, the cross section to produce any number of any species of hadrons with no cuts in phase space. This cross is of the type we have analysed in the previous two sections, since it only depends on the center of mass energy of the $e^+ e^-$ pair. Therefore, we can set $Q = \sqrt{s}$.

If one observes an event display of one of these collisions at very large $Q \gg \Lambda$, see for example figure (1.6), this looks like a very complicated observable, which lots of particles in the final state. Furthermore, those particles are hadrons, whose production mechanism is not under good theoretical control. Nevertheless, the discussion in the previous sections tells us that we can describe this cross section in QCD using perturbation theory. Choosing $\mu = Q$ to avoid large logs, we can expand the cross section

$$\sigma_{e^+e^- \rightarrow \text{hadrons}} = \sigma_0(Q) + \alpha(Q)\sigma_1 + \dots \quad (1.82)$$

Therefore, in spite of being a complicated observable, with many low energy and non-perturbative processes occurring on an event-by-event basis, as long as we do a fully inclusive measurement, σ_0 is given by the lowest order diagram in perturbative QCD, which is independent of α_s . This diagram is shown in figure (1.6).

This leading order diagram is, in fact, identical to the leading order QED diagram of $e^+e^- \rightarrow \mu^+\mu^-$, up to the trivial factor of the electric charge of the produced quarks, Q_f . Since in the cross section we must sum over all final states, the annihilation into hadrons is

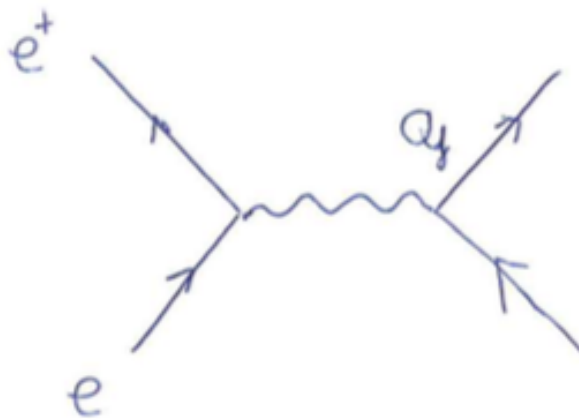


Figure 1.6: Leading order Feynman graph for e^+e^- annihilation into hadrons.

enhanced by an additional N -factor with respect to the annihilation into muons, because of the colour degrees of freedom. Therefore, the fraction

$$R = \frac{\sigma_{e^+e^- \rightarrow \text{hadrons}}}{\sigma_{e^+e^- \rightarrow \mu^+\mu^-}} = N \sum_f Q_f^2, \quad (1.83)$$

Where the sum runs over the number of *active* flavours, that is, the quarks with masses lighter than the Q . This is simple to understand, since to produce a $q - \bar{q}$ pair we need a center of mass energy of at least two times the mass of the quark. The experimental measurement of this quantity is shown in figure (1.7) At low energies, the R parameter shows a lot of structure,

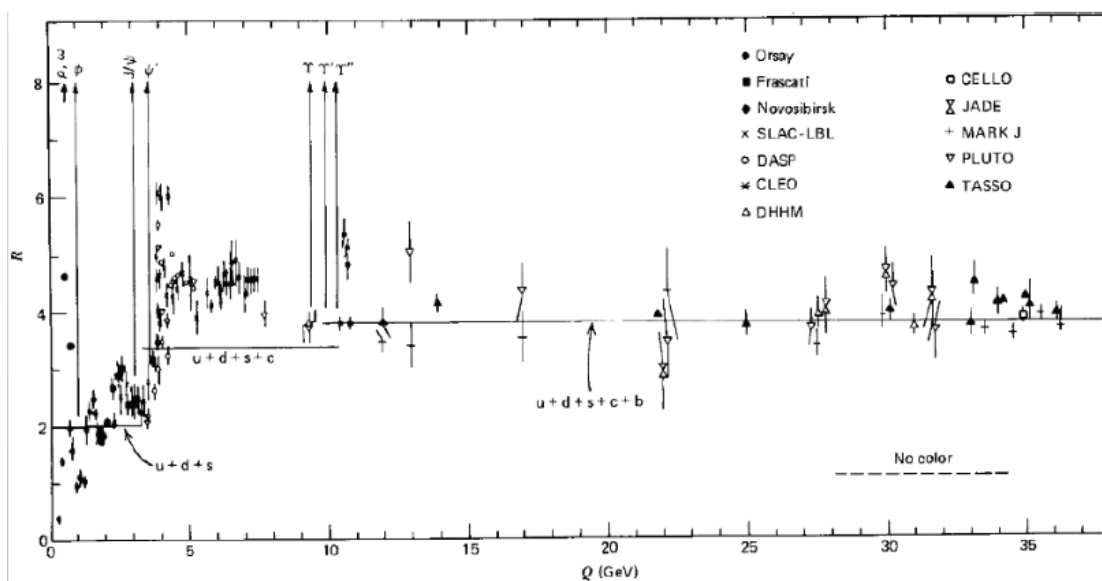


Figure 1.7: Measurement of the R parameter, as defined in Eq. (1.83).

corresponding to the formation of hadronic vector resonances at different scales. In between

these resonances, R is approximately flat, according to the corresponding number of active quarks. At high \sqrt{s} the measured ratio of cross section agrees well with Eq. (1.83) with all quarks, but the top quark, active. This measurement constitutes an experimental verification that there are indeed $N = 3$ colours. In later subsections we will attempt to determine this asymptotic value of the R parameter with higher accuracy in QCD by computing the next-to-leading correction to the annihilation cross section. However, we may anticipate the result here, by quoting the next to leading order result. To second order in α the calculation of this QCD process at arbitrary μ is given by

$$R(Q, \mu) = N \sum_f Q_f^2 \left(1 + \frac{\alpha(\mu)}{\pi} + \mathcal{O}(\alpha^2) \right), \quad (1.84)$$

While in principle any value of μ is equally valid, since this is an observable and therefore renormalisation-group invariant, our analysis of the previous section instructs us to choose $\mu = Q$ to obtain a better accuracy of this fixed order calculation. At this order, the need for this choice is not apparent, however, if we compute the same observable at next to next to leading order, we obtain

$$R(Q, \mu) = N \sum_f Q_f^2 \left(1 + \frac{\alpha(\mu)}{\pi} + \left(\frac{b_0}{4} \log \frac{Q^2}{\mu} + c_2 \right) \left(\frac{\alpha(\mu)}{\pi} \right)^2 + \mathcal{O}(\alpha^3) \right), \quad (1.85)$$

where b_0 is only a function of the number of colours and flavours, equation (1.55) and $c_2 = 0.6619N - 0.1152n_f$ is also a number for a fixed number of colours and flavours. At this order it becomes apparent why we must choose $\mu = Q$ (or at least of the same order), since otherwise the large logarithm that appears in the next-to-next-to leading order could lead to a large contribution, rendering the perturbative expansion useless.

A question now arises on how to evaluate α . In principle, the coupling constant depends on all flavours in QCD, independently of the masses, since renormalisation is a statement about the UV behaviour. On the other hand, just as the overall pre-factor depends on the number of active flavours, it makes no sense that the coupling constant depends on heavy flavour degree of freedom of mass $M \gg \mu$. These quarks must decouple from the calculation, as we will see below.

1.10 Heavy Quark Decoupling

As we have already mentioned, the $\overline{\text{MS}}$ is nowadays the scheme of choice for performing perturbative computations in QCD. This is due in part to its simplicity, which in particular implies that the different renormalisation constants in this scheme are independent on the renormalised mass parameter of the different matter fields (quarks) of the theory. This is a tremendous simplification to find solutions for RG flow equations. However, this property also leads to a problem, the apparent non-decoupling of heavy particles in the gauge theory parameters. What this means is that, as mentioned before, the expression for the β -function

depends on all the quarks that feel the strong force, since they all contribute to loop corrections. And this observation is rather unphysical, since it cannot be true that low energy processes with typical scale Q much smaller than the mass M of some quark know about the existence of this quark. The observation we have just described is what it is known as heavy quark decoupling.

In other more physical schemes, such as momentum subtraction scheme, that decoupling can be proven. In $\overline{\text{MS}}$ however, it must be introduced by hand. Since this latter procedure is standard we will streamline the main steps for this decoupling in these lecture notes. Note, however, that this is not just a physical requirement; if we do not perform this decoupling, at low energies $Q \ll M$, because of this separation of scales any given $\overline{\text{MS}}$ computation will exhibit large logarithmic corrections $\log M/Q$ which could spoil the perturbative evaluation and demand a resummation. What we will present below is, in effect, such resummation.

In our discussion of the decoupling we will be employing perturbation theory. Therefore, we must ensure that for the quarks we will be decoupling the QCD coupling constant evaluated at a scale comparable to the quark mass is small. The values of the $\overline{\text{MS}}$ mass $m_R(\mu)$, tabulated by the particle data group, are

$$m_u(2 \text{ GeV}) = 2.15 \pm 15 \text{ MeV} \quad m_c(m_c) = 1.28 \pm 0.025 \text{ GeV} \quad (1.86)$$

$$m_d(2 \text{ GeV}) = 4.90 \pm 20 \text{ MeV} \quad m_b(m_b) = 4.18 \pm 0.03 \text{ GeV} \quad (1.87)$$

$$m_s(2 \text{ GeV}) = 93.5 \pm 2 \text{ MeV} \quad m_t(m_t) = 173.3 \pm 0.8 \text{ GeV} \quad (1.88)$$

Therefore, the u , d and s quarks are considered light, since their mass is smaller than Λ , while the other three are considered heavy.

The main idea behind the decoupling procedure is to describe the low energy QCD interactions with $Q \ll M$, with M the mass of either heavy quark, with a low energy effective theory with n'_f quarks, which correspond to the number of active flavours at the corresponding energy scale. These are the light quarks plus any quark with $m_q \ll Q$.

For sufficiently low energy processes, that is, if we neglect all corrections of the type Q/M , it is easy to guess what the low energy effective theory is: it is just QCD with n'_f flavours. What it is not clear is what the relations between the coupling and masses in the low energy theory, g'_R , m'_R , and the coupling and masses in full QCD, g_R , m_R , are. The criterium to make sure that the low energy effective theory and QCD agree is that for all processes involving only the active (light) flavours, at momenta $Q \ll M$ both theories yield the same answer for all observables. In other words that the scattering matrix in both theories agree in that limit.

To implement this condition, let us start thinking about the problem from the point of view of the bare theories. Since we know that in both cases the bare Lagrangian is the bare Lagrangian of $\text{SU}(N)$ Yang Mills theory with the corresponding number of flavours, we can formally specify either theory by specifying their bare coupling constant and bare masses of the light flavours. Similarly, the bare theories possess bare (light) fields with arbitrary normalisations. Denoting with $'$ -variables the parameters and fields of the low energy theory, we may relate the two set of bare objects via a set of multiplicative constants, known as

decoupling constants

$$\psi'_{(0)} = \xi_{\psi(0)}^{1/2} \psi_{(0)} \quad A'_{(0)} = \xi_{A(0)}^{1/2} A_{(0)} \quad c'_{(0)} = \xi_{c(0)}^{1/2} c_{(0)} \quad (1.89)$$

$$g'_{(0)} = \xi_{g(0)} g_{(0)} \quad \lambda'_{(0)} = \lambda_{(0)} \quad m'_{(0)} = \xi_{m(0)} m_{(0)} \quad (1.90)$$

where we have imposed the same gauge in both theories by setting the same gauge fixing parameter. Since the bare parameters are divergent, so are the bare coupling constants.

As we have seen in previous section, renormalisation implies that the bare quantities in both theories will be multiplied by different divergent renormalisation constants, which differ in full QCD and in the low energy theory through their dependence in the number of flavours. This implies that there are analogous multiplicative relations for the renormalised fields via renormalised decoupling constants

$$\psi'_R = \xi_{\psi R}^{1/2} \psi_R \quad A'_R = \xi_{AR}^{1/2} A_R \quad c'_R = \xi_{cR}^{1/2} c_R \quad (1.91)$$

$$g'_R = \xi_{gR} g_R \quad \lambda'_R = \xi_{AR} \lambda_R \quad m'_R = \xi_{mR} m_R \quad (1.92)$$

where the relation between the bare and renormalised decoupling constant are straight forward. For the particular case of the coupling, this is given by

$$\xi_{gR} = \frac{Z_g}{Z'_g} \xi_{g(0)} \quad (1.93)$$

Note that since the renormalised decoupling constants relate renormalised quantities, which are finite, they are also finite and can be determine order by order in perturbation theory. In addition, since both Z_g and Z'_g are scale dependent, so must ξ_{gR} be. It is easy to determine the renormalisation group equation for this variable

$$\frac{\partial \log \xi_{gR}}{\partial \log \mu} = \frac{1}{g'_R} \beta' - \frac{1}{g} \beta \quad (1.94)$$

where we have used the relation between the β -function and the derivative of the renormalisation constant, equation (1.47). This expression is an exact relation provided we know the β functions of both theories to all orders in perturbation theory.

The evolution equation (1.94) allows us to determine the decoupling constant at any scale provided we can determine its value at some reference scale. To determine this value we must do what is known as a **matching calculation**. That is, ensuring that at some scale of choice μ the results of the low energy theory agree with those of the full theory. In these lecture notes we will focus on two of the decoupling constants, ξ_{AR} and ξ_{gR} .

To determine the ξ_{AR} we will focus in one particular correlation function that involves only gluonic fields, the gluon propagator, which for notational convenience we write as

$$D_{\mu\nu}^{AB}(k) = \int d^n x e^{ik \cdot x} \langle A_{R\mu}^A(x) A_{R\nu}^B(0) \rangle \quad D'_{\mu\nu}{}^{AB}(k) = \int d^n x e^{ik \cdot x} \langle A'^A_{R\mu}(x) A'^B_{R\nu}(0) \rangle \quad (1.95)$$

Using the definition of the decoupling constants above, these two propagators are related as

$$D_{\mu\nu}^{AB}(k) = \frac{1}{\xi_{AR}} D'_{\mu\nu}{}^{AB}(k) + \mathcal{O}\left(\frac{k^2}{M^2}\right) \quad (1.96)$$

where the last term reminds us that as the momentum k approaches the heavy quark mass M , we should include power-suppressed corrections. However, we may neglect those corrections as long as we have $k^2 \ll M^2$. Using the all order relations in arbitrary gauge

$$D_{\mu\nu}^{AB}(k) = \frac{-i}{(k^2 + i\epsilon)(1 + \Pi(k^2))} \delta^{AB} \left(g_{\mu\nu} - \frac{k_\mu k_\nu}{k^2} \right) + \frac{-i}{k^2 + i\epsilon} \frac{k_\mu k_\nu}{k^2} \lambda_R \delta^{AB} \quad (1.97)$$

where it is understood that we are working with the regularised quantities and where Π is the gluon self energy

$$\text{Diagram: a circle with two wavy lines attached} \equiv -i\pi_{AB,\mu\nu}(k) \quad \text{with} \quad \pi_{AB,\mu\nu}(k) = \delta_{AB} (k^2 g_{\mu\nu} - k_\mu k_\nu) \Pi(k^2) \quad (1.98)$$

Therefore, we can use equation (1.96) to relate the decoupling parameter to the gluon self-energy as

$$\xi_{AR}(\mu) = \frac{1 + \Pi(k^2 = 0, \mu, M)}{1 + \Pi'(k^2 = 0, \mu)} \quad (1.99)$$

where we have made explicit that in full QCD the gluon self energy depends on the mass of the heavy quark that decouples from the spectrum. This is an exact relation which is valid at all orders in perturbation theory. We may further simplify this relation if we assume that the renormalised mass of the light quarks is zero $m_R = 0$, since in that case the self energy of the low energy effective theory is a scaleless integral which in dim reg evaluates to zero

$$m_R = 0 \rightarrow \Pi'(0, \mu) = 0 \rightarrow \xi_{AR}(\mu) = 1 + \Pi(k^2 = 0, \mu, M) \quad (1.100)$$

For heavy quarks, such that $M \gg \Lambda$ we can also consider large renormalisation scales and evaluate the decoupling constant in a power series in α . The evaluation of $\Pi(k = 0)$ at one loop is straight forward. The relevant diagrams are shown in section (1.2). At leading order we can separate the one loop evaluation of Π into two distinct contribution, one coming from loop correction of light degrees of freedom and another one coming from the heavy quark loop

$$\Pi(k^2) = \Pi_l(k^2, \mu) + \Pi_h(k^2, \mu, M) \quad (1.101)$$

As for the low energy effective theory, in the limit of massless light quarks, $\Pi_l(k^2 = 0, \mu)$ vanishes in dimensional regularisation since it is given by a scale-less divergent integral. Analysing the finite part of the fermion loop contribution to the gluon self energy, equation (1.15) in $\overline{\text{MS}}$ -scheme we obtain

$$\xi_{AR} = 1 + \frac{1}{3} T_F \frac{\alpha}{\pi} \log \left(\frac{\mu^2}{M(\mu)^2} \right) + \mathcal{O}(\alpha^2) \quad (1.102)$$

From this computation we can readily extract ξ_{gR} . A simple way to proceed is to use the relation of the coupling with the different renormalisation constants, equation (1.41) both in the full theory and in the low energy effective theory to determine

$$\xi_{gR} = \frac{\xi_{1R}}{\xi_{\psi R} \xi_{AR}^{1/2}} \quad \text{where} \quad \xi_{1R} \equiv \frac{Z_1}{Z_1'} \quad (1.103)$$

with Z_1 the gluon-fermion vertex. Since we cannot write any leading loop correction involving the heavy quark for neither this vertex nor the light quark propagator, the leading order correction for both $\xi_{\psi R}$ and ξ_{1R} start at $\mathcal{O}(\alpha^2)$. Therefore to order α the decoupling constant for g is

$$\xi_{gR} = 1 - \frac{1}{6} T_F \frac{\alpha}{\pi} \log \left(\frac{\mu^2}{M(\mu)^2} \right) + \mathcal{O}(\alpha^2) \quad (1.104)$$

which implies that the α' of the low energy effective theory is related to the full α by

$$\alpha'(\mu) = \alpha(\mu) \left(1 - \frac{1}{3} T_F \frac{\alpha(\mu)}{\pi} \log \left(\frac{\mu^2}{M(\mu)^2} \right) + \mathcal{O}(\alpha^2) \right) \quad (1.105)$$

There are several interesting features about expression (1.105). First of all, at leading order, $\alpha' = \alpha$. This means that at order α^0 , the coupling constants (and the fields) of the effective low energy theory and the full theory are the same. However, once loop correction start to appear, those parameters differ by a normalisation, and we may think of the coupling constant and the fields as discontinuous across the heavy quark threshold. The second important piece of information is the appearance of $\log \mu^2/M(\mu)^2$ in the leading correction. Similarly to what happened with the energy of the $e^+ - e^-$ annihilation, the renormalisation scale emerges as a log of the ratio with the other mass scale in the problem. Because of this, the expansion parameter is not just α but $\alpha \log \mu^2/M(\mu)^2$. Therefore, while in principle we are free to choose any value of the scale μ , the fixed order computation is only well behaved as long as we choose

$$\mu \approx \mu_M \quad \text{with} \quad \mu_M \equiv M(\mu = M) \quad (1.106)$$

such that the log is small (in fact it is zero⁵ for $\mu = \mu_M$). For this reason, the perturbative decoupling analysis we have performed only makes sense for heavy quarks, in the sense of quarks with $M \gg \Lambda$.

If we want to determine the decoupling parameter (or the effective low energy coupling constant) at any other scale parametrically different from M we must re-sum a set of diagrams that are logarithmically enhanced. This can be easily done by using the renormalisation group equations, either by solving the β' -equation in the low energy theory or by solving the renormalisation group equation (1.94). This procedure is in fact important if we want to decouple several heavy quarks with masses parametrically separated $\Lambda \ll M_1 \ll M_2 \ll M_3 \dots$, as it occurs in QCD, where we have three different heavy quark. In order to avoid large logarithms of the type $\log m_b^2/m_t^2$ we must follow a sequential procedure, in which we first decouple the heaviest of the quarks (m_t), which relates $\alpha^{(n_f=5)}$ and $\alpha^{(n_f=6)}$ at about the top mass scale, then we use the renormalisation group equation to evolve down to $\mu \sim m_b$ to later perform the matching between $\alpha^{(n_f=4)}$ and $\alpha^{(n_f=5)}$ and so on. Having understood this sequential procedure, we can now give accurate values to the n_f -dependent Λ , which are to be used in the corresponding range of energies. In $\overline{\text{MS}}$ -scheme these are (extracted from the

⁵Note also that while selecting $\mu = \mu_M$ implies that the coupling constant is continuous across the transition, this is not the case for order α^2 , in which the coupling is discontinuous for this choice of scale

PDG)

$$\Lambda_{\overline{\text{MS}}}^{(6)} = 89 \pm 6 \text{ MeV} \quad (1.107)$$

$$\Lambda_{\overline{\text{MS}}}^{(5)} = 210 \pm 14 \text{ MeV} \quad (1.108)$$

$$\Lambda_{\overline{\text{MS}}}^{(4)} = 292 \pm 16 \text{ MeV} \quad (1.109)$$

$$\Lambda_{\overline{\text{MS}}}^{(3)} = 332 \pm 17 \text{ MeV} \quad (1.110)$$

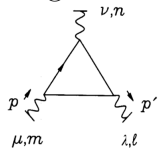
$$(1.111)$$

1.10.1 Going beyond $\mathcal{O}(1/M^0)$

The analysis we have performed so far only gives us the dynamics when the external momentum is much much smaller than the heavy quark mass we are decoupling. In the limit we have studied, provided we used the correct low energy coupling constant and masses the results of the low energy effective theory and the full theory are the same. However, we expect that with sufficient precision we should be able to notice the existence of this heavy quark, since it must modify the interaction by some power of the ratio of Q/M with Q the relevant scale in the process. This is in fact suggested by the relation (1.96), where we stated that the equality of the two propagators is only true up to corrections of this type.

In principle, since we know the full theory, we could simply answer this question by expanding any given cross section in powers of Q/M . However, here we want to analyse those corrections from the point of view of the low energy effective theory. The questions we are asking is whether by reasoning within the low energy theory we could guess or constrain the existence and properties of some unknown hypothetical heavier particle. In our example we will assume that this is a heavy quark that is coupled to gluons as any other quark, but the techniques we will use are general and can be used to study the effect at low energies of any unknown heavy particle within or beyond the standard model.

Even if we do not have enough energy to produce those heavy particles, their presence in the theory is signalled by the generation of new interactions of the light fields induced by loops of those massive objects. A simple example in QCD is the fermion-loop contribution to the three gluon vertex



$$\equiv \Gamma_{h\mu\nu\lambda}^{m,n,l}(p, p', M, \mu) \quad \text{after renormalisation} \quad (1.112)$$

When the fermion mass is much larger than the momenta of the gluons, we can expand Γ_h in powers of p/M and p'/M . The leading order term takes the form of a counter-term and it contributes to ξ_{gR} via the Z'_1 . Going to quadratic order, and after coming back to configuration space we expect that this diagram leads to a 1PI contribution of the form

$$\Gamma_{h\mu\nu\lambda}^{m,n,l}(p, p', M, \mu) \sim \frac{\partial^2}{M^2} AA\partial A \quad (1.113)$$

where two powers of ∂ come from the expansion of two of the quark propagators⁶ and the additional one comes from gluon-fermion vertex. Since the interactions must be gauge invariant, we can reproduce this structure with a unique gauge invariant combination of fields with the same mass dimension as the above combination. Therefore, we may understand the effect of the massive particle as introducing a new interaction of the form

$$\mathcal{L}_{\text{HQG}} = c_G \frac{1}{M^2} f^{ABC} g F_{\mu\nu}^A F^{B\mu}{}_\rho F^{C\nu\rho} \quad (1.114)$$

where c_G is a dimensionless coupling constant that controls the interaction of this new vertex⁷. Note also that this term has the correct dimensionality for the Lagrangian, since it has overall mass dimension 4. The interaction is however non-renormalisable, since the operator is dimension six. But this is not a problem, since we know that we are not describing a UV-complete theory; the non-renormalisability is a consequence of forgetting that in the UV there is an additional quark with renormalisable interactions.

If we do not know the value of the heavy quark mass, but we suspect that there is some additional degree of freedom, we could add a term like that of equation (1.114) and try to constraint it either by doing measurements or by comparing to a full theory once new physics are known. If we are only working with the low energy theory and we have no candidate for the mass, we could introduce into the renormalised Lagrangian a dimension 6 operator as

$$\delta\mathcal{L}_G = \rho_{RG}(\mu) \frac{1}{\mu^2} \mathcal{O}_G \quad \text{with} \quad \mathcal{O}_G \equiv g_R(\mu) \mu^\epsilon F_{R\mu\nu}^A F_R^{B\mu}{}_\rho F_R^{C\nu\rho} \quad (1.115)$$

where $\rho_{RG}(\mu)$ is some renormalised parameter with mass dimension 0, and we have used the scale μ to take care of the dimensions.

This new interaction term depends on the scale in two ways. On the one hand, there is the explicit dependence on μ , that takes care of the dimensionality. On the other hand, the introduction of the higher-dimension operator \mathcal{O}_G leads to new divergences associated to radiative corrections which must be absorbed into renormalisation constants. As an example, one of the diagrams contributing to this divergence is


 $\equiv Z_{1G} \quad (1.116)$

where the dot at the centre represents the new three gluon vertex. We can use this quantity to define the relation between the renormalised and bare versions of this operator

$$\mathcal{O}_{0G} = Z_{1G} \mathcal{O}_{RG}, \quad (1.117)$$

which implies that the operator has an anomalous dimension, which, in analogy with the rest of the parameters in the gauge theory we determine as

$$\gamma_{1G} \equiv \mu \partial_\mu \log Z_{1G} \quad (1.118)$$

⁶The leading order term, with no derivatives, contributes to the decoupling constant. A term with one single derivative coming from the propagator vanishes due to Dirac algebra.

⁷Note that we have included a power of the coupling constant in the vertex, which is in principle arbitrary. This is convenient, since it ensure that c_G remains dimensionless in dimensional regularisation

By computing all the radiative corrections of the type of those in the diagram above, at one loop order, this anomalous dimension is

$$\gamma_{1G} = \frac{g_R^2}{16\pi^2} (12N + 2b_0) , \quad (1.119)$$

where b_0 is the parameter appearing in the one-loop β -function Eq. (1.55). This anomalous dimension controls how the operator changes under renormalisation.

As we have done before with all other parameters in the Lagrangian, to make sure that the interaction Lagrangian is finite, we have to consider the coupling $\rho_{RG}(\mu)$ as connected with a bare (and divergent) coupling via a (divergent) parameter as

$$\frac{1}{\Lambda_0^2} = Z_G(\mu) \frac{\rho_{RG}(\mu)}{\mu^2} \quad (1.120)$$

where Λ_0 is a dimension 1 divergent coupling constant. Matching the two forms of renormalising the interaction Lagrangian, it is easy to see the relation between the different renormalisation constants.

$$Z_G(\mu) = \frac{Z_{1G}}{Z_g Z_A^{3/2}} \quad (1.121)$$

where the Z_g and Z_A factor arise from renormalising the fields that form the new operator. By taking logarithmic derivative, the anomalous dimension of dimensionless coupling $\rho_{RG}(\mu)$ is related to the rest of the anomalous dimension, which we have already determined as

$$\gamma_G = \gamma_{1G} - \gamma_g - \frac{3}{2}\gamma_A \quad (1.122)$$

This analysis does not fix the value of the coupling constant ρ_{RG} but only how it changes with scale. Provided we determine its value at some scale, we can then determine its value at some other scale by integrating the anomalous dimension

$$\rho_{RG}(\mu) = \rho_{RG}(\mu_0) \exp \left\{ - \int_{\mu_0}^{\mu} \frac{d\mu'}{\mu'} \gamma_G(g_R(\mu')) \right\} \quad (1.123)$$

The initial value $\rho_{RG}(\mu_0)$ must be determined from additional information. One possible way is to by performing measurements of three gluon interactions and observing deviations from the QCD result that can be put in this form. However, if we know the macroscopic theory we can determine this coefficient by an explicit calculation.

A concrete example is the case when we are considering the effects of a very massive quark. There, we can use the QCD to compute the three gluon vertex at external momenta that are small as compared to the heavy quark mass. We can then expand the three point function in powers of p/M with p any of the external momentum. In general, this correction will also depend on the renormalisation scale, and in order to avoid large logs, we can choose $\mu = M$. Doing so, we find that the leading correction possesses a term of the form

$$\delta\Gamma_{h\mu\nu\lambda}^{m,n,l}(p,p',M,\mu) = \frac{c_G(M)}{M^2} g(M) V_{\mu\nu\lambda}(p,p') \quad (1.124)$$

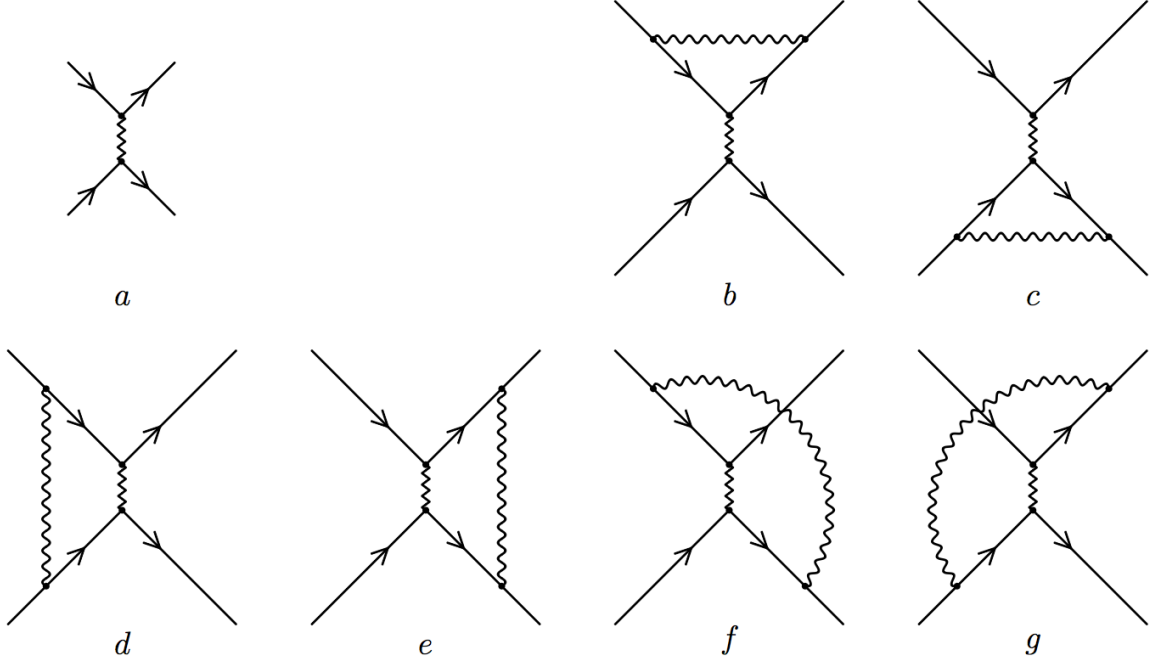


Figure 1.8: Radiative corrections to the four fermion operators O_i . Diagram a) is the tree level, while all other diagrams are radiative corrections. The zigzag line represents a point, and only indicates which fermions are connected by γ -matrices. Figure taken from 0908.4392.

where $V_{\mu\nu\lambda}(p, p')$ is combination of the external momentum that arises from the operator \mathcal{O}_G . At one loop order

$$c_G(M) = \frac{\alpha}{1440\pi} T_F \quad (1.125)$$

Therefore, we can make the effective low energy theory and QCD with a heavy quark match provided we identify

$$\rho_{RG}(M) = c_G(M) \quad (1.126)$$

which provides the initial value of the evolution equation. After this identification, QCD with a heavy quark and the effective theory described by $\delta\mathcal{L}_G$ are equivalent for all gluonic interactions as long as the momentum of the gluon is small as compared to the mass of the quark and to order $\mathcal{O}(1/M^2)$.

We may now want to extend this analysis to obtain an effective theory valid for all light degrees of freedom, not just gluons, but also light quarks. The ideology is the same. We know

that loop diagrams will generate new interactions between quarks that are not included in the QCD Lagrangian. In general, we will expect that these interactions will generate any possible additional effective vertex that is allowed by symmetries. Therefore, if we want to write the most general Lagrangian, we should identify all possible dimension-6 operators. In addition to \mathcal{O}_G , these are

$$\mathcal{O}_1 = g^2 \sum_{f,f'=1}^{nf} \bar{q}_f T^a \gamma^\mu q_f \bar{q}_{f'} T^a \gamma_\mu q_{f'} \quad \mathcal{O}_2 = g^2 \sum_{f,f'=1}^{nf} \bar{q}_f T^a \gamma_5 \gamma_\mu q_f \bar{q}_{f'} T^a \gamma_5 \gamma^\mu q_{f'} \quad (1.127)$$

$$\mathcal{O}_3 = g^2 \sum_{f,f'=1}^{nf} \bar{q}_f \gamma^\mu q_f \bar{q}_{f'} \gamma_\mu q_{f'} \quad \mathcal{O}_4 = g^2 \sum_{f,f'=1}^{nf} \bar{q}_f \gamma_5 \gamma^\mu q_f \bar{q}_{f'} \gamma_5 \gamma_\mu q_{f'} \quad (1.128)$$

And we can again write the leading correction to the Lagrangian as

$$\delta \mathcal{L}_{light} = \sum_i^4 \frac{\rho_i}{\mu^2} \mathcal{O}_i \quad (1.129)$$

As in the case before, radiative corrections to these operators are divergent when considering diagrams of the type of those displayed in figure (1.8). However, unlike the previous case, the divergences of each individual diagram do not cancel independently, but we need to consider all of them to be able to introduce renormalisation constants, which are now a matrix. These mixing comes from the insertion of the γ -matrices in the gauge vertex, which changes the spin structure of the operator. The relation between the bare and renormalised quantities are given by

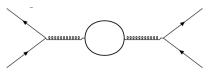
$$\mathcal{O}_{0i} = Z_{ij}(\mu) \mathcal{O}_{Rj} \quad (1.130)$$

Therefore, the anomalous dimension of the operator and of the coupling of this new operators in the Lagrangian are also matrices

$$\mu \partial_\mu \rho_i = -\gamma_{ij} \rho_j \quad (1.131)$$

The radiative corrections mix these operators.

As before, the fact that the operators develop non-trivial anomalous dimensions implies that the coupling constants ρ_i depend on the scale. We can deduce the evolution of each of these constants as before. This does not determine the value of those constants at any given scale, but only how to connect one scale to another. Once again, to be able to determine the value of the corrections additional data is needed. If we now focus on the case of QCD with one heavy flavour, the leading order diagram (in g_R) is



where the thick line in the loop represents the heavy quark.

Expanding those correlation functions in powers of the external momentum over the mass of the heavy quark, we can determine the leading corrections to the corresponding four fermion point function. Since these calculations depend on the ratio of μ/M it is convenient to choose

$\mu = M$ to avoid large logs. The explicit computation of these terms lead to initial values for the constants $\rho_i(M)$. Choosing those values the predictions of the effective theory agree with those of QCD plus a heavy quark to order $1/M^2$.

As you may notice, we have not written all possible dimension-6 operators we can think of. The reason is that not all of them are independent. Possible choices like

$$D^\mu F_\lambda^A \mu D^\nu F^{A\lambda\nu} \quad (1.132)$$

can be related to the previously discussed operators by using the classical equations of motion. Therefore, these operators do not introduce new vertex.

With this steps we have summarised the ideology for constructing an effective field theory for unknown physics at short distances. We can parametrise the corrections of the short distance physics on the known low energy physics by including higher and higher dimension operators, which come associated with higher and higher momentum corrections induced by the new physics. The strategy is then to classify all possible independent operators at a given dimensionality and associate couplings to those terms. By doing a matching calculation as we have described, we can give values to the parameters of the low energy theory so that they agree at a given order in a $1/M$ expansion.

Finally, following this ideology, we may wonder why we have started with dimension-6 operators and not with dimension-5. For QCD the answer is simple, we simply cannot find a gauge invariant dimension-5 operator that we could use. In QED, with a heavy fermion, however, such operator exists

$$\mathcal{O}_5 = \bar{\psi} F^{\mu\nu} \sigma_{\mu\nu} \psi \quad (1.133)$$

However, this operator flips the helicity of electrons, which cannot happen in the limit of massless electrons. Therefore, any such contribution in the Lagrangian must be multiplied by the electron mass.

Chapter 2

The limits of perturbation theory

2.1 Infrared divergences. Inclusive and Exclusive processes

In the previous chapter we have focussed on understanding small distance phenomena in QCD. We have seen that at very high energy a number of divergences appeared, that we have managed to regularise and subtract to make QCD a sensible theory of nature for any scale we can probe. In this chapter we will discuss a new set of divergences which, although they affect other gauge theories such as QED, are of special relevance for QCD. These are called infrared and collinear divergences.

To make our discussion more concrete, let us concentrate on one particular observable: the annihilation cross section we discussed in Section 1.9. To compute the next-to-leading order correction to the annihilation cross section we must first identify the relevant QCD diagrams that we need to compute. Following what we have learned in the previous section, we only need to consider the cross section with additional coupling insertions. At the level of the amplitude, there are two graphs we must consider to determine the next-to-leading order *amplitude*. Expanding the amplitude as

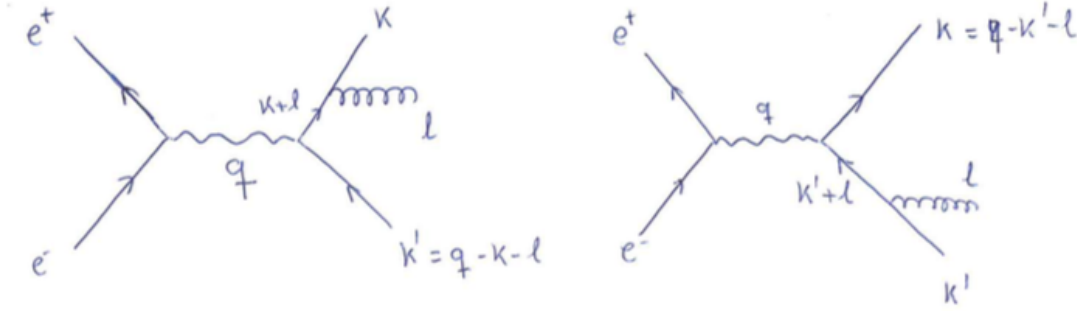
$$\mathcal{M} = \mathcal{M}^{(0)} + \mathcal{M}^{(1)} + \mathcal{M}^{(2)} + \dots \quad (2.1)$$

with the index indicating the order of the g expansion, the diagrams contributing $\mathcal{M}^{(1)}$ are shown in figure (2.1).

These correspond to the contribution of real emissions of final state gluons to the final cross section. Using the QCD Feynman rules these diagrams are given by

$$\begin{aligned} \mathcal{M}^{(1)} = & \bar{u}(k) (igt^a) \not{\epsilon}(l) \frac{i}{\not{k} + \not{l}} (-ie) \not{\epsilon}(q) (i) v(k') + \\ & + \bar{u}(k) (-ie) \not{\epsilon}(q) (i) \frac{i}{-\not{k}' - \not{l}} (igt^a) \not{\epsilon}(l) v(k'), \end{aligned} \quad (2.2)$$

where $\epsilon(l)$ and $\epsilon(q)$ are the polarisation of the gluon and the virtual photon respectively.

Figure 2.1: Diagrams contributing to $\mathcal{M}^{(1)}$.

This amplitude reveals something worrisome. In the massless limit, which as we have seen is the relevant limit for high-energy processes, the amplitude has divergent denominators

$$\frac{1}{\not{k} + \not{l}} = \frac{\not{k} + \not{l}}{2k \cdot l} = \frac{\not{k} + \not{l}}{2k^0 l^0 (1 - \cos \theta)}, \quad (2.3)$$

with θ the angle between the quark and the gluon, which show apparent divergences when the external gluon is soft $l^0 \ll 1$ or when the gluon is collinear with the quark $\theta \sim 0$. Analogous divergences appear for the second diagram. To evaluate whether these indeed lead to a divergence in the cross section, let us focus on the infrared dynamics and perform and *infrared approximation*. This amounts to neglecting the emitted gluon momentum in numerators, while keeping it in denominators, since, as we have seen, in the quark propagator this leads to non trivial divergences. In this limit the amplitude can be simplified significantly by using the following identities:

$$\not{k}' v(k') = 0, \quad \bar{u}(k) \not{k} = 0, \quad (2.4)$$

$$\not{k}' \gamma_\nu v(k') = 2k'_\nu v(k'), \quad \bar{u}(k) \gamma_\nu \not{k}' = 2\bar{u}(k) k_\nu \quad (2.5)$$

where we have use Dirac's equation in the first line and in the second line the anti-commutation relations of γ_ν .

With this approximations the next-to-leading order amplitude is

$$\mathcal{M}^{(1)} \approx \bar{u}(k)(-ie)\not{\epsilon}(q)v(k)(ig)\left(\frac{k \cdot \epsilon(l)}{k \cdot l} - \frac{k' \cdot \epsilon(l)}{k' \cdot l}\right)t^a \quad (2.6)$$

$$\approx \mathcal{M}^{(0)}g\left(\frac{k \cdot \epsilon(l)}{k \cdot l} - \frac{k' \cdot \epsilon(l)}{k' \cdot l}\right)t^a, \quad (2.7)$$

where in the second line we have factored out the leading order matrix element. Because of this factorisation, in the infrared approximation the effect of gluon emission can be viewed as a multiplicative factor of the overall cross section. Note also that, as expected, this amplitude is transverse, since it vanish after replacing $\epsilon(l) \rightarrow l$. Taking the square of the matrix element, summing over gluon polarisation and multiplying by the gluon phase space and corresponding

flux factors, the contribution of this matrix element to the cross section is given by

$$\sigma_1^R = \sigma_0 C_F g^2 \int \frac{d^3 l}{(2\pi)^3} \frac{1}{2l^0} \frac{2k \cdot k'}{(k \cdot l)(k' \cdot l)} \quad (2.8)$$

where we have used that $\text{tr} \{t^a t^b\} = C_F N$ and N is absorbed into the leading order cross section, and that the sum over polarisation $\sum \epsilon_\mu \epsilon_\nu^* \sim -g_{\mu\nu}$ for transverse structures.

The integral in Eq. (2.8) is divergent in several ways

1. UV divergence: as l becomes large, the integral is divergent as

$$\frac{d^3 l}{l^3} \sim \log \quad (2.9)$$

However, this is nothing to worry about, since we have performed an approximation which is valid only for soft momentum. Possible UV divergences of the true integral should have been dealt by the renormalisation procedure.

2. Infrared (IR) divergence: when the gluon momentum is soft l , the integral is also of the form above and also diverges logarithmically in the infrared. This is a problem, since this is a divergence in the region the field theory is not altered by renormalisation.
3. Collinear divergence: the polar angle integration θ , with θ the angle between the gluon and the quark-antiquark axis in the centre of mass frame is

$$\int \frac{dx}{1-x^2} = \frac{1}{2} \log \frac{1+x}{1-x} \quad (2.10)$$

with $x = \cos \theta$, which is also divergent whenever $\theta = 0, \pi$, *i. e.* whenever the emitted gluons are collinear with the quark or the antiquark. This is also a physical divergence, emerging in for Minkowski signature, and cannot, therefore, be removed via renormalisation.

This seems frustrating. As soon as we study our first radiative correction we find an uncontrolled divergence which apparently cannot be removed. Furthermore, this appears for a very simple observable, in which no kinematic cuts are applied and certainly something that can be measured and should be finite. Luckily, under close examination we can conclude that we have not computed all the contribution to the next-to-leading order *cross section*. In fact, terms there are contributions from the next-to-next-to leading order amplitude which also contribute to the next to leading order cross section. Indeed, squaring the matrix element

$$\mathcal{M}\mathcal{M}^\dagger = \mathcal{M}^{(0)}\mathcal{M}^{(0)\dagger} + \mathcal{M}^{(1)}\mathcal{M}^{(1)\dagger} + \mathcal{M}^{(2)}\mathcal{M}^{(0)\dagger} + \mathcal{M}^{(0)}\mathcal{M}^{(2)\dagger} \quad (2.11)$$

Therefore, there are contributions to the next-to-leading order cross section which depend on $\mathcal{M}^{(2)}$, those in which there are no gluons in the final state. These are the virtual correction shown in figure (2.2) To evaluate those we need to compute those loop corrections,

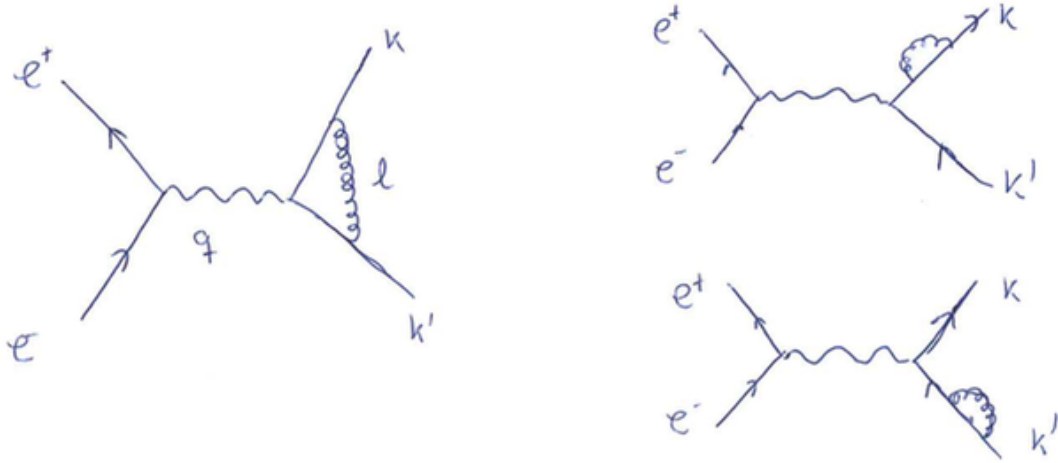


Figure 2.2: Virtual corrections

which demand regularisation. The self energy corrections displayed in the right hand side of figure (2.2) vanish using dimensional regularisation in $\overline{\text{MS}}$ -type schemes, since for these scale-less divergent integrals vanish after regularisation. The vertex correction gives a finite contribution. Clearly, this diagram leads to similar IR&Coll divergences, since the quark and anti-quark propagators in the loop lead to terms of the type

$$\frac{1}{k \cdot l \, k' \cdot l} \quad (2.12)$$

which are also divergent.

Evaluating the vertex correction in IR -approximation one obtains

$$\sigma_1^V = -\sigma_0 C_F \frac{g^2}{2\pi^2} \int \frac{dl}{l} \frac{dx}{1-x^2}, \quad (2.13)$$

which cancels the real contribution identically. Therefore the virtual correction in this observable cancel both the infrared and collinear divergences of the total cross section and the result is finite. Within the infrared approximation the next-to-leading order correction vanishes identically; however this is an artefact of the approximation, which is only valid to capture the IR&Coll divergent contribution. The full calculation yields

$$R = R_0 \left(1 + \frac{\alpha_s}{\pi} \right). \quad (2.14)$$

The cancellation of divergences we have described is not specific of this fully inclusive observable. This is one example of the Kinoshita-Lee-Nauenberg theorem which states that for suitably define inclusive cross section, infrared and collinear divergences cancel.

The cancellation above is essential to make sense of this correction. Only because the observable we have considered is inclusive, we must include both real and virtual contributions,

and this new type of divergences cancel. However, if we would have liked to determine the cross section of the fully exclusive quark-antiquark-gluon final state, the cross section would be divergent, since it would be only given by σ_R and no virtual correction are present. For this reason, only measurements which are not fully exclusive are under good theoretical control in perturbative QCD. In the next section we will describe other less inclusive measurements that can be performed in e^+e^- and that can be reliably computed.

2.1.1 Jets in e^+e^-

The total annihilation cross section we analysed in the preceding section is an interesting observable, but it provides limited information about the microscopic behaviour of how hadrons are produced in e^+e^- . To gain more insights, we would like to have access to other observables in which energy or angular distributions can be determined and contrasted with experiments. In this way we have more sensitive tools both to test QCD and to search for physics beyond the standard model. Experimentally, we can define as many observables as our imagination can produce. However, although all those observables provide information about the microscopic processes, not all of them can be reliably calculable in perturbative QCD. Therefore, it is important to think about which type of observables make sense in a perturbative analysis.

An obvious first candidate of a new "observable" is the emission rate of a single gluon. This provides information on how gluons are coupled to quarks. However, this is not a good observable. We have already analysed the diagrams that control this emission, figure (2.1) and seen that this rate possesses both IR&Coll divergences. We may interpret the collinear divergence in physical terms: while the emission of a gluon from the quark is in principle suppressed by an additional power of α , this emission rate is enhanced by a $\log \theta$ term, which make the radiation of almost collinear gluons non-suppressed. This means that in high-energy processes we expect that most of the energetic particles in hard annihilations will be produced in collimated sprays, since there are not suppressions for these collinear processes. These sprays are called jets and they are indeed observed in e^+e^- annihilations. Similarly, the emission of soft particles at any angle is not suppressed either, since the soft divergence can compensate for the smallness of α_s and lead to soft radiation between the jets, or inter-jet radiation. An sketch of this structure is shown in figure (2.3).

The above discussion of a jet is simply descriptive. To be able to determine the production rate of those sprays of particles it is necessary to provide a precise definition of what we mean with a jet. This definition is not unique and, in fact, not all possible definitions can be reliably computed in QCD. In this lecture we will describe Serman-Weinberg jets, which depend on two parameters, ϵ and δ . In an e^+e^- collision an event contributes to the 2-jet cross section if we can find 2 cones of opening angle δ such that the fraction of the total energy of the event contained in those cones is greater than $1 - \epsilon$. These parameters are displayed in figure (2.3). Note that this definition is well suited for e^+e^- collisions where the total energy in the event is known, but not so much for hadronic collisions.

We will now compute the two jet cross section, integrating over all possible jet axis. At

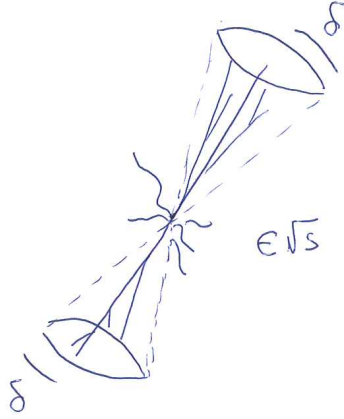


Figure 2.3: Sketch of a typical jet event. The parameters of the Serman-Weinberg jet definition are also shown.

leading order, all the energy of the event goes into two quarks and, therefore, into two jets of (arbitrarily small) opening angle. As a consequence,

$$\sigma_0^{2\text{jets}} = \sigma_0, \quad (2.15)$$

the total annihilation cross section at this order.

At next to leading order, the emission of gluons can take energy out of a given cone, and the cross section at this order differs from the total cross section. There are three distinct processes that contribute to the jet cross section:

- Emission of *hard* gluons with energy greater than ϵE emitted at angle $\theta < \delta$ from either the quark or the antiquark. We will call this contribution σ_1^H , which in the infra-red approximation is given by

$$\sigma_1^H = C_F \frac{g^2}{2\pi^2} \sigma_0 \int_{\epsilon E}^E \frac{dl_0}{l_0} \left[\int_0^\delta \frac{d\theta \sin \theta}{1 - \cos^2 \theta} + \int_{\pi-\delta}^\pi \frac{d\theta \sin \theta}{1 - \cos^2 \theta} \right]. \quad (2.16)$$

- Emission of *soft* gluons with energy $\delta E < \epsilon E$ at any angle with respect to the quark. Since these gluons are below the energy cut, they do not alter the jet cross section. We call this contribution σ_1^S . In the infrared approximation this is given by

$$\sigma_1^S = C_F \frac{g^2}{2\pi^2} \sigma_0 \int_0^{\epsilon E} \frac{dl_0}{l_0} \int_0^\pi \frac{d\theta \sin \theta}{1 - \cos^2 \theta}. \quad (2.17)$$

- Virtual corrections. Since at this order virtual corrections do not have real gluon emission, all the virtual correction computed in the last chapter contributes to the jet cross section. In the infrared approximation

$$\sigma_1^V = -C_F \frac{g^2}{2\pi^2} \sigma_0 \int_0^{\epsilon E} \frac{dl_0}{l_0} \int_0^\pi \frac{d\theta \sin \theta}{1 - \cos^2 \theta}. \quad (2.18)$$

Putting all these terms together, the two jet cross section is given by

$$= \sigma_1^H + \sigma_1^S + \sigma_1^V \quad (2.19)$$

$$= -\sigma_0 \left(\frac{g^2}{2\pi^2} C_F \int_\epsilon^E \frac{dl_0}{l_0} \int_\delta^{\pi-\delta} \frac{d\theta \sin \theta}{1 - \cos^2 \theta} \right). \quad (2.20)$$

As expected, the virtual corrections lead to the cancellation of the IR&Coll divergences. However, these leave an imprint into the cross section, which depends logarithmically on the jet definition parameters. In the $\delta \ll 1$ limit we obtain

$$\sigma^{2\text{jets}} = \sigma_0 \left(1 - \frac{g^2}{\pi^2} C_F \log \epsilon \log \delta \right). \quad (2.21)$$

The two jet cross section decreases both as ϵ and δ decrease. The second effect is easy to understand, since requiring the angle of emission to be smaller and smaller reduces also the phase space for emissions. What is less intuitive is that the reduction of the energy cut also reduces the cross section, which means that demanding the observation of events with less and less soft radiation is rarer and rarer.

The inspection of Eq. (2.21) also shows that the accuracy of the perturbative computation also depends on the parameters used for the jet definition. For either small ϵ or δ , the combination $\alpha \log \epsilon \log \delta$ can be of order one, which means that this leading order calculation is inaccurate and resummations of terms like those must be performed.

Finally from this computation, we can also easily determine the three jet cross section. Since at next to leading order the total cross section must be either formed by two or three final particle events, we must have

$$\sigma^{\text{tot}} = \sigma^{2\text{jets}} + \sigma^{3\text{jets}}, \quad (2.22)$$

we conclude

$$\sigma^{3\text{jets}} = \sigma_0 \frac{g^2}{\pi^2} C_F \log \epsilon \log \delta \quad (2.23)$$

2.1.1.1 IR&Coll divergences in dimensional regularisation

While the analysis above gives the correct answer, there are a number of technical steps that we could have treated with more care. In particular, there are a number of divergent integrals that we have manipulated and it would be desirable to have a more systematic way to regularise and manipulate IR&Coll divergent contributions. Luckily, as for the analysis of UV divergences, dimensional regularisation is well suited for this task.

As we have seen, when regularising one-loop UV-divergent integrals terms proportional to $\Gamma(\epsilon)$ appear. These terms indicate that the integral is convergent for any dimension smaller than 4 (in particular for any dimension close to 4 from below). Because the integral becomes convergent in smaller number dimensions, the integral is UV-divergent. Unlike UV divergent integrals, infrared divergent integrals become convergent when the number of dimensions increase, $n > 4$, since then the powers of momentum in the numerator of the integral dominate

over the powers of momentum in the denominator. Therefore, when regularising IR-divergent integrals terms proportional to $\Gamma(-\epsilon)$ appear, which indicate that the integral is finite for $n > 4$.

As a concrete example, let us analyse one of the integrals that appears in the infrared limit of the virtual correction term in the e^+e^- annihilation cross section. This is given by

$$I_{\text{IR}}(Q^2, m) = g_{\text{R}}^2 \mu^{2\epsilon} \frac{Q^2}{2} \int \frac{d^n k}{(2\pi)^n} \frac{-i}{k^2 + i\epsilon} \frac{1}{2p_1 \cdot k + k^2 + i\epsilon} \frac{1}{-2p_2 \cdot k + k^2 + i\epsilon} \quad (2.24)$$

where p_1 and p_2 are the four-momenta of the outgoing quarks, which for this analysis we will take as massive with $p_1^2 = p_2^2 = m^2$ and $Q = (p_1 + p_2)^2$. This integral also appears in the QED virtual corrections of decays of a heavy bosons into leptons. At large k this integral is convergent. However, as k becomes softer and softer, we expect the integral to be divergent in the IR for any $\epsilon \geq 0$. As already stated and unlike UV divergences, the integral becomes convergent for $n > 4$ ($\epsilon < 0$).

The loop momentum integral can be easily performed. After introducing Feynman parameters, rotating to Euclidean space and using the identity (1.8), the integral becomes

$$I_{\text{IR}}(Q^2, m) = \frac{\alpha}{4\pi} (4\pi\mu^2)^\epsilon \Gamma(1 + \epsilon) \int_0^1 dx \int_0^{1-x} dx' \frac{Q^2}{(-xx'Q^2 + (x + x')^2 m^2 - i\epsilon)^{1+\epsilon}} \quad (2.25)$$

Since this is nothing else than some rewriting of equation (2.24), this integral is also divergent. In this form, the divergence arises from the poles of the denominator. In general those poles do not lead to a divergence in the integral, as long as the contour of integration in complex plane can be chosen to avoid the pole. However, the integrand possesses a pole at $x = x' = 0$, which coincides with the edge of the integration region and, therefore it makes the integral divergent for $\epsilon \geq 0$.

To isolate the IR divergence, we can fix the sum $x + x'$ to be a number $x + x' = w$ and integrate over all possible values of w by introducing unity into the integral in the form of

$$1 = \int_0^1 dw \delta(w - x - x') \quad (2.26)$$

where the limits of integration are consistent with the region of integration in x' , which ensures that the sum $x + x' \leq 1$. After integrating over x' and introducing the variable $u = x/w$, we can write

$$I_{\text{IR}}(Q^2, m) = \frac{\alpha}{4\pi} (4\pi\mu^2/Q^2)^\epsilon \Gamma(1 + \epsilon) \int_0^1 dw \frac{1}{w^{1+2\epsilon}} \int_0^1 du \frac{1}{(-u(1-u) + \frac{m^2}{Q^2} - i\epsilon)^{1+\epsilon}} \quad (2.27)$$

The u integral is now convergent in the limit $\epsilon \rightarrow 0$, since the pole of the integrand does not coincide with the limits of integration for general Q/m . As expected, the divergence is moved to the w integral; however, this integral possesses a representation in terms of gamma function

$$\int_0^1 dw \frac{1}{w^{1+2\epsilon}} = \frac{\Gamma(-2\epsilon)}{\Gamma(1 - 2\epsilon)} = \frac{1}{-2\epsilon} \quad (2.28)$$

This expression in terms of $\Gamma(-2\epsilon)$ makes explicit the observation that the integral is only well defined for $\epsilon < 0$, which is again a consequence of the fact that we are dealing with an IR divergent. To remind ourselves of this fact, when expressing this integral in terms of poles in ϵ it is useful to keep the minus sing in the denominator, to remind us ourselves that we are regularising an IR divergence.

Performing the u integration we obtain

$$I_{\text{IR}}(Q^2, m) = \frac{\alpha}{2\pi} \frac{1}{-\epsilon} \left(\frac{4\pi\mu^2}{Q^2} \right)^\epsilon \times \left\{ \left[\frac{1 - 2m^2/Q^2}{\beta} \right] \log \frac{\beta + 1}{\beta - 1} - 1 \right\} + \mathcal{O}(\epsilon^0) \quad (2.29)$$

with $\beta = \sqrt{1 - 4m^2/Q^2}$. This parameter shows that the cross section exhibits a threshold behaviour when $Q^2 > 4m^2$, which is the limit for the formation of a $q\bar{q}$ pair. As stressed above, this integral is only well defined for $\epsilon < 0$, which reflects its IR origin.

The above exercise has shown us how dimensional regularisation also defines IR divergent quantities. However, since we are keeping a non-zero mass, the integral is not collinear divergent. The mass of the quarks has, in fact, regularised the collinear divergence, since it is impossible to split a time-like momentum into the sum of another time-like momentum with the same mass and a light-like momentum. In other words, if the momentum of the fermion is time-like, $p \cdot k$ never vanishes. The non-zero mass calculation is nevertheless important, since in QED similar IR divergences appear in the interactions of photons with fermions. As we have argued, for inclusive observables, the real contributions to the cross section posses an identical divergence with opposite sign that makes the cross section finite.

In QCD it is important to understand the massless limit, not only because of the high-scale behaviour of the fermion masses, but also because gluons are massless and we can have loops of massless gluons, which also lead to collinear divergent integrals. As expected, the expression above diverges in the massless limit and additional care must be taken when $m = 0$. In addition to the IR-divergence in the w -integration, when $m = 0$ also the u -integral becomes divergent. But this divergence can also be treated in dimensional regularisation. Indeed

$$\int_0^1 du \frac{1}{(-u(1-u))^{1+\epsilon}} = (-1)^{1-\epsilon} \frac{\Gamma(-\epsilon)^2}{\Gamma(-2\epsilon)} \approx -\frac{2}{-\epsilon} + \mathcal{O}(\epsilon) \quad (2.30)$$

This additional power of inverse ϵ implies that in the massless limit the divergence of the integral I_{IR} is stronger than in the $m \neq 0$ case, since, taking into account the w -integral, it now diverges as $1/\epsilon^2$. This is the manifestation of the collinear divergence.

From the arguments of the previous subsection, we know that this additional divergence must be cancelled by the the real contribution. The origin of this second ϵ -pole in the real contribution is indeed the collinear divergence. This arises as a result of the the integration of the angular part of the phase space of the gluon. In particular, denominators of the form $p \cdot k$ lead to integrals of the type

$$\int_{-1}^1 \frac{d(\cos \theta)}{1 - \cos(\theta)} \quad (2.31)$$

which is divergent in the upper limit. Nevertheless, this integral is only divergent for $n \leq 4$ dimension. For $n > 4$ the integral is regularised because the volume element of a higher dimensional sphere possesses a stronger dependence on the polar angle, θ . Since the divergences are cured in larger number of dimension, these collinear divergences are more similar to IR divergences than to UV divergences.

In general, the volume element of a d -sphere may be related to the volume element the $d - 1$ -sphere obtained by fixing one of the angular variables as

$$\int d\Omega_d = \int_0^\pi d\theta \sin^{d-1}(\theta) \int d\Omega_{n-2} \quad (2.32)$$

Because of symmetry in the azimuthal plane, we can always identify this angle with the angle between the external momentum and the loop momentum. So, we can always choose the angles in n -dimensions such that $p \cdot k = E_p \omega (1 - \cos \theta)$. When we now consider real emission processes, we must integrate over the gluon on-shell momentum. The phase space for this integration in n -dimensions is

$$\int \frac{d^{n-1}k}{2\omega} \quad (2.33)$$

where the ω -denominator reflects the on shell condition $\omega^2 = \sum_i^{n-1} k_i^2$. This phase space includes an integration over a $n - 2$ sphere, instead of the $n - 1$ sphere that appears in the Wick rotated quantities. Therefore, in n -dimensions, the final phase-space factors imply

$$\int d\Omega_{n-2} \frac{1}{1 - \cos \theta} = \Omega_{n-3} \int_{-1}^1 dx \frac{(1 - x^2)^{-\epsilon}}{1 - x} = \Omega_{n-3} \frac{\sqrt{\pi} \Gamma(-\epsilon)}{\Gamma(1 - \epsilon)} \quad (2.34)$$

which leads to a pole in the $1/\epsilon$ expansion for negative ϵ . This divergence in the angular integration, which only occurs in the $m = 0$ limit cancels the virtual contribution to the cross section, provided we consider sufficiently inclusive observables.

2.1.1.2 Infrared and Collinear Safety

One of the consequences of the analysis of IR&Coll divergences we have performed in the previous sections is that not all observables that one can think of can be reliably computed in perturbative QCD. Good observables are those that, like the total cross section or the two jet cross section, include virtual correction that cancel infra-red and collinear divergences. Otherwise the observable is sensitive to small non-perturbative scales in the processes, which go beyond perturbation theory. This does not mean that those observable cannot be measured; it simply means that it is not possible to obtain reliable predictions from perturbative QCD.

A set of observables that can be computed in perturbative QCD are what is known as infrared and collinear safe observables. An observable depending of the momenta of n particles $\{k_1, k_2, \dots, k_n\}$ is infrared and collinear safe if for any pair of particles $\{i, j\}$

$$\mathcal{O}\{k_1, \dots, k_i, k_j, \dots, k_n\} \rightarrow \mathcal{O}\{k_1, \dots, k_i + k_j, \dots, k_n\}, \quad (2.35)$$

whenever either k_i or k_j become soft or the pair becomes collinear with one another. The first condition ensures that the observable is insensitive to soft emissions. The second one ensures that collinear splittings do not change the observable. These observables are, in fact, well defined to all orders in perturbation theory.

As a final remark, let us mention that the Stermann-Weinberg definition of jets we have analysed in the previous section is not, in fact, infra-red and collinear safe, since if the combination of a pair of hard gluons can take the resulting product outside of the angular region δ . In fact, at order α^2 these processes lead to a non cancellation of IR&Coll. divergences in that case.

2.1.1.3 The anti- k_t jet reconstruction algorithm

To conclude our discussion about jets and for completeness, let us describe here a jet reconstruction algorithm that is both IR&Coll safe. Although this is not unique, this has become the standard choice for jet analysis at the LHC. This is a sequential algorithm known as the jet reconstruction algorithm.

What the algorithm does is to group all particles in a QCD event into jets. To do so, we must define some distance between the particles observed in one given event. Since all particles are measured by detectors surrounding the collisions point, this is an angular distance between the direction of motion of the particles. This is analogous to the angular cut in the Stermann-Weinberg definition of jets. The distance also takes into account the momentum of the particles and it depends on a single jet parameter, the jet reconstruction radius R , which is analogous to δ for SW-jets.

The distance is formulated in terms of the standard variables for collider physics. Specially in hadronic collisions, the beam axis of the collision is special, and it is standard to treat differently the momenta of particles transverse to the beam and the momenta along the beam direction. A common parametrisation of the momentum of particles in this set up is

$$p = (m_T \cosh y, p_T \cos \phi, p_T \sin \phi, m_T \sinh y) \quad (2.36)$$

where we have introduced

- $p_T = \sqrt{p_x^2 + p_y^2} \equiv$ transverse momentum
- $\phi \equiv$ azimuthal angle, *i. e.* the angle of the particle in the plane transverse to the beam.
- $y = \frac{1}{2} \log \frac{E+p_z}{E-p_z} \equiv$ rapidity.
- $m_T = \sqrt{m^2 + p_T^2} \equiv$ transverse mass.

The variables p_T , m_T , and ϕ are invariant under boosts (along the beam axis). The variable y is not invariant under boosts, but it is additive. This means that, for example, the rapidity

in the lab frame y , is related to the rapidity in the c.o.m frame \hat{y} via the rapidity of the c.o.m. y^* as

$$y = y^* + \hat{y}. \quad (2.37)$$

Both the variables ϕ and y are angular variables, in the sense that they parametrise the solid angle around the collision point.

The steps that the anti- k_T algorithm follow are the following

Step 1. List of particles on a given event.

Step 2. For every pair of particles compute the inter-particle distance given by

$$d_{i,j} = \min \left(\frac{1}{p_{Ti}^2}, \frac{1}{p_{Tj}^2} \right) \frac{(\phi_i - \phi_j)^2 + (y_i - y_j)^2}{R^2} \quad (2.38)$$

and for every particle, compute the distance to the beam axis as

$$d_{i,B} = \frac{1}{p_{Ti}^2} \quad (2.39)$$

Step 3 Determine the minimum all the previous distances. If the minimum distance is $d_{i,j}$, between particle i and particle j , substitute this pair by a new particle that recombines those two by summing their four-momenta. If the minimum distance is $d_{i,B}$ for some particle i , we call that particle a jet and we remove it from the list.

Step 4 With the remaining particles after step 3, repeat the procedure until no particles are left, or, in other words, all particles are clustered into jets.

The result of this procedure is a number of jets which are indeed IR&Coll safe. Because the way it is constructed, the algorithm starts from the particles with the largest transverse momentum clustering those particles that are nearby to it, within an angular distance R . After those particles are clustered, the algorithm moves to the next hard particle left, and so on until the procedure is concluded.

2.1.2 Deep Inelastic Scattering

Having analysed QCD processes with no hadrons in the initial state, we now move to the next step in complexity and study high-energy lepton-hadron interactions. In particular, we focus on the inelastic scattering of an electron off a hadron such that the hadron is totally destroyed. The process is inclusive in the sense that we will characterise the cross section in terms of variables of the incoming e and p and on the scattered e only, without specifying the rest of the products of the scattering. This is a historically important process, since it led to the development of the parton model and the discovery of quarks.

The diagrams representing this process to leading order in the electromagnetic coupling α_{em} is shown in figure (2.4).

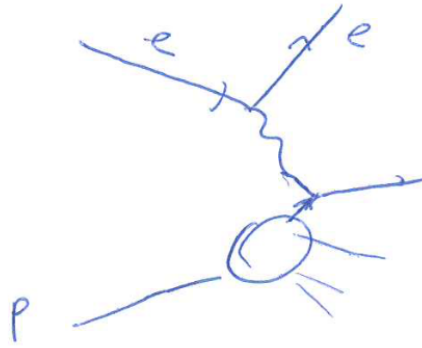


Figure 2.4: Sketch of the DIS process.

The cross section depends on the following invariant variables

$$Q^2 \equiv -q^2 = -(k' - k)^2, \quad x_{\text{Bj}} = \frac{Q^2}{2pq}, \quad (2.40)$$

$$y = \frac{qp}{kp}, \quad \nu = pq. \quad (2.41)$$

In the rest frame of the proton, the last two invariants admit a simple interpretation

$$\nu = M_p (E' - E) \quad \text{Energy lost by the electron,} \quad (2.42)$$

$$y = 1 - \frac{E'}{E} \quad \text{fraction of energy lost by the electron.} \quad (2.43)$$

In full generality, we can separate the QED and hadronic part of the process. To all orders in α_s , we may write the amplitude of the process as

$$\mathcal{M} = e \bar{u}(k') \gamma^\alpha u(k) \frac{1}{q^2} \langle X | j_\alpha(0) | p \rangle, \quad (2.44)$$

where $j_\alpha(0)$ is the electromagnetic current on the strong fields evaluated at the origin of space

$$j_\alpha(x) = \sum_f e Q_f \bar{q}(x) \gamma_\alpha q(x), \quad (2.45)$$

and the state $|X\rangle$ is a generic hadronic state as a result of the scattering and $|p\rangle$ is the incoming proton state. After squaring this matrix element

$$\frac{d\sigma}{dQ^2 dx_{\text{Bj}}} \propto L_{\alpha\beta} W^{\alpha\beta}, \quad (2.46)$$

where we have separated the contributions of the cross section into a leptonic contribution, given by the leptonic tensor

$$L_{\alpha\beta} \equiv e^2 \text{Tr} [\not{k} \gamma_\alpha \not{k}' \gamma_\beta], \quad (2.47)$$

which can be expressed in terms of products of k and k' , and a hadronic tensor

$$W_{\alpha\beta} = \frac{1}{4\pi} \sum_X \langle p | j_\alpha^\dagger(0) | X \rangle \langle X | j_\alpha^\dagger(0) | p \rangle (2\pi)^4 \delta(q + p - p_X), \quad (2.48)$$

where p_X is the total four-momentum of the state X and we have also summed over all possible final hadronic states. This expression may be further simplified using the fact that X is a full set of states. It is easy to see that

$$(2\pi)^4 \delta(q + p - p_X) = \int dz e^{i(q+p-p_X)z}. \quad (2.49)$$

Similarly, using the momentum operator \hat{P}

$$\langle p | j_\alpha^\dagger(0) | X \rangle e^{i(p-p_X)z} = \langle p | e^{i\hat{P}z} j_\alpha^\dagger(0) e^{-i\hat{P}z} | X \rangle = \langle p | j_\alpha^\dagger(z) | X \rangle. \quad (2.50)$$

Putting these relations together, we have

$$W_{\alpha\beta} = \frac{1}{4\pi} \int dz e^{iqz} \langle p | j_\alpha^\dagger(z) j_\beta(0) | p \rangle, \quad (2.51)$$

i. e., we have expressed the hadronic tensor as a correlator of electromagnetic currents evaluated on the proton. This expression is valid to *all orders* in the strong coupling constant and is sensitive both to perturbative and non-perturbative physics. The number of free functions in the hadronic tensor can be significantly reduced by using the conservation of the electromagnetic current

$$\partial_\mu j^\mu(x) = 0, \quad (2.52)$$

which implies that the hadronic tensor is transverse $q^\alpha W_{\alpha\beta} = q^\beta W_{\alpha\beta} = 0$. We can therefore constraint its tensorial structure to be

$$\begin{aligned} W_{\alpha\beta}(p, q) &= \left(g_{\alpha\beta} - \frac{q_\alpha q_\beta}{q^2} \right) F_1(x_{\text{Bj}}, Q^2) \\ &+ \left(p_\alpha + \frac{1}{2x} q_\alpha \right) \left(p_\beta + \frac{1}{2x} q_\beta \right) \frac{1}{\nu} F_2(x_{\text{Bj}}, Q^2). \end{aligned} \quad (2.53)$$

Neglecting the mass of the hadron, at high energies the cross section reduces to

$$\frac{d^2\sigma}{dx dQ^2} = \frac{4\pi\alpha_{em}^2}{Q^4} \left[(1 + (1-y)^2) F_1(x_{\text{Bj}}, Q^2) + \frac{1-y}{x} (F_1(x_{\text{Bj}}, Q^2) - 2x_{\text{Bj}} F_2(x_{\text{Bj}}, Q^2)) \right] \quad (2.54)$$

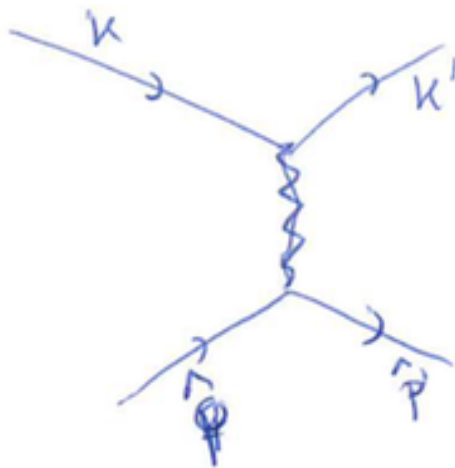


Figure 2.5: Lowest order diagram for electro-quark scattering

This expression is general and it makes no assumptions on the structure of the proton. It parametrises the scattering cross section in terms of two functions, F_1 and F_2 that are properties of the scattered hadron. In the next section we will evaluate these function in a particular model for the proton.

2.1.2.1 The parton model

In the parton model, the proton is seen, at least at high-energies, as a collection of almost free partons, quarks and gluons, which carry a given fraction of the proton momentum $\hat{p} = \zeta p$. In this model, the DIS cross section at leading order is controlled by the scattering of the electron off a quark within the proton. For this microscopic process, the leading order cross section is easy to compute.

The matrix element of the $e - q$ scattering at leading order is shown in figure (2.5). The amplitude is given by

$$\mathcal{M}^{(0)} = \frac{e^2 Q_f}{q^2} \bar{u}(\hat{p}') \gamma^\mu u(\hat{p}) \bar{u}(k') \gamma_\mu u(k) \quad (2.55)$$

After averaging over initial states and summing over final states, the square matrix element is given by

$$\frac{1}{2} \sum_{\text{pol}} |\mathcal{M}^{(0)}|^2 = \frac{e^4 Q_f^2}{4q^4} N \text{tr} [\hat{p}' \gamma^\mu \hat{p} \gamma^\nu] \text{tr} [k' \gamma_\mu k \gamma_\nu] , \quad (2.56)$$

$$= 8 \frac{Q_f^2 e^4}{q^4} N [k \cdot \hat{p} k' \cdot \hat{p}' + k' \cdot \hat{p} k \cdot \hat{p}'] \quad (2.57)$$

which, leads to the partonic cross section

$$\begin{aligned}\frac{d\hat{\sigma}}{dQ^2} &= \frac{1}{16\pi\hat{s}^2} \frac{1}{2} \sum_{\text{pol}} |\mathcal{M}^{(0)}|^2 \\ &= \frac{2\pi\alpha^2 Q_f^2}{Q^4} (1 + (1-y)^2)\end{aligned}\quad (2.58)$$

This simple finding has important consequences for the structure functions of electro-hadron collisions in the parton model. Let us remember that in the parton model the momentum of the quark is a fraction of the momentum of the incoming proton. In fact, the assumption that the proton is made of almost free quarks fixes the value of $x_{\text{Bj}} = \zeta$, the fraction of momentum taken by the quark. Indeed,

$$\hat{p}'^2 = 0 = (\hat{p} + q)^2 = 2\hat{p} \cdot q - Q^2 = 2\zeta p \cdot q - Q^2 = 2\nu(\zeta - x_{\text{Bj}}) \quad (2.59)$$

Using this result, we can express the cross section for $e - p$ scattering

$$\frac{d\sigma}{dQ^4 dx} = \frac{4\pi\alpha_{em}^2}{Q^2} (1 + (1-y)^2) \frac{1}{2} Q_f^2 \delta(x_{\text{Bj}} - \zeta) \quad (2.60)$$

Which we can interpret as the scattering of an electron off a hadron made of a single quark which carries all the momentum of the quark. Therefore, if the hadron has a distribution of partons with a density of quarks carrying a momentum fraction $f_q(\zeta)$ the cross section is

$$\frac{d\sigma}{dQ^4 dx} = \frac{4\pi\alpha_{em}^2}{Q^2} \sum_f (1 + (1-y)^2) \frac{1}{2} Q_f^2 f_f(x_{\text{Bj}}). \quad (2.61)$$

The parton distribution function (PDF) f_f are non-perturbative objects which characterise the hadron target. These cannot be computed in perturbation theory and need to be determined experimentally. Nevertheless, given their interpretation as density of partons of a given species within the hadron, they must satisfy a number of integral constraints or sum rules. One of them is that summing over all partons the net momentum is the proton momentum, which implies

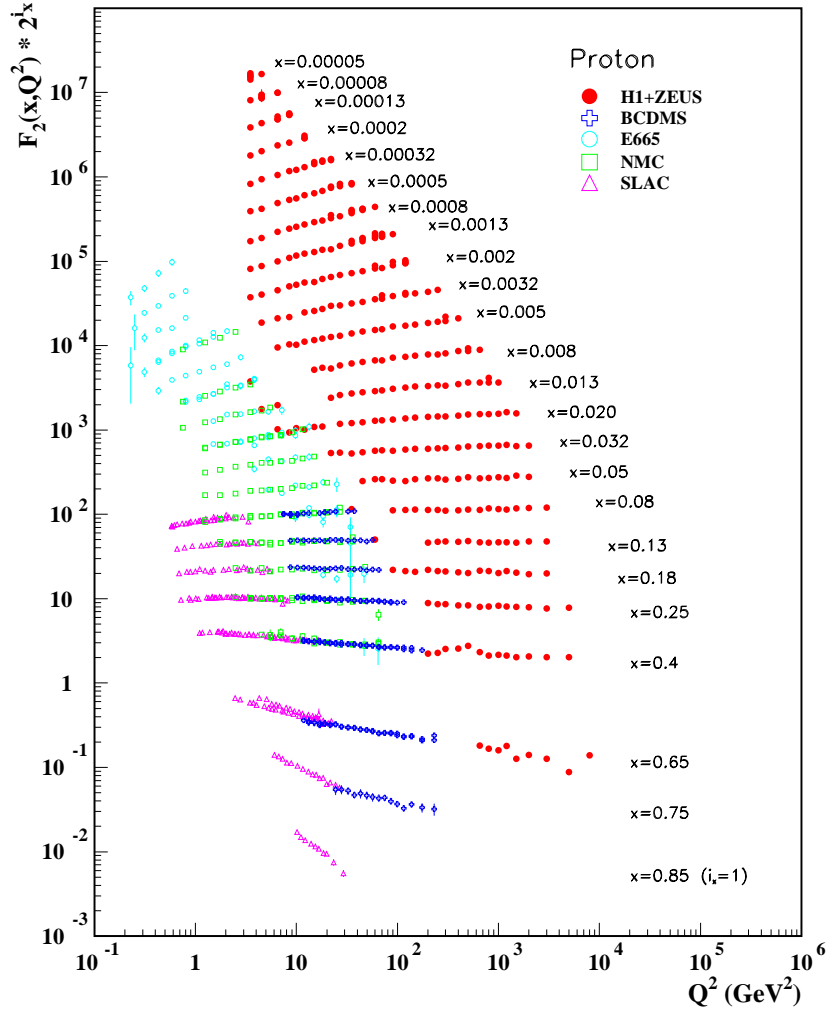
$$\sum_f \int_0^1 dx x f_f(x) = 1 \quad (2.62)$$

Similarly, the total number of quarks must coincide with the known quark content of the hadron. For the particular case of the proton, the sum rules read

$$\int_0^1 dx (f_u(x) - f_{\bar{u}}(x)) = 2 \quad (2.63)$$

$$\int_0^1 dx (f_d(x) - f_{\bar{d}}(x)) = 1 \quad (2.64)$$

$$\int_0^1 dx (f_s(x) - f_{\bar{s}}(x)) = 0 \quad (2.65)$$

Figure 2.6: Measurements of F_2 from different experiments

Comparing Eq. (2.61) with Eq. (2.54), the parton model provides very strong predictions for the structure functions F_1 and F_2 .

$$F_1(x, Q^2) = \sum_f \frac{1}{2} Q_f^2 f_f(x_{Bj}), \quad (2.66)$$

$$F_2(x, Q^2) = 2x F_1(x, Q^2). \quad (2.67)$$

The second relation is known as Callan-Gross relation, and it is a consequence of the fact that quarks possess spin $1/2$. The first relation, known as Bjorken scaling, implies that the function F_1 is only a function of x_{Bj} and independent of Q^2 . This is a consequence of the fact that the electron scatters off a point-like object. Should the scattering proceed off an extended object of typical transverse size σ_p , we would have expected that the number of partons within a transverse area $1/Q^2$ would be given by the ratio $1/(\sigma_p Q^2)$, which shows a strong dependence

on Q^2 , in contrast to the parton model prediction.

Measurements of F_2 by different experiments are shown in figure (2.6). This structure functions is indeed very weak functions of Q , and if the interval of Q is not (logarithmically) large, F_2 can be well approximated by a constant. The early measurements of this functions performed in SLAC showed indeed this behaviour which serve as a confirmation of Bjorken scaling and the parton model. However, for large ranges of Q scaling violations are observed. In the next subsection we will see how these violations arise from radiative correction of the DIS process.

2.1.2.2 Radiative corrections in DIS

We would like to be able to determine the leading order QCD correction of the predictions of the parton model for the value of the structure functions characterising DIS. As in the case of jets, radiative corrections lead to IR&Coll. divergences; but in this case, the cancellation of real and virtual corrections is more intricate than in that case.

To simplify our analysis let us introduce some more notation. We will separate from the partonic matrix element the contribution of the external parton leg $u(\hat{p})$ and the rest of the diagram, such that

$$\mathcal{M}^{(0)} \equiv \tilde{\mathcal{M}}^{(0)} u(\hat{p}), \quad (2.68)$$

So that the partonic cross section is given by

$$\sigma = \frac{N}{\hat{p}^0} \tilde{\mathcal{M}}^{(0)} \frac{1}{2} \sum \bar{u}(\hat{p}) u(\hat{p}) \tilde{\mathcal{M}}^{(0)\dagger} = \frac{N}{\hat{p}^0} \tilde{\mathcal{M}}^{(0)} \frac{\not{\hat{p}}}{2} \tilde{\mathcal{M}}^{(0)\dagger} \quad (2.69)$$

We now study the radiation of a gluon from the incoming quark. The diagram is shown in figure (2.7) Using the notation introduced above, this diagram is

$$\mathcal{M}^{(1)} = \tilde{\mathcal{M}}^{(0)}(\hat{p} - l) \frac{i(\not{\hat{p}} - \not{l})}{(\hat{p} - l)^2} (ig) t^a \not{\epsilon}(l) u(\hat{p}) \quad (2.70)$$

We see that once again the quark propagator leads to a possible collinear divergence when $l \cdot k = 0$, that is, when the intermediate quark has very small virtuality. Since in DIS we do not specify the gluon momentum l and we must integrate over all possible values. To focus on the most important region, we introduce the light-cone decomposition of the gluon momentum

$$l = (1 - z) \hat{p} + l_{\perp} + \xi \eta, \quad (2.71)$$

where \hat{p} is the (light-like) momentum of the incoming quark, η is another light-like momentum and l_{\perp} is a space-like momentum which satisfies

$$\eta \cdot \hat{p} = 2\hat{p}^0, \quad l_{\perp} \cdot \hat{p} = l_{\perp} \cdot \eta = 0 \quad (2.72)$$

In coordinates in which $\hat{p} = (1, 0, 0, 1)\hat{p}^0$, these four vectors are

$$\eta = (1, 0, 0, -1), \quad l_{\perp} = (0, l_x, l_y, 0). \quad (2.73)$$

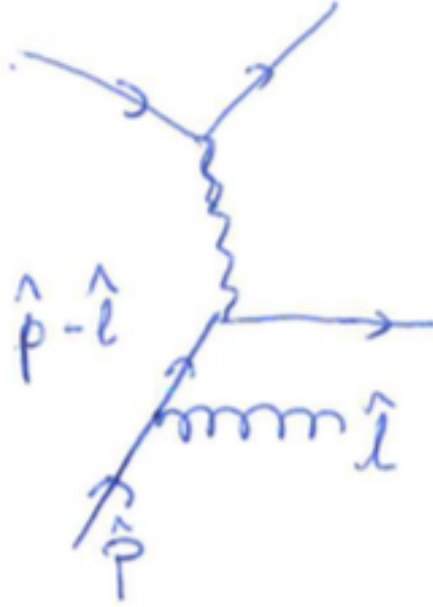


Figure 2.7: Real emission in DIS

In terms of these variables, the gluon phase space is

$$\frac{d^3l}{(2\pi)^3 2l^0} = \frac{1}{2} \frac{d^2l_\perp}{(2\pi)^3} \frac{dz}{1-z}, \quad (2.74)$$

Note also that in the requirement that the gluon momentum is light-like fixes all the components of the four momentum once the transverse momentum with respect to the quark l_\perp and the fraction of the quark momentum taken by the gluon $(1-z)$ are fixed

$$\xi = \frac{l_\perp^2}{4\hat{p}^0(1-z)}. \quad (2.75)$$

Similarly, the pole of the propagator is given by

$$(l - \hat{p})^2 = -\frac{l_\perp^2}{1-z}, \quad (2.76)$$

and, therefore, the collinear divergence occurs when $l_\perp \rightarrow 0$.

The apparent divergence in the cross section after squaring the amplitude is $1/l_\perp^4$. However, this is not the case, since there is a cancelation in the numerator that makes the leading \hat{p} term vanish. This cancelation is a consequence of the on-shell conditions $\epsilon \cdot l = 0$ and $\hat{p}u(\hat{p})$. After a few commutation and using the decomposition Eq. (2.72) and neglecting terms proportional to ξ in the high energy limit we have

$$(\hat{p} - l)\not{\epsilon}u(\hat{p}) = (2\epsilon \cdot p + \not{\epsilon}l)u(\hat{p}) \quad (2.77)$$

$$\approx \left(-2\frac{\epsilon \cdot l_\perp}{1-z} + \not{\epsilon}l_\perp \right) u(\hat{p}). \quad (2.78)$$

Therefore, the numerator of the square matrix element is proportional to l_\perp^2 , which leads to an overall $1/l_\perp^2$ divergence. Putting everything together we find

$$|\mathcal{M}^{(1)}|^2 = g^2 C_F \frac{2(1+z^2)}{l_\perp^2} \tilde{\mathcal{M}}^{(0)}(p-l) \frac{\not{p}}{2} \tilde{\mathcal{M}}^{(0)\dagger}(p-l) \quad (2.79)$$

We now multiply by the corresponding flux factor to compute the correction to the cross section

$$\sigma_1^R = g^2 C_F \int \frac{d^2 l_\perp^2}{(2\pi)^3} dz \frac{1+z^2}{1-z} \frac{N}{\hat{p}^0} \tilde{\mathcal{M}}^{(0)}(p-l) \frac{\not{p}}{2} \tilde{\mathcal{M}}^{(0)\dagger}(p-l) \quad (2.80)$$

$$\approx g^2 C_F \int \frac{d^2 l_\perp^2}{(2\pi)^3} dz \frac{1+z^2}{1-z} \frac{N}{(\hat{p}-l)^0} \tilde{\mathcal{M}}^{(0)}(p-l) \frac{\not{p}-\not{l}}{2} \tilde{\mathcal{M}}^{(0)\dagger}(p-l) \quad (2.81)$$

where in the second identity we have assumed that the gluon is almost collinear with the quark, since we are focussing in the $l_\perp \rightarrow 0$ limit. Using Eq. (2.69)

$$\sigma_1^R = \frac{\alpha_s C_F}{2\pi} \int dz \frac{1+z^2}{1-z} \frac{dl_\perp^2}{l_\perp^2} \hat{\sigma}_0(z\hat{p}). \quad (2.82)$$

As in the case of jets, the emission of gluons factorises into a universal part, which only depends on the gluon kinematics and the leading order cross section, which depends of the process. However, the arguments of the leading order cross section depends on the gluon kinematics, unlike the e^+e^- case. Also, this real emission cross section is both collinear ($l_\perp \rightarrow 0$) and soft ($z \rightarrow 1$) divergent. However, as before, we need to consider virtual corrections.

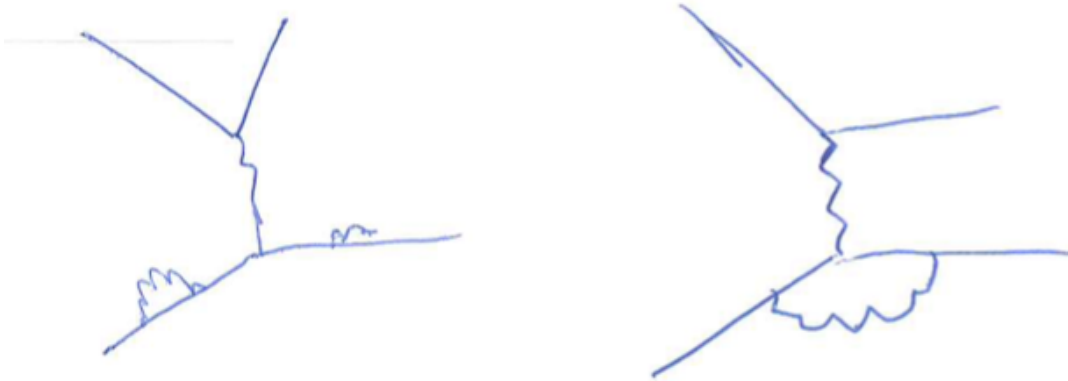


Figure 2.8: Virtual corrections in DIS

The diagrams that contribute to those corrections are shown figure (2.8). The self-energy corrections in that figure vanish in dimensional regularisation. Therefore, the only non-vanishing correction is the vertex correction. However, this correction does not alter the kinematics of the scattered quark. As a consequence the correction can only be a divergent piece multiplying the leading order cross section for the incoming momentum \hat{p} . After

computing the integral we obtain

$$\sigma_1 = \frac{\alpha_s C_F}{2\pi} \int dz \frac{1+z^2}{1-z} \frac{dl_\perp^2}{l_\perp^2} [\hat{\sigma}_0(z\hat{p}) - \hat{\sigma}(\hat{p})] . \quad (2.83)$$

The virtual correction cancels the soft divergence $z \rightarrow 1$. The way it does it is by subtracting the cross section value at the $z = 1$. In essence we can view the final result after taking into account the virtual correction as transforming the divergent $(1+z^2)/(1-z)$ function in the interval $(0, 1)$ into a *distribution*, in which the function is regularised. To specify that this is indeed a distribution we introduce the notation

$$P_{qq}(z) = \left(\frac{1+z^2}{1-z} \right)_+ , \quad (2.84)$$

such that when convoluted with any function

$$\int_0^1 dz \left(\frac{1+z^2}{1-z} \right)_+ f(z) = \int_0^1 dz \left(\frac{1+z^2}{1-z} \right) (f(z) - f(1)) . \quad (2.85)$$

We therefore can split the process as

$$\sigma_1 = \frac{\alpha_s C_F}{2\pi} \int dz \frac{dl_\perp^2}{l_\perp^2} P_{qq}(z) \sigma_0(z\hat{p}) . \quad (2.86)$$

Note that the function P_{qq} is universal, in the sense that any process that will be initiated by a quark will lead to this function as a radiative correction. We have therefore factorised the process into a universal part and a process dependent cross section. This separation has a simple physical interpretation. In the collinear limit, the quark virtuality is small, which means that it has a very long life-time to emit the almost collinear gluon. This means that the process by which the quark emits this gluon must decouple from the rest of the diagram, which occurs at a much shorter time, given by the virtuality of the exchanged photon. This factorisation can be made much more precise, but this goes beyond the scope of these lectures.

There is one remaining problem: the virtual correction does not cancel the *collinear* divergence. This is a consequence of the fact that the virtual corrections cannot alter the parton kinematics. This non-cancellation implies that our naive parton model cannot be correct, since it cannot predict the cross section beyond leading order. In the next section we will study which modifications we need to introduce to the parton model to render the cross section finite.

2.1.2.3 Scaling violation

To deal with the uncanceled collinear divergence we will follow a strategy very similar to what it is done for renormalisation. There, the UV divergences are absorbed into the parameters of the Lagrangian via multiplicative constants, such that the bare parameters are divergent, while the renormalised ones are finite. Here, the object which we can use to renormalise is the

parton distribution function, which, as it was the case for the parameters of the Lagrangian, is an object that we cannot compute (in perturbation theory), but we need to determine experimentally.

The calculation we analysed in the previous subsection is the cross section at partonic level. To obtain the cross section at hadronic level we must convolute the partonic cross section with the (bare) PDF

$$\sigma = \int dx f_q^{(0)}(x) \hat{\sigma}(xp), \quad (2.87)$$

Using our perturbative computation, this expression is still collinear divergent, since convoluting with the (bare) PDF does not change the collinear kinematics. Introducing a collinear regulator λ , which is a minimum transverse momentum the gluon can have, we obtain

$$\sigma = \int dx dz f_q^{(0)}(x) \left(\delta(z-1) + \frac{\alpha_s C_F}{2\pi} \log \left(\frac{Q^2}{\lambda^2} \right) P_{qq}(z) \right) \sigma_0(zxp) \quad (2.88)$$

where we have cut off the small l_\perp limit of the integral by the infrared regulator. The upper cut-off is of order of the transverse momentum exchange Q , as can be easily estimated by demanding that the final scattered parton is massless. The full cross section is obtained taking the cut-off to zero.

As for renormalisation we would like to "multiplicatively" renormalise the bare PDF such that it absorbs the logarithmic divergence. But since this is a function of the momentum, instead of multiplying by a (divergent) constant, we convolute the PDF with a (divergent) correction. As in renormalisation, we introduce an arbitrary scale, called the factorisation scale μ_F to separate the contribution of the cutoff. Using the trivial fact that

$$\log \frac{Q^2}{\lambda^2} = \log \frac{Q^2}{\mu_F^2} + \log \frac{\mu_F^2}{\lambda^2} \quad (2.89)$$

we redefine

$$f_q(x, \mu_F^2) = \int dy dz f_q^{(0)}(y) \left(\delta(1-z) + \frac{\alpha_s C_F}{2\pi} P_{qq}(z) \log \frac{\mu_F^2}{\lambda^2} \right) \delta(x-yz) \quad (2.90)$$

This redefinition absorbs the collinear divergence to leading order: additional factors may be found order by order in perturbation theory. Similarly, we may redefine the partonic cross section as

$$\hat{\sigma}(\hat{p}, \mu_F^2) = \hat{\sigma}_0(\hat{p}) + \frac{\alpha_s C_F}{2\pi} \log \frac{Q^2}{\mu_F^2} \int dz P_{qq}(z) \sigma_0(z\hat{p}). \quad (2.91)$$

This expression coincides with the partonic cross section including the emission of gluons with transverse momentum $l_\perp > \mu_F$. The rest is absorbed into the PDF.

A heuristic explanation of what the procedure we have just described means is the following: the PDF provides the distribution of partons within the hadron. But the distribution of those partons can be easily changed by almost collinear emissions, which can alter the kinematics and flavour of the parton we are interacting with. Similarly, the process of interaction can be altered by collinear emissions off the incident quark. What the factorisation

$$\begin{aligned}
P_{qq}^{(0)}(x) &= P_{\bar{q}\bar{q}}^{(0)}(x) = C_F \left(\frac{1+x^2}{1-x} \right)_+ , \\
P_{qg}^{(0)}(x) &= P_{\bar{q}g}^{(0)}(x) = T_f (x^2 + (1-x)^2) , \\
P_{gq}^{(0)}(x) &= P_{g\bar{q}}^{(0)}(x) = C_F \frac{1+(1-x)^2}{x} , \\
P_{gg}^{(0)}(x) &= 2C_A \left[z \left(\frac{1}{1-z} \right)_+ + \frac{1-z}{z} + z(1-z) + \left(\frac{11}{12} - \frac{n_f}{6C_A} \right) \delta(1-x) \right]
\end{aligned}$$

Figure 2.9: Leading order splitting functions. Figure taken from P.Nason, Introduction to QCD

scale provides is a separation between the radiative processes we include as part of the proton structure and those that contribute to the real emissions in the cross section. Once this is determined, we can factorise the cross section between the properties of the target, as codified by the PDF, and the partonic interactions. The scale separating these assignments is μ_F

To determine the full cross section we must therefore choose a value of μ_F to compute the partonic cross section Eq. (2.91) and convolute it with the PDF at that same μ_F . Since μ_F is arbitrary, all choices should give the same answer in a complete computation. However, as it was the case for the running coupling constant, in a fixed order calculation some choices reduce the uncertainty in the computation. Examining Eq. (2.91) it becomes apparent that we must choose $\mu_F = \xi Q$, with ξ an order one number, to avoid the presence of a large log. Therefore, we must also evaluate the PDF in the same scale $\mu_F \sim Q$. As a consequence of radiative corrections the PDF depends then on both x_{Bj} and Q , although the dependence on Q is weak, since its only logarithmically. The dependence of the PDF on the scale is known as scaling violation, since radiative corrections break Bjorken scaling.

2.1.2.4 DGLAP evolution

Although the PDF must be determined experimentally, we do not need to determine them at all possible scales. We can relate the dependence from one scale to another via an evolution equation. Indeed, taking a derivative with respect to the scale of Eq. (2.90) we obtain

$$\mu^2 \frac{\partial}{\partial \mu^2} f_q(x, \mu^2) = \frac{\alpha_s C_F}{2\pi} \int_0^1 dy dz f_q^{(0)}(x) P_{qq}(z) \delta(x - yz). \quad (2.92)$$

Integrating out one of the variables and noticing that to the accuracy that we have performed, we can replace the bare partition function with the full partition function, we obtain

$$\mu^2 \frac{\partial}{\partial \mu^2} f_q(x, \mu^2) = \frac{\alpha_s C_F}{2\pi} \int_x^1 \frac{dy}{y} f_q(y, \mu_F^2) P_{qq}\left(\frac{x}{y}\right). \quad (2.93)$$

This equation has a simple interpretation. As we have discussed, μ is the maximum value of the collinear gluons that are included in the PDF. If we now increase this scale by a small

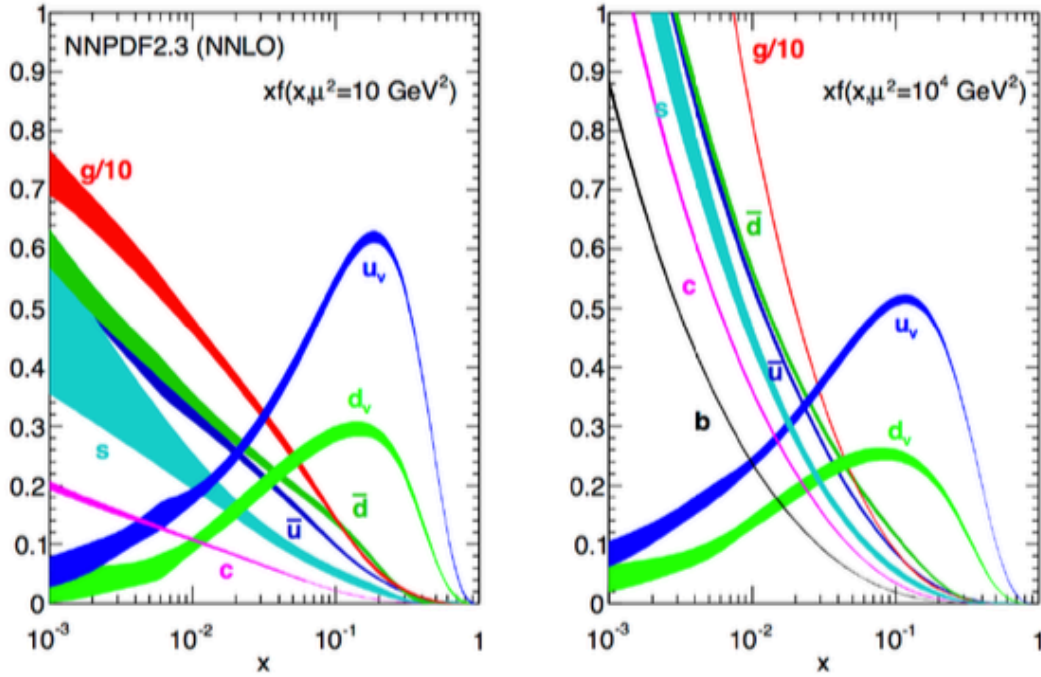


Figure 2.10: PDF at two different scales.

amount, the PDF will change, since we allow for additional radiation off the quarks. The new PDF at this bigger scale is given by the convolution of the PDF at the smaller scale times the probability of emission. Since the emission takes away some energy, the PDF at the smaller scale will be evaluated at a different value of the momentum fraction y , such that after emission of a gluon with momentum $1 - z$ the final quark possesses a momentum $x = yz$.

Our calculation up to now has been oversimplified, since we have only considered processes in which the scattered quark comes from a quark that emits a gluon. However, we could have also included processes like $g \rightarrow q\bar{q}$. This makes the evolution also sensitive to the gluon distribution, since, following the previous interpretation, the quarks at one given scale can also come from the conversion of gluons from a smaller scale into quark pairs. In general, all PDF are coupled and the evolution equations take the generic form

$$\mu^2 \frac{\partial}{\partial \mu^2} f_i(x, \mu) = \sum_{ij} \int_x^1 \frac{dy}{y} P_{ij} \left(\frac{x}{y} \right) f_j(y, \mu_F^2), \quad (2.94)$$

where the splitting P_{ij} can be determined in perturbation theory and they are shown in figure (2.9). These are important equations, which are known as the DGLAP (Dokshitzer, Gribov, Lipatov, Altarelli, Parisi) equations. These are the basis to determine the parton distribution functions from experimental data on $e - p$ collisions (and also hadron hadron collision).

In essence, the procedure to determine the PDF is to start with some parametrisation of the distribution function at some reference scale $\mu_F^2 \sim 10 \text{ GeV}^2$ and use the evolution equation

to constraint data at different values of x and Q . The initial parametrisation may be of the form of some prescribed functional form or, in more modern approaches, chosen via a neural network trained to fit the data. A state-of-the-art determination of the PDF is shown in figure (2.10)

2.1.3 Parton Showers and MonteCarlo Simulations

Up to now we have focussed on fixed order QCD calculations, which, in principle, can be extended to higher and higher order by continuing the perturbative series. However, in practice, the number of diagrams grows fast and it makes it very hard to go beyond NNLO. Furthermore these fixed order computations are good for sufficiently inclusive measurements or for particularly simple final states. However, a generic hadron-hadron collisions event has a lot of activity which make it very hard or even impossible to describe them in fixed order perturbative computation.

To describe those complicated events we need to perform approximations, which concentrate in regions of phase space that are kinematically enhanced. As we have seen, the presence of collinear and infrared divergences tells us that the dominant momentum regions in physical cross sections are precisely in the regions where these divergences occur.

To make the discussion concrete, let us consider a diagram in which an almost on shell parton with (small) virtuality $t=p_a^2$ splits into two partons with virtualities $p_c^2, p_b^2 \ll t$. The relevant scale to compare the virtuality of the parent parton is the energy of the parton, $E_a \gg p_a^2$. Similarly, we will assume that the virtualities of the decay products are much larger than Λ_{QCD} , so that the coupling constant is small. A sketch of this branching process is shown in figure (2.11)

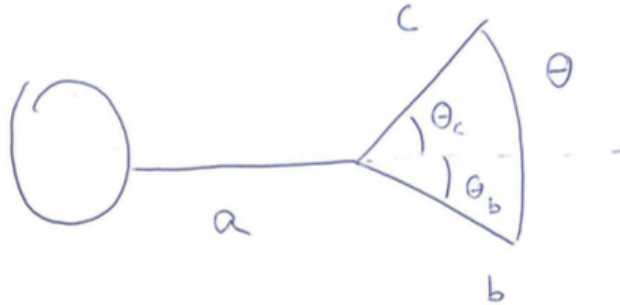


Figure 2.11: Sketch for the splitting dynamics.

Let us examine the kinematics of the branching process. After fixing the four momenta of the decay products, the virtuality of the parent parton is given by

$$t = p_b^2 + p_c^2 + 2E_b E_c (1 - v_b v_c \cos(\theta)) \approx z(1-z)E_a^2 \theta^2, \quad (2.95)$$

where $\mathbf{v}_i = \mathbf{p}_i/E_i$ and in the right hand side we have neglected the virtualities of the decay products and assume that the angle between the particles is small. In this approximation it

is clear that the virtuality of the parent parton is small when either one of the decay products is soft or when the splitting angle is small. In this case, the $1/t$ dependence of the parton propagator in the diagram will lead to an enhancement of the cross section, reminiscent of the infrared and collinear singularities.

In the almost on-shell limit, the propagator of the intermediate particle simplifies significantly. Indeed, using the completeness relation of the external polarisation factors, it is easy to show that close to the pole the numerator of the propagator can be expressed as the sum over external polarisations of the on-shell particles

$$\left. \frac{-g_{\mu\nu}}{k^2} \right|_{k^2 \rightarrow 0} \rightarrow \frac{\sum_{\text{pol}} \epsilon(k) \epsilon^*(k)}{k^2}, \quad (2.96)$$

$$\left. \frac{\not{p}}{p^2} \right|_{p^2 \rightarrow 0} \rightarrow \frac{\sum_{\text{pol}} u(p) \bar{u}(p)}{p^2}, \quad (2.97)$$

which allows us to separate the contribution of the production of the almost on-shell particle from the subsequent splittings. In particular, assuming that the process in figure (2.11) is mediated by a gluon, we may written as

$$\mathcal{M}_{n+1} = \mathcal{M}_n \frac{1}{t} i g f^{abc} \epsilon^{*\alpha} \epsilon^\beta \epsilon^\gamma [g_{\alpha\beta} (-p_a - p_b)_\gamma + g_{\beta\gamma} (p_b - p_c)_\alpha + g_{\gamma\alpha} (p_c + p_a)_\beta], \quad (2.98)$$

where we have used that the p_a momentum flows into the vertex and, as before, \mathcal{M}_n is the diagram producing the on shell gluon with polarisation ϵ^α . As mentioned, the amplitude already splits into the production of the gluon times and an additional factor encoding the gluon splitting. Taking the square of the amplitude and summing over polarisations one can obtain (see for example Ellis, Stirling and Webber)

$$|M_{n+1}|^2 = |M_n|^2 \frac{4g^2}{t} \hat{P}_{gg}(z) \quad (2.99)$$

where $\hat{P}_{gg}(z)$ is the un-regularised gluon splitting function

$$\hat{P}_{gg}(z) = C_A \left[\frac{1-z}{z} + \frac{z}{1-z} + z(1-z) \right]. \quad (2.100)$$

Note that this splitting function is divergent at $z = 1$ and no “+”-prescription appears (yet). For this reason we call this object the un-regularised splitting function. Similar computations can be done for all other channels, where a similar factorisation of the square amplitudes between the production of the n-particle state and the subsequent splitting occurs. Note that this also means that, at least in the almost on-shell limit, the splitting distribution is universal, independent of the process that leads to the production of the parent parton.

To show that the full cross section also factorises, we must also show that the phase space for the process can be separated in a similar fashion. The phase space of production of n particles will be given by

$$d\phi_n = \dots \frac{d^3 p_a}{(2\pi)^3} \frac{1}{2E_a} \quad (2.101)$$

while the phase space after splitting is given by

$$d\phi_{n+1} = \dots \frac{d^3 p_b}{(2\pi)^3} \frac{1}{2E_b} \frac{d^3 p_c}{(2\pi)^3} \frac{1}{2E_c} \quad (2.102)$$

Fixing the momentum of particle p_b we can use momentum conservation ($\mathbf{p}_a = \mathbf{p}_b + \mathbf{p}_c$) to trade $d^3 p_c = d^3 p_a$. We may now introduce unity into the integral as

$$1 = \int dz dt \delta \left(z - \frac{E_b}{E_a} \right) \delta(t - z(1-z)E_a^2 \theta^2). \quad (2.103)$$

Using simple kinematics, demanding that the momentum of the decay products transverse to \mathbf{p}_a vanishes, in the small angle approximation we obtain

$$\theta_b = (1-z)\theta \quad (2.104)$$

and change variables to integrate over θ_b . Eliminating the p_b and θ_b integrals via the introduced δ -functions we end up with

$$\frac{d^3 p_b}{(2\pi)^3} \frac{1}{2E_b} \frac{d^3 p_c}{(2\pi)^3} \frac{1}{2E_c} = \frac{d^3 p_a}{(2\pi)^3} \frac{1}{2E_a} \frac{dt dz d\phi}{4(2\pi)^3}. \quad (2.105)$$

And, as claimed, the phase space factorises. Putting all together, we find a factorised expression for the cross section

$$d\sigma_{n+1} = d\sigma_n \frac{dt}{t} dz \frac{\alpha_s}{2\pi} \hat{P}_{ab}, \quad (2.106)$$

which separates the cross section into a process-independent universal factor, and the cross section to produce an on-shell particle. Note that the presence of $dt/t \sim d \log t$ signals once again the collinear singularity, since, as we have seen, t vanishes at small angle. In a given process, this singularities are regulated by the fact that the virtualities of the decay product do not vanish identically, leading to terms of the order

$$\alpha_s \log \frac{p_b^2}{p_a^2}, \quad (2.107)$$

Therefore, if one examines processes with very different initial and final virtuality, this ratio of logs of scales indicates that the multiple radiations are likely, since the smallness of α_s is compensated by the large \log . These factors are also behind the emergence of virtuality ordered showers. If at each step in the shower there is a jump in the virtuality, the factorisation of the process we have described before appears at each splitting with enhancing factors as the above. Emissions in which the virtualities are not ordered are possible, but their rate is much smaller than those of a strong ordering as a consequence of the above logarithmic enhancement.

The end result of the showering process we have described is a complicated event with multiple almost collinear quark and gluons. An sketch of this process in a hadronic collision is summarised in figure (2.12). Ultimately, all these partons must decay into hadrons via a

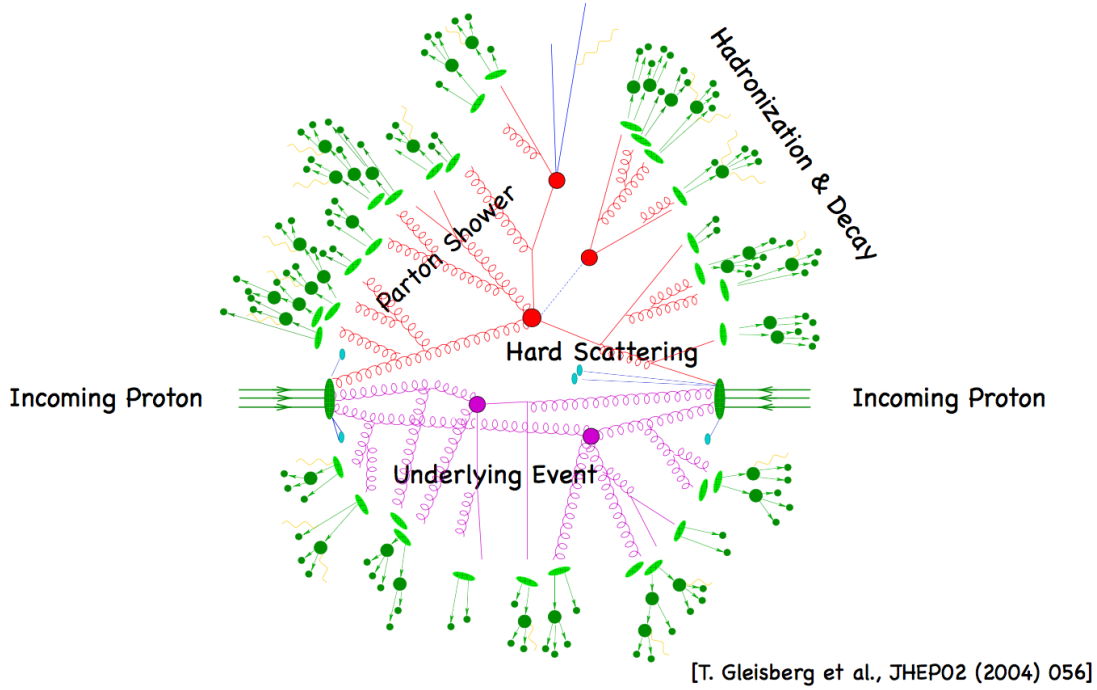


Figure 2.12: Sketch of a hadronic event with multiple jet showers.

non-perturbative process which is currently not accessible to first principle QCD calculations. However, if we are only interested in determining the mean number of hadrons of a given species h produced in a collision, we may encode this process by a set of *fragmentation function*

$$D_i^h(x; t) \quad (2.108)$$

which represent the density of hadrons of species h produced by a parton of type i (with i being any quark flavour or gluon) with virtuality $p^2 = t$ that carries a fraction $x = E^{\text{hadron}} / E^{\text{parton}}$ of the energy of the parton. These are very similar to the parton distribution function of DIS, which we described in detail in section(2.1.2). While we do not know how to compute this function, we can use the branching picture described above to determine how this object changes from one scale to another.

Let us consider the fragmentation functions of a parton at two different, but close scales, t' and t with $t' = t + \delta t$ and δt small. Certainly, without the showering process we described above, the two fragmentation functions $D_i^h(x, t + \delta t)$ and $D_i^h(x, t)$ would be identical. However, the collinear shower process we describe above shows that the fragmentation function will change by a small amount. For simplicity of the notation and since the generalisation is straight forward, let us assume that there is a single type of partons. Then we can write

$$D^h(x, t + \delta t) = D^h(x, t) + \delta D^h(x, t) \quad (2.109)$$

The showering process described above leads to two distinct contributions to the change in $\delta D^h(x, t)$. On the one hand, the parton with virtuality $t + \delta t$ will have a small probability

to radiate and produce a daughter parton with a fraction $z = E^{daughter}/E^{parent}$ of the momentum of the original (parent) parton. This daughter parton, in turn, will fragment with the splitting function at scale t . But since the momentum of the daughter parton differs from that of the parent parton, the splitting function is evaluated at a different momentum, $x' = E^{hadron}/E^{daughter} = x/z$. In addition, since the other particle produced in the splitting is also a gluon, the daughter with momentum $E^{daughter} = (1-z)E^{parton}$ also contributes to the fragmentation function with $x' = x/(1-z)$. Using the splitting probability determined above we conclude that number of hadrons produced by the a parton at scale $t + \delta t$ will be

$$\delta D_{in}^h(x, t) = \frac{\delta t}{t} \int_0^1 dx' dz \frac{\alpha_s}{2\pi} \hat{P}_{gg}(z) D(x', t) (\delta(x - zx') + \delta(x - (1-z)x')) . \quad (2.110)$$

We can integrate x' integral right way by solving the δ -function; using the fact that $\hat{P}_{gg}(z)$ is symmetric under $z \rightarrow (1-z)$, equation (2.100), this integration leads to

$$\delta D_{in}^h(x, t) = \frac{\delta t}{t} \int_0^1 dz \frac{\alpha_s}{2\pi} 2\hat{P}_{gg}(z) D\left(\frac{x}{z}, t\right) . \quad (2.111)$$

Complementary, the same splitting process reduces the number of partons with energy E^{parent} that are susceptible to hadronise. This reduction is proportional to the emission probability of daughter partons with any momentum fraction, and we have:

$$\delta D_{out}^h(x, t) = -\frac{\delta t}{t} \int_0^1 dz \frac{\alpha_s}{2\pi} \hat{P}_{gg}(z) D(x, t) . \quad (2.112)$$

Putting together these two contributions, we find that the change total change in the fragmentation function is

$$\delta D^h(x, t) = \delta D_{in} - \delta D_{out} \quad (2.113)$$

$$= \frac{\delta t}{t} \int_0^1 dz \frac{\alpha_s}{2\pi} \hat{P}_{gg}(z) \left[\frac{2}{z} D\left(\frac{x}{z}, t\right) - D(x, t) \right] . \quad (2.114)$$

This is an interesting result which parallels what we have already saw in section (2.1.2). As we have motivated by our analysis of the gluon-gluon splitting function, equation (2.100), the splitting functions that we obtain from a branching analysis as we have performed are generically divergent in the $z \rightarrow 1$ limit, which reflects the IR&Coll singularity of the splitting process. Nevertheless, the integral above regularises de splitting function, since it subtracts the $z = 1$ limit. This is equivalent to the +-prescription in DIS, which we described in section (2.1.2). However, unlike in that case, the subtraction is slightly more complicated, since the two gluons produced in the splitting contribute to the fragmentation function. We may then take this subtraction as the definition of the regularised fragmentation function.

To work out the explicit form of the regularised splitting function, and using the symmetry of equation (2.100), we note that

$$\int_0^1 dz \hat{P}_{gg}(z) = 2C_A \int_0^1 dz \left(\frac{z}{1-z} + \frac{1}{2}z(1-z) \right) . \quad (2.115)$$

Then, we can define the regularised splitting function as

$$P_{gg}(z) = 2C_A \left(\left(\frac{z}{1-z} + \frac{1}{2}z(1-z) \right)_+ + \frac{1-z}{z} + \frac{1}{2}z(1-z) \right) \quad (2.116)$$

where, as in section (2.1.2)

$$\int dz \left(\frac{z}{1-z} + \frac{1}{2}z(1-z) \right)_+ f(z) = \int dz \left(\frac{z}{1-z} + \frac{1}{2}z(1-z) \right) (f(z) - f(1)) \quad (2.117)$$

Taking δt as infinitesimally small, we may write the change of the fragmentation function as a differential equation that takes the form

$$t\partial_t D^h(x, t) = \int_x^1 \frac{dz}{z} \frac{\alpha_s}{2\pi} P_{gg}(z) D\left(\frac{x}{z}, t\right), \quad (2.118)$$

where we have removed the $\hat{}$ from the splitting function to remind us that this is the regularised splitting function defined in equation (2.116). We have also changed the lower limit of integration since the splitting function vanishes for $x > 1$ because of simple kinematics. Quite remarkably, this is the same DGLAP evolution equation that we obtained for parton distribution function in deep inelastic scatterings by demanding that the definition of the number of partons would be independent of the factorisation scales that controls the transverse size of partons. As in DIS we may give this equation a similar interpretation by noticing that the virtuality of the parton may be taken as an arbitrary scale that factorises a perturbative contribution to the QCD cross section from the non-perturbative contribution to the production cross section. A similar analysis to the one we did in DIS can be performed for fragmentation functions; but since here the non-perturbative state is specified, the analysis is much more cumbersome and we will not address it in these lecture notes¹.

The expression of evolution equations with the regularised splitting function is suitable for analytical computations but hard to evaluate numerically. For this reason we look for a simplified expression which does not require the regularised splitting function. To do so, let us introduce the Sudakov form factor

$$\Delta(t) = \exp \left\{ - \int_{t_0}^t \frac{dt'}{t'} \int dz \frac{\alpha_s}{2\pi} \hat{P}(z) \right\}. \quad (2.119)$$

It is easy to see that if D satisfies the DGLAP equation, then

$$t\partial_t \left(\frac{D(x, t)}{\Delta(t)} \right) = \int \frac{dz}{z} \frac{\alpha_s}{2\pi} \hat{P}(z) \frac{D(x/z, t)}{\Delta(t)}. \quad (2.120)$$

This equation has a formal solution given by

$$D(x, t) = \Delta(t) D(x, t_0) + \int_{t_0}^t \frac{dt'}{t'} \frac{\Delta(t)}{\Delta(t')} \int \frac{dz}{z} \frac{\alpha_s}{2\pi} \hat{P}(z) D(x/z, t') \quad (2.121)$$

¹The interested reader may find the full analysis in "Foundations of Perturbative QCD", John Collins, Cambridge University Press, 2011

This expression admits a simple interpretation. The first term may be interpreted as the contribution of processes in which no radiation occurs, since the fragmentation function at x remains the same between the two scales. The pre-factor $\Delta(t)$ may be then interpreted as the probability of no radiation between the initial and final scale. This interpretation also help us to understand the second term. The fragmentation function at scale t is related to the fragmentation at scale t' via the radiation of a parton that changes the kinematics of the initial parton; the ratio of Sudakov form factors can be interpreted as the probability that there is no further radiation between t' and t .

This interpretation is the basis for Monte-Carlo event generators. Given some initial virtuality, the distribution of branchings at some other scales follows the distribution $\Delta(t)/\Delta(t_0)$. The value of t may be found randomly, by generating an arbitrary number $R \in (0, 1)$ and solving

$$\frac{\Delta(t)}{\Delta(t_0)} = R. \quad (2.122)$$

After finding the scale, we can determine the fraction of momentum of the emitted parton z according to the splitting distribution \hat{P} . This procedure generates a shower up to a non-perturbative value of $t \sim \Lambda_{QCD}$. At this point, current MonteCarlo generators connect with different models for hadronisation which convert the partonic distribution at the end of the shower into hadrons, either via clustering or via classical string dynamics. We will not describe those models in these lectures. For a brief description see Ellis, Stirling and Webber.

2.2 The Operator Product Expansion

Complementing the purely perturbative analysis that we have performed in the previous sections, in this section we will explore a different technique that can complement purely perturbative analyses with non-perturbative physics. This technique is based on the observation that high energy processes are determined by interactions that occur at very short distances, such that from a far away observer they seem to occur at a point.

The above reasoning can be made more precise by analysing individual QCD processes at all orders in the strong coupling constant. We have already done one of those analysis in describing DIS, section (2.1.2), where we found the proton-electron inelastic cross section can be expressed in terms of the hadronic tensor, eq. (2.51), which we repeat here from convenience

$$W_{\alpha\beta} = \frac{1}{4\pi} \int d^4z e^{iqz} \langle p | j_\alpha^\dagger(z) j_\alpha^\dagger(0) | p \rangle , \quad (2.123)$$

where j_μ is the electromagnetic current operator. Following identical steps, the total annihilation cross section of e^+e^- into hadrons can also be expressed as a product of two currents to all orders in the strong coupling constant

$$\sigma_{e^+e^- \rightarrow \text{hadrons}} = -\frac{8\pi\alpha_{\text{em}}}{3Q^4} \int d^4z e^{iqz} \langle \Omega | j^\mu(z) j_\mu(0) | \Omega \rangle \quad (2.124)$$

where $q = (Q, \mathbf{0})$ is the four-momentum of the e^+e^- pair in the center of mass of the collision and Ω the vacuum.

In both these cases we see that the processes we are interested in may be expressed as the product of two operators, the electromagnetic current in both cases, displaced from one another by a distance $z \sim 1/Q$, which decreases as the momentum increases. As the distance becomes shorter, we would like to express this product of operators in an expansion in the displacement. This is the operator product expansion.

From a more formal point of view, we may consider the more general case of the correlation function of a product of operators O_a and O_b with a displacement z with a number of operators ϕ_i situated far away from them with a displacement y_i

$$G_{ab}(x; y_1, y_2, \dots, y_n) = \langle O_a(x) O_b(0) \phi_1(y_1) \dots \phi_n(y_n) \rangle \quad (2.125)$$

We may think of the operators ϕ_i operators as those associated with the detectors of the particles. From the far away point y_i the two operators O_{ab} seem to be in the same point. Therefore, we can approximate their action as a certain disturbance at the origin which we may generate by a complete set of local operators $\{\mathcal{O}_n\}$. With this ideology, the displacement between the two appears only as the coefficient of this expansion. This means, that we can write the operator identity

$$O_a(x) O_b(0) = \sum_n C_{ab}^{(n)}(x) \mathcal{O}_n(0) \quad (2.126)$$

where the operators $\{O_n\}$ are evaluated at the origin and the $C_{ab}^{(n)}(x)$ are complex function (as opposed to operators) that depend on the separation between the two initial operators O_{ab} . Since this relation holds at the level of operators, this implies that similar relations can be written for *any* correlation function that involves the product of these operators

$$G_{ab}(x; y_1, y_2, \dots, y_n) = \sum_n C_{ab}^{(n)}(x) G_n(y_1, y_2, \dots, y_n) \quad (2.127)$$

$$G_n(y_1, y_2, \dots, y_n) \equiv \langle \mathcal{O}_n(0) \phi_1(y_1) \dots \phi_n(y_n) \rangle \quad (2.128)$$

The complex functions $C_{ab}^{(n)}(x)$ are common to all those correlation functions.

Since the product of operators is singular, so will be the functions $C_{ab}^{(n)}(x)$, which we expect will diverge as $x \rightarrow 0$. Up to radiative effects, we can determine the short distance divergence from the (engineer) dimension of the different operators in the identity (2.126). If the operators $O_{a,b}$ have mass dimension $d_{a,b}$ and the operator \mathcal{O}_n mass dimension d_n , dimensional analysis shows that the short distance divergence of the coefficients is

$$C_{ab}^{(n)}(x) \sim \frac{1}{x^{d_a+d_b-d_n}}, \quad (2.129)$$

For this reason, it is convenient to order the possible operators O_n in increasing order of mass dimension, so that the first coefficient $C_{ab}^{(1)}(x)$ is the most divergent at short distance.

Another obvious condition derived from the identity (2.126) is that the symmetry properties in both sides of the equality must be the same. Therefore, the quantum numbers of the operators \mathcal{O}_n must be the same as those of the product of operators $O_a O_b$.

Finally, as we have stressed in the first chapter, with few exceptions, high-dimension local operators receive divergent radiative corrections which need to be renormalised. This means that in any computation we perform all the terms in the sum in (2.126) depend on the renormalisation scale. Therefore, after renormalisation also the complex functions $C_{ab}^{(n)}(x)$ depend on the renormalisation scale and

$$O_{Ra}(x, \mu) O_{Rb}(0, \mu) = \sum_n C_{Rab}^{(n)}(x, \mu) \mathcal{O}_{Rn}(0, \mu) \quad (2.130)$$

Here it is worth pausing for a second to discuss the meaning of the renormalisation scale in this expression. Since we are separating the dynamics for small values of x from the rest of the operators insertions far from the origin, the OPE procedure implicitly implies a factorisation between short and long distance physics. In this way, all the high-energy contributions are included into the coefficient functions $C_{ab}^{Rn}(x, \mu)$ while the long distance dynamics are encoded in the (correlation functions of the) local operators \mathcal{O}_{Rn} . For any given correlation function $G_n(y_1 \dots y_n)$ renormalisation is independent of the separation x , which we may interpret that the modes we are integrating cannot resolve this separation. Therefore, we can think of the renormalisation-scale dependence of the identity (2.130) as separating short and long distance fluctuations. In other words, we may think the procedure as having $\mathcal{O}_{Rn}(0, \mu)$ absorb the contribution of all fluctuation with $k < \mu$ while the fluctuations with $k > \mu$ contribute the

coefficients $C_{ab}^{\text{Rn}}(x, \mu)$. The scale μ may be thought of as the (arbitrary) separation between this regimes, and behaves very similarly to the factorisation scale identified in PDFs. Since this separation is arbitrary, the coefficient function also satisfy a Callan-Symanzik equation given by

$$\left(\mu \frac{\partial}{\partial \mu} + \beta \frac{\partial}{\partial g_{\text{R}}} + \gamma_a + \gamma_b - \gamma_n \right) C_{ab}^{\text{Rn}}(x, \mu) = 0 \quad (2.131)$$

where γ_{abn} are the anomalous dimensions of the different operators, defined as $\gamma_i = d \log Z_i / d \log \mu$. As we did for the annihilation cross section, we can convert this equation into an equation for the x dependence of the coefficient functions after noting that $C_{ab}^{\text{Rn}}(x, \mu)$ is a function of the product $x\mu$,

$$C_{ab}^{\text{Rn}}(x, \mu) = \frac{1}{x^{d_a+d_b-d_n}} f_{ab}^{\text{Rn}}(x\mu) \quad (2.132)$$

Repeating the same steps as in that case, the solution to this equation is given by

$$C_{ab}^{\text{Rn}}(x, \mu) = \frac{1}{x^{d_a+d_b-d_n}} f^n(\bar{g}) \exp \left\{ - \int_{1/x}^{\mu} d \log t (\gamma_a + \gamma_b - \gamma_n) \right\} \quad (2.133)$$

with \bar{g} the running coupling constant, equation (1.64) and $f^n(g)$ a function of the coupling that needs to be determined at some scale. As in the case for the cross section, the particular choice of $\mu = 1/x$ ensures that there are no large logarithms in a particular evaluation of this constants. Nevertheless, this analysis also shows that at any given μ the short distance behaviour of this function is not just controlled by its engineer dimension but also by the radiative corrections. Since QCD is asymptotically free, these type of corrections become less and less relevant at sufficiently short distances.

2.2.1 OPE analysis of $e^+ - e^-$

To make the analysis above more concrete, we would like to discuss a particular example, that of the total annihilation cross section into hadrons. As we have stated in equation (1.64), this cross section may be expressed in terms of the product of two electromagnetic currents. We would then like to discuss the OPE analysis of this product.

Since $j_\mu(x)j_\nu(0)$ is a Lorentz scalar, the lowest dimension operator that contributes to this expansion is the identity $\mathbb{1}$. The next Lorenz scalar that can be constructed from the elementary fields of the Lagrangian is the dimension three operator constructed from quark fields

$$\bar{q}(0)q(0) \quad (2.134)$$

However, this operator breaks explicitly chirality, which is conserved in the current current correlator. Therefore, it can only contribute to the expansion if chiral symmetry is not a symmetry of the Lagrangian, i.e., for non-vanishing quark masses, and its contribution must vanish in the chiral limit. For this reason the relevant operator is dimension 4 and is given by

$$\mathcal{O}_2(0) = m\bar{q}(0)q(0) \quad (2.135)$$

At dimension four, there is another operator that can be constructed entirely from gauge fields, which is given by

$$\mathcal{O}_3(0) = \frac{\alpha_s}{\pi} F_{\mu\nu}(0) F^{\mu\nu}(0) \quad (2.136)$$

Additional higher-dimension operators may be constructing by either multiplying more elementary fields or taking additional (covariant) derivatives. As in the analysis of effective theories, the strategy to determine all these operators we need to determine the most general operators compatible with the dimensions of the product.

Up to dimension four, the OPE relation reads

$$j^\mu(x) j_\mu(0) = c^{(1)}(x) \mathbb{1} + c^{(2)}(x) m \bar{q}(0) q(0) + c^{(3)}(x) \frac{\alpha_s}{\pi} F_{\mu\nu}(0) F^{\mu\nu}(0) + \dots \quad (2.137)$$

At short distances, these coefficients behave as

$$c^{(1)} \sim \frac{1}{x^6} \quad c^{(2)} \sim \frac{1}{x^2} \quad c^{(3)} \sim \frac{1}{x^2} \quad (2.138)$$

and higher-dimension operators become less and less singular. Since the cross section is proportional to the Fourier transform of the vacuum expectation value of this product

$$\begin{aligned} \int d^4 z e^{iqz} \langle \Omega | j^\mu(z) j_\mu(0) | \Omega \rangle &= \\ c^{(1)}(q) + c^{(2)}(q) \langle \Omega | m \bar{q}(0) q(0) | \Omega \rangle + c^{(3)}(q) \langle \Omega | \frac{\alpha_s}{\pi} F_{\mu\nu}(0) F^{\mu\nu}(0) | \Omega \rangle \end{aligned} \quad (2.139)$$

where we have used the vacuum is normalised to 1. From the short distance behaviour above we see that

$$c^{(1)} \sim q^2 \quad c^{(2)} \sim q^{-2} \quad c^{(3)} \sim q^{-2} \quad (2.140)$$

and therefore, at high energy, the cross section is dominated by the leading term in the expansion, while the contribution of higher order operators lead to power suppressed corrections to the cross section.

Before trying to evaluate each of these coefficients, let us note that the correlation we are studying is not time ordered, unlike the correlation functions that appear in the perturbative expansion. The analysis for time ordered correlators, or any other correlation function is identical to the one we have performed. Since the basis of operators \mathcal{O}_n are evaluated at the origin, all the difference between different correlation function is the expression for the expansion coefficients. Furthermore, not all those are independent since the optical theorem relates different correlation function as

$$\int d^4 z e^{iqz} \langle \Omega | j_\mu(z) j_\mu(0) | \Omega \rangle = \frac{1}{2} \text{Im} \Pi_{\mu\nu}(q) \quad (2.141)$$

where

$$\Pi_{\mu\nu}(q) \equiv i \int d^4 z e^{iqz} \langle \Omega | \mathcal{T} j_\mu(z) j_\nu(0) | \Omega \rangle \quad (2.142)$$

Therefore, calling $c_{\Pi}^{(n)}(q)$ the OPE coefficients of the time-ordered product $\Pi_{\mu\nu}$ we have

$$c^{(n)}(q) = \frac{1}{2} \text{Im } c_{\Pi}^{(n)}(q) \quad (2.143)$$

We may now discuss how to compute the OPE coefficients. Since QCD is asymptotically free, at sufficiently high q we can use perturbation theory to determine them. Let us focus on the leading coefficient and defer the discussion of the power corrections. Since the OPE is valid at operator level, we can determine the coefficient in any state that suits best the computation. A particularly simple choice is the perturbative vacuum $|0\rangle$, since the expectation values of all the other local operators vanish in this state. The evaluation of the Π tensor in this state is nothing else than the QCD contribution of the photon self-energy, which at leading order is given by diagram a) in figure (1.1). Using the standard techniques

$$i\Pi_{\mu}^{\mu}(q) = +Q_f^2 e^2 N_c \int \frac{d^4 k}{(2\pi)^2} \text{tr} \left[\gamma^{\mu} \frac{i \not{k}}{k^2} \gamma_{\mu} \frac{i (\not{q} + \not{k})}{(q+k)^2} \right] \quad (2.144)$$

This expression is, of course, UV divergent, as the photon self energy is. However, this divergence can be renormalised by including (QED) counter-terms; up to scheme dependence, the renormalised expression is given by

$$i\Pi_{R\mu}^{\mu}(q) = i\Pi_{\mu}^{\mu}(q) - i\Pi_{\mu}^{\mu}(0) \quad (2.145)$$

The integral is also collinear divergent. Although the divergence can be treated in dimensional regularisation, in this particular case and at this order it is much simpler to keep a non-zero mass for the quarks, which we may view as an infrared regulator. Putting all together, we find

$$c_{\Pi}^{(1)}(q) = \Pi_{R\mu}^{\mu}(q) = -Q_f^2 e^2 N_c q^2 \left[\frac{1}{4\pi^2} \log \frac{-q^2}{m^2} - \frac{5}{6} \right] \quad (2.146)$$

where we have used that this perturbative computation yields exactly the first coefficient function. For time-like momentum $q^2 > 0$ the coefficient function $c_{\Pi}^{(1)}(q)$ possesses an imaginary part, which is in fact independent of the regulator. We can therefore read the leading OPE contribution to the total cross section as

$$c^{(1)}(q) = -\frac{1}{2} Q_f^2 \alpha_{em} N_c q^2 \quad (2.147)$$

which, together with equation (2.124) yields the well known result

$$\sigma(e^+e^- \rightarrow \text{hadrons}) = \frac{4\pi\alpha_{em}^2 N_c}{q^2} \sum_f Q_f^2, \quad (2.148)$$

which coincides with the purely perturbative contribution we derived in section (1.9). Since this is nothing else than evaluation of the current-current correlator in the perturbative vacuum, it is clear that the α_s -expansion of the annihilation cross section coincides identically

with the α_s expansion of the OPE coefficient $c^{(1)}(q)$. Therefore, perturbation theory only provides information about this contribution to the cross section.

We now turn to the power corrections induced by the sub-leading terms in the OPE expansion. These terms only contribute to the cross section because the QCD vacuum $|\Omega\rangle$ differs from the perturbative vacuum $|O\rangle$. In the QCD vacuum there are non-vanishing condensates, i. e., non-zero expectation values of operators with vacuum quantum numbers. These are very similar to Bose-Einstein condensates in condensed matter physics. However, since vacuum physics are the physics of long distances, these quantities are non-perturbative and can be only determined either by measurements or by non-perturbative methods, such as lattice calculations. On dimensional grounds, these condensates must be set by Λ_{QCD} . Explicit determinations of these non-perturbative corrections lead to

$$\langle\Omega|\bar{q}(0)q(0)|\Omega\rangle = -(0.25\text{ GeV})^3 \quad \text{for u and d quarks} \quad (2.149)$$

$$\langle\Omega|\frac{\alpha_s}{\pi}F_{\mu\nu}(0)F^{\mu\nu}(0)|\Omega\rangle = (0.33\text{ GeV})^4 \quad (2.150)$$

The first of these condensates is called the chiral condensate (since it's non-vanishing expectation value is related to chiral symmetry breaking in QCD) and the second is called the gluon condensate. Expectation values of other operators exist in the vacuum and they contribute to further terms in the OPE.

As we have seen, at high energies these give non-perturbative contributions to the cross section which are suppressed by order Λ^4/Q^4 with respect to the leading OPE contribution. Even though the magnitude of the condensate is non-perturbative, the large q behaviour of the coefficients $c^{(n)}(q)$ can be computed in perturbation theory. As before, since the OPE holds at the level of operators, we are free to choose any state to evaluate the correlator. Therefore, we may choose the perturbative states of one free quark, $|q\rangle$, and one free gluon, $|g\rangle$ to evaluate the chiral and gluon condensates respectively. We will not review the computation in this notes.

2.2.2 Sum-rules and power corrections to the R parameter

While the discussion above is apparently satisfying, there is some small problem with the arguments that we have overlooked. In our discussion we have been too vague with what we mean when we say that the separation between the two operators is small. In Minkowski space, while two operators may be evaluated at a large spacial distance, if the two operators insertions are along the light-cone, the interval between the two points is actually zero. To be precise, the OPE is only strictly valid if the two operators insertions occur at two space-like separated points, where the concept of large separation is well defined. Therefore, in momentum space this occurs when the exchanged momentum is large and space-like. This is unlike the annihilation cross section we have studied, which involves large time-like momentum.

The problems of a direct application of OPE as we have done in the previous section become manifest when comparing to e^+e^- data. There, as we saw in the analysis of the R parameter, several peaks appear whenever a neutral vector resonance, such as Υ or the $J\psi$, is

produced. However, the OPE prediction involves simple powers, which do not reproduce this behaviour. The reason for this discrepancy is easy to understand. Close to the resonance, the R parameter may be approximated by the Breit-Wigner-like distribution

$$R(Q^2) \sim \frac{1}{Q^2 - M(M - i\Gamma)} \quad (2.151)$$

with M and Γ the mass and width of the resonance. The presence of a pole close to the real Q^2 axis says that an expansion in powers of $1/Q$ does not work around the resonance.

Even though this quantity is intrinsically time-like, we can still use OPE to constraint the annihilation cross section. To do so, we will exploit the analytic properties of the current-current correlation function. If we focus on the T-ordered current current correlator, $\Pi_\mu^\mu(q^2)$, we know that this must posses a Källén-Lehmann spectral representation, which predicts the analytic structure of this correlator in the complex Q^2 plane. In particular, in addition to a few isolated poles, associated to vector resonance, the correlator possesses a branch cut along the positive Q^2 axis starting from the threshold of production of the lowest hadronic state. The knowledge of this analytic structure will be instrumental to constraint the cross section.

Since we know that OPE is valid for large space-like momentum, let us choose a large reference scale Q_0 and analyse the correlator in the vicinity of $q^2 = -Q_0^2$. Because of the previous discussion, in this region $\Pi_\mu^\mu(q^2)$ is analytic. Therefore, contour integrals around $q^2 = -Q_0^2$ are easily evaluated. Let us, in particular, study the integral

$$I_n = -\frac{4\pi\alpha_{\text{em}}}{3} \oint \frac{ds}{2\pi i} \frac{1}{(s + Q_0^2)^{n+1}} \frac{\Pi_\mu^\mu(s)}{s} \quad (2.152)$$

where the contour is shown in figure (2.13) left. Using the residue theorem, this integral yields

$$I_n = -\frac{4\pi\alpha_{\text{em}}}{3} \frac{1}{n!} \frac{d^n}{d^n s} \left(\frac{\Pi_\mu^\mu(s)}{s} \right) \Big|_{s=-Q_0^2} \quad (2.153)$$

Because the correlator is evaluated at a large space-time momentum, these derivative can be computed with the OPE expression, in terms of the coefficients $c_{\text{H}}^{(n)}(q)$.

Since the correlator is analytic in the complex Q^2 plane, the contour of integration of the above expression can be deformed into the contour shown in figure (2.13) left, which surrounds the brach cut along the real axis. Closing the path infinitely far away from the origin, and since we know the asymptotic large Q behaviour of the correlator from OPE, the integral in this new contour is non-vanishing only around the brach cut. Therefore we have

$$I_n = -\frac{4\pi\alpha_{\text{em}}}{3} \int_0^\infty \frac{ds}{2\pi i} \frac{1}{(s + Q_0^2)^{n+1}} \frac{\text{Disc } \Pi_\mu^\mu(s)}{s} \quad (2.154)$$

where $\text{Disc } \Pi_\mu^\mu(s)$ is the discontinuity of the correlator across the cut.

We can relate this discontinuity with the with the imaginary part of $\Pi_\mu^\mu(q^2)$. Since for energies lower than that of the pion mass the annihilation cross section into hadrons must

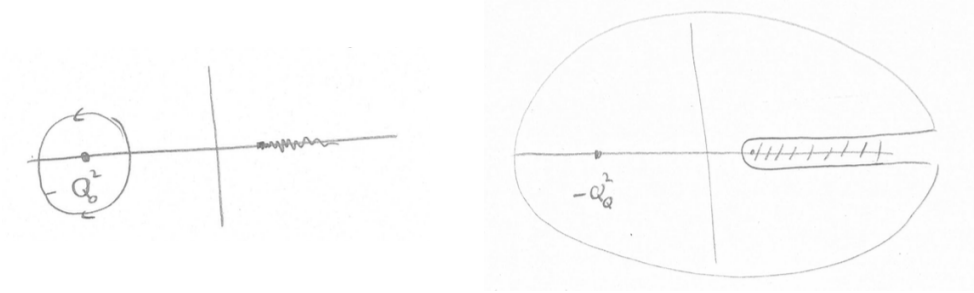


Figure 2.13: Contours of integration for the derivation of sum rules.

vanish, by virtue of the optical theorem, equation (2.141) we know that close to $q^2 = 0$, $\Pi_\mu^\mu(q^2)$ is real. Since in this region, this function is also analytic, it verifies that

$$\Pi_\mu^\mu(s) = (\Pi_\mu^\mu(s^*))^* \quad (2.155)$$

with $s = q^2$. If we now analytically continue both sides of this equation to the regions above and below the cut we obtain that the real and imaginary parts of the correlator satisfy

$$\text{Re}\Pi_\mu^\mu(q^2 + i\epsilon) = \text{Re}\Pi_\mu^\mu(q^2 - i\epsilon) \quad (2.156)$$

$$\text{Im}\Pi_\mu^\mu(q^2 + i\epsilon) = -\text{Im}\Pi_\mu^\mu(q^2 - i\epsilon) \quad (2.157)$$

Since across the cut the current-current correlator becomes discontinuous, we can use this expression to relate this discontinuity with the imaginary part of the correlator.

$$\text{Disc } \Pi_\mu^\mu(q^2) = 2i \text{Im } \Pi_\mu^\mu(q^2 + i\epsilon) \quad (2.158)$$

Finally, we can use the optical theorem, equation (2.141) to relate the imaginary part of the correlator to the total cross section via equation (2.124) and write

$$I_n = \frac{1}{\pi} \int_0^\infty ds \frac{s}{(s + Q_0^2)^{n+1}} \sigma(s) \quad (2.159)$$

Using the evaluation of this integral in a contour close to $q^2 = -Q_0^2$, equation (2.153) we arrive to the following integral constraint on the annihilation cross section

$$\frac{1}{\pi} \int_0^\infty ds \frac{s}{(s + Q_0^2)^{n+1}} \sigma(s) = -\frac{4\pi\alpha_{\text{em}}}{3} \frac{1}{n!} \frac{d^n}{ds^n} \left(\frac{\Pi_\mu^\mu(s)}{s} \right) \Big|_{s=-Q_0^2} \quad (2.160)$$

where now the right hand side can be rigorously evaluated via OPE since involves large space-like momenta, as we have already stressed. For sufficiently large Q_0 , the OPE coefficients $c_{\Pi}^{(n)}$ can be reliably computed in perturbation theory, since they are evaluated at non-perturbative values. Therefore by combining those perturbative computations of the coefficients and the measured data on the cross section, we can constrain non-perturbative quantities, meaning the condensates, that characterise the QCD vacuum.

Therefore, by performing integrals of the measured cross section we can have direct access to the non-perturbative physics that control the different condensates in the vacuum.

2.3 Confinement

We have seen that perturbative QCD describes well high-energy, large q^2 processes, since at these scale the strong coupling constant α_s becomes small. However, when the typical momentum exchanged is of order of mesons or hadron mass, the coupling constant grows and perturbation theory stops being applicably. At this scales we know from observation that the quarks and gluons reorganise themselves into hadrons, which cannot be simply described in terms of the microscopic Lagrangian. While the detailed mechanism by which this confinement phenomenon is not yet well understood, there are some non-perturbative techniques that allow us to connect the QCD Lagrangian with the observed spectrum of hadrons. In this section we will describe some of those techniques. However, to understand the physics of these methods, we will need to review a few phenomenological facts about hadrons.

2.3.1 Regge Trajectories and QCD strings

Prior to the discovery of QCD there where an intense search for patterns that could allow us to understand the physics of the very many hadrons that emerged in collider experiments. One of the most spectacular observations that emerged from those studies was that there is a strong linear scaling between the angular momentum and the squared of the mass of different mesons. This linear relation is shown in figure (2.14) for different mesons and may be parametrised as

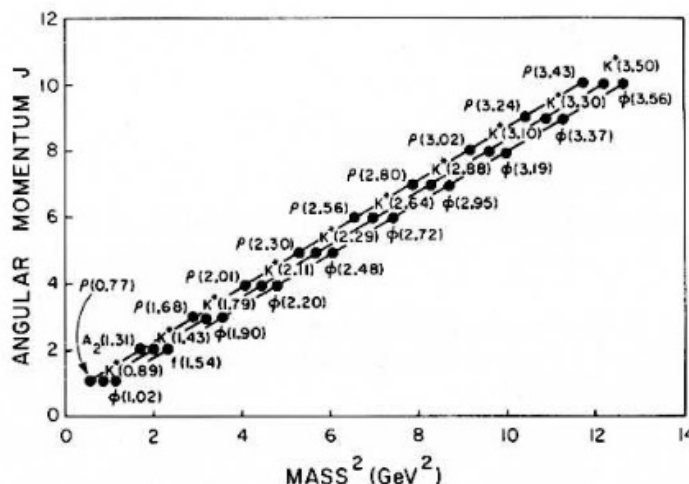
$$J(M^2) = \alpha_0 + \alpha' M^2 \quad (2.161)$$

where the slope α' was observed to be the same for many families of mesons which shared the same symmetries, while the intercept α_0 depended of the family of mesons. These linear relations are known as Regge trajectories. The extracted value of the common slope parameter is

$$\alpha' = 0.8 - 0.9, \text{ GeV}^{-2} \quad (2.162)$$

This simple systematics were explained by a surprisingly simple model. As we know that mesons are formed by $q - \bar{q}$ pairs, by assuming that the two quarks spin around one another while connected by a classical string with string tension

$$\sigma = \frac{1}{2\pi\alpha'}, \quad (2.163)$$



to their mass $E_B \ll M$, and we can think of them as a non-relativistic system interacting with one another via an effective potential. Since they are non-relativistic, they are correctly described by the Schrödinger equation

$$i\partial_t Q = \left(-\frac{\nabla^2}{2M} + V \right) Q \quad (2.164)$$

where Q is the heavy quark field and V is the potential it feels due to the presence of the antiquark. There is an analogous equation for the antiquark.

Despite of the simplicity of these ideas, for a judiciously chosen potential the Schrödinger equation provides a very good description of the spectra of charmonium and bottomonium states. Combining perturbative and non perturbative input this potential is parametrised as

$$V = -\frac{4}{3} \frac{\alpha_c}{r} + \sigma r \quad (2.165)$$

with $\alpha_c = 0.39$ and $\sigma = 0.182 \text{ GeV}^{-2}$. The first part captures the $1/r$ Coulomb dependence of a one-gluon exchange model, which should be a good approximation at short distances, where the theory is weakly coupled. The second part captures linear rise of energy between the $\bar{Q} - Q$ pair expected from the QCD-string model, with the string tension parameter σ agreeing with the value extracted from the analysis of Regge trajectories.

From this potential another way to describe confinement becomes apparent. QCD is confining because quarks cannot exist in isolation and must always appear in the form of hadrons. In the potential this is a consequence of the fact that the energy necessary to separate a pair of heavy quark and infinite distance diverges, and therefore, they cannot exist in isolation. This divergent energy is directly sensitive to the string tension.

The dynamics of heavy quarks allows us give a field theory description of the inter-quark potential. In the non-relativistic limit, the quark and antiquark field decoupled and are represented by two independent two-dimensional spinors. The dynamics of these quarks is controlled by the Heavy Quark effective theory Lagrangian

$$L_{HQ} = Q^\dagger i (\partial_t - ig A_0^A t^A) Q + Q^\dagger \frac{(\nabla^i - ig A_i^A t^A)^2}{2M} Q + \mathcal{O}\left(\frac{1}{M^2}\right) \quad (2.166)$$

where Q is the quark field and A_μ is the gluonic field, governed by the YM-Lagrangian. At this order in the $1/M$ expansion, the Lagrangian is nothing else than a covariant version of the Schrödinger Lagrangian. While this form is easy to guess from physics reasoning, this HQ Lagrangian can be directly obtained from the QCD Lagrangian via field redefinitions and expansion in powers of M . An equivalent Lagrangian (with opposite sign for the gauge coupling constant g) may be written for the heavy antiquark \bar{Q} , which at this order becomes an independent degree of freedom.

To define our criterium for confinement, we will work in the strict $M \rightarrow \infty$ limit, which implies that the second term of the HQ Lagrangian drops. As a consequence, the heavy quark fields do not change their position in space: if we place an infinitely heavy object in a point

it will remain at that point. This, in particular, implies that heavy quark fields situated at different points anti-commute with one another. Selecting the correct normalisation for the quark field, we can set the commutation relation

$$\{Q^\dagger(x), Q(y)\} = 2\pi\delta(x - y) \quad (2.167)$$

and similarly for \bar{Q} . In this limit, the Q and \bar{Q} fields anti-commute with one another.

Even though these quarks cannot move, there are dynamics associated with the interaction of the quarks with the gluon field. While the quark sits in a given position, its colour field can change as a result of gluon interaction. This repainting of the quark may be expressed as a group transformation of the quark field. After a given time t , the quark will have colour rotated by a phase $U(t)$

$$Q(t) = U(t)Q(0) \quad (2.168)$$

This phase can be determined by the equations of motion of the heavy quark, which in the $M \rightarrow \infty$ limit are simply

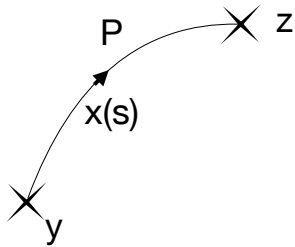
$$(\partial_t - igA_0^a t^a) Q = 0 \rightarrow (\partial_t - igA_0^a t^a) U(t) = 0 \quad (2.169)$$

with the condition $U(0) = 1$. As in quantum mechanics, this equation can be solved as a Dyson series, which yields

$$U(t, x) = \mathcal{T} \exp \left\{ ig \int_0^t dt' A_0^A(t', x) t^A \right\} \quad (2.170)$$

where \mathcal{T} is the T-order symbol.

In addition to describing the time-propagation of an infinitely heavy quark, this object is called a temporal Wilson lines. Wilson lines are important line-like objects in field theory and they can be defined connecting two arbitrary space-time points, y^μ and z^μ via an arbitrary path P as



$$U_P(z, y) = \mathcal{P} \exp \left\{ ig \int_0^1 ds \frac{dx^\mu}{ds} A_\mu^A(x^\mu(s)) t^A \right\} \quad (2.171)$$

with $x^\mu(s)$ the curve that parametrises the path P that starts at $x^\mu(0) = y^\mu$ and ends at $x^\mu(1) = z^\mu$. Here the path ordered symbol \mathcal{P} is analogous to the \mathcal{T} but instead of ordering the expansion of the exponential in time it is ordered in the path variable s . Choosing $y^\mu = (0, x, 0, 0)$, $z^\mu = (t, x, 0, 0)$ and $x^\mu(s) = (ts, x, 0, 0)$ we recover the expression for the

temporal Wilson line, equation (2.170). For any arbitrary point along the path, this object verifies

$$\frac{d}{ds}U_P(s) = ig \frac{dx^\mu}{ds} A_\mu^A t^A U_P(s) \quad (2.172)$$

which reduces to the heavy quark evolution equation for the previously specified path.

One of the many reasons why these Wilson line operators are interesting is because they have interesting properties under gauge transformation. If we perform a local gauge rotation with an element of $SU(N)$, \mathcal{G} , such that the gauge field transforms as

$$\hat{A}'_\mu = \mathcal{G} \hat{A}_\mu \mathcal{G}^\dagger + i \mathcal{G} \partial_\mu \mathcal{G}^\dagger \quad (2.173)$$

with $\hat{A} = A^A t^A$, then the Wilson line transforms as

$$U'_P(z, y) = \mathcal{G}(z) U_P(z, y) \mathcal{G}'(y) \quad (2.174)$$

this is, it transforms as the gauge rotations at the beginning and end of the path. This nice feature implies, as expected, that quark field given by equation (2.168) transforms with the local gauge transformation at the final point

$$Q'(t, x) = \mathcal{G}(t, x) Q(t, x) \quad (2.175)$$

After discussing some of the general properties of Wilson lines, we can return to the analysis of the heavy quark dynamics. In particular, we can determine the HQ propagator

$$iG_{HQ}(x, y) = \langle 0_{HQ} | Q(x) Q^\dagger(y) | 0_{HQ} \rangle \quad (2.176)$$

where here $|0_{HQ}\rangle$ is any state in the gauge theory with no heavy quarks. As is standard, this is just a green function of the evolution equation

$$(\partial_t - ig A_0^a t^a) iG_{HQ}(x, y) = \delta^4(x - y) \quad (2.177)$$

which may be solved as

$$iG_{HQ}(x, y) = \theta(t_x - t_y) \delta^3(\mathbf{x} - \mathbf{y}) U(t_x, t_y; \mathbf{x}) \quad (2.178)$$

We see that we can interpret the Wilson line as the heavy quark propagator.

We now consider the dynamics of a $Q - \bar{Q}$ pair separated by a fixed distance. At initial time t_0 , we could generate this state by acting on the heavy quark vacuum with the creation of operators of the quarks and antiquarks at the space points \mathbf{x} and \mathbf{y} respectively. However, this is not a gauge invariant state. A simple generalisation of the previous operator, that creates a gauge invariant combination of HQ pairs is given by

$$M^\dagger(t_0, \mathbf{x}, \mathbf{y}) = Q^\dagger(t_0, \mathbf{y}) U_s(t_0, \mathbf{y}, \mathbf{x}) \bar{Q}^\dagger(t_0, \mathbf{x}) \quad (2.179)$$

where $U_s(t_0, \mathbf{y}, \mathbf{x})$ is a space Wilson line along a straight line between the points \mathbf{x} and \mathbf{y} at fixed $t = t_0$. When acting on the Heavy Quark vacuum this operator generates a disturbance with the quantum number of heavy quarkonia.

We may now study the time-evolution of this disturbance by computing the overlap of the state after a later time t with the state created at t_0

$$\begin{aligned} iG_M(t, \mathbf{x}', \mathbf{y}', t_0, \mathbf{x}, \mathbf{y}) &\equiv \langle M(t, \mathbf{x}', \mathbf{y}') M(t_0, \mathbf{x}, \mathbf{y}) \rangle \\ &= \langle \bar{Q}(t, \mathbf{x}') U_s(t, \mathbf{x}, \mathbf{y}) Q(t, \mathbf{y}') Q^\dagger(t_0, \mathbf{y}) U_s(t_0, \mathbf{y}, \mathbf{x}) \bar{Q}^\dagger(t_0, \mathbf{x}) \rangle \end{aligned} \quad (2.180)$$

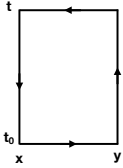
where we have used that the hermitian conjugate of a Wilson line gives a Wilson line over the same path but in opposite direction $U_s(t, \mathbf{y}, \mathbf{x})^\dagger = U_s(t, \mathbf{x}, \mathbf{y})$. Since the Q and \bar{Q} anti-commute with each other, we can relate this correlator with the propagator of the quark and antiquark

$$iG_M(t, \mathbf{x}', \mathbf{y}', t_0, \mathbf{x}, \mathbf{y}) = \text{tr} \{ U_s(t, \mathbf{x}', \mathbf{y}') iG(t, \mathbf{y}', t_0, \mathbf{y}) U_s(t_0, \mathbf{y}, \mathbf{x}) i\bar{G}(t, \mathbf{x}', t_0, \mathbf{x}) \} \quad (2.181)$$

where \bar{G} is the propagator of the heavy antiquark, which is analogous to that of the Q but with an hermitian conjugate Wilson line, and the trace is taken over colour indexes. Using equation (2.178) we can find for the propagator

$$iG_M(t, \mathbf{x}', \mathbf{y}', t_0, \mathbf{x}, \mathbf{y}) = W(t, t_0, \mathbf{x}, \mathbf{y}) \delta^3(\mathbf{x}' - \mathbf{x}) \delta^3(\mathbf{y}' - \mathbf{y}) \quad (2.182)$$

Where the rectangular Wilson loop W is a Wilson line along a closed loop connecting the initial and final positions of the quark and the antiquark.



$$W(t, t_0, \mathbf{x}, \mathbf{y}) = \text{tr} \{ U_s(t, \mathbf{x}, \mathbf{y}) U(t, t_0; \mathbf{y}) U_s(t_0, \mathbf{y}, \mathbf{x}) U(t_0, t; \mathbf{x}) \}$$

Since the path of this loop is closed, the Wilson loop is gauge invariant. This non-local object tells us how the disturbance created by the heavy quark pair propagates in time under a fixed gluonic field A_μ . All the analysis we have performed is valid independently of the form of this field. Therefore, we can simply average over the gluonic fields in vacuum via the QCD partition function and define the heavy quark pair correlator as the result of this average. Using that vacuum is translational invariant

$$iG_M(t, \mathbf{x}', \mathbf{y}', t_0, \mathbf{x}, \mathbf{y}) = \langle W(t, t_0, |\mathbf{x}, -\mathbf{y}|) \rangle \delta^3(\mathbf{x}' - \mathbf{x}) \delta^3(\mathbf{y}' - \mathbf{y}) \quad (2.183)$$

$$\langle W(t, t_0, r) \rangle = \int \mathcal{D}\phi e^{iS_{QCD}} W(t, t_0, r; A) \quad (2.184)$$

where $r = |\mathbf{x} - \mathbf{y}|$ and ϕ represents all the fields of QCD without the heavy quark.

We can now make contact with the analysis of the heavy quark dynamics under the influence of a potential, equation (2.164). Since G_M represents the evolution of a $Q\bar{Q}$ pair, it must be governed by the Schrödinger equation, and therefore

$$(i\partial_t - V(r)) \langle W(t, t_0, r) \rangle = 0 \quad (2.185)$$

From this equation, we can now identify the potential from the time derivative of W . However, there is certain arbitrariness in the way we defined the operator M , since we could

have chosen any path to connect the heavy pair. To remove this arbitrariness, we will consider the long time limit Wilson loop; in this limit, the Wilson loop becomes effectively time-translational invariant and, by virtue of equation (2.185), the log of the expectation value of W depends linearly in time. The effect of the initial preparation of the state is only a transient which must decay far away from the creation point. Therefore, we may identify the potential as

$$V(r) = \lim_{t \rightarrow \infty} i \partial_t \log \langle W \rangle \quad (2.186)$$

2.3.2.1 The Area Law

The relation we have just derived between the potential and the expectation value of the rectangular Wilson loop allows us to establish a criterium to understand whether QCD or any other gauge theory is confining. As we discussed, confinement implies that the energy to separate a $Q\bar{Q}$ -pair diverges and, according to the effective string model at long distances this divergence is linear $V(r \rightarrow \infty) \rightarrow \sigma r$. This implies that, at long distances

$$\lim_{\mathcal{T} \rightarrow \infty} \left\langle W \left(-\frac{\mathcal{T}}{2}, \frac{\mathcal{T}}{2}, r \right) \right\rangle = e^{i\sigma r \mathcal{T}} \quad (2.187)$$

Since the Wilson loop is a property that can be easily computed via lattice QCD, this is a standard test of confinement Which is called the Wilson test. For completeness, let us remark that lattice QCD computations are performed in Euclidean time (τ), that is, after a Wick rotation of the time-coordinate to the imaginary axis

$$\tau = -it \quad (2.188)$$

where the expectation value of the Wilson loop becomes

$$\langle W \rangle = e^{-\sigma \mathcal{A}} \quad (2.189)$$

where $\mathcal{A} = r\mathcal{T}_E$ is the area of the rectangle enclosed by the Wilson loop. This is another way to express the confinement criterium, known as the Areal Law. According to this criterium, if the expectation value of the Wilson loop over any (sufficiently large) loop show an exponential suppression proportional to the area of the loop, then the theory is confining and the constant of proportionality is the string tension. If, on the contrary, the theory is not confining, as QED, then the expectation value of W is also exponentially suppressed, but this suppression is only proportional to the perimeter of the loop.

2.3.3 Confinement/deconfinement transition

Our discussion above has focussed on how to determine whether a theory is confining or not, at least at zero temperature. However, even if a theory is confining, we could expect that this property disappears at sufficiently high temperature. It is easy to imagine how this would happen. Since temperature gives us an idea of the typical momentum of particles, when

$T \gg \Lambda_{\text{QCD}}$ all exchanges among quarks and gluons will be hard, and the interactions between them become small. We would like then to understand whether there is some sort of transition between the confined ground state of QCD and the finite temperature configuration.

Let us first say a few words of how finite temperature is introduced in QFT. As in quantum mechanics, a thermal state is an ensemble of states in which the probability to find any given state is only a function of the state's energy and is given by the Boltzmann weight. We may represent this ensemble via a density matrix

$$\rho_T = \sum_n e^{-E_n/T} |n\rangle \langle n| \quad (2.190)$$

where $\{|n\rangle\}$ is the set of eigenvectors of the Hamiltonian, and therefore a complete basis of states, and $\{E_n\}$ are its energies.

Thermal averages of any operator may be taken by evaluating the expectation value of the operator over any of the states according to their weight, which is the same as to take the trace of the operator with the density matrix

$$\langle \mathcal{O}(t, \mathbf{x}) \rangle = \sum_n e^{-E_n/T} \langle n | \mathcal{O}(t, \mathbf{x}) | n \rangle \equiv \text{Tr} \{ e^{-H\beta} \mathcal{O}(t, \mathbf{x}) \} \quad (2.191)$$

with $\beta = 1/T$.

We may now notice that H is the generator of time translations. Therefore, we can interpret the factor $\exp\{-H\beta\}$ as journey in complex time for a extent $\tau = \beta$. After this identification, it is easy to see that finite temperature implies that correlators will be periodic in imaginary time. After a few simple manipulations

$$\langle \mathcal{O}(t, \mathbf{x}) \rangle = \text{Tr} \{ e^{-H\beta} \mathcal{O}(t, \mathbf{x}) e^{H\beta} e^{-H\beta} \} = \text{Tr} \{ \mathcal{O}(t - i\beta, \mathbf{x}) e^{-H\beta} \} \quad (2.192)$$

which using the cyclicity of Tr , we can express as

$$\langle \mathcal{O}(t, \mathbf{x}) \rangle = \langle \mathcal{O}(t - i\beta, \mathbf{x}) \rangle \quad (2.193)$$

After a Wick rotation, in Euclidean time, this relation implies that expectation values (and correlators) are periodic

$$\langle \mathcal{O}(\tau, \mathbf{x}) \rangle = \langle \mathcal{O}(\tau - \beta, \mathbf{x}) \rangle \quad (2.194)$$

These manipulations establish a very useful formal relation between a thermal QFT and its Euclidean counterpart. The study of thermal properties of the theory is equivalent to the study of the Euclidean field theory in a space with periodic (Euclidean) time coordinate. The period of this coordinate can be identified with the temperature as $\beta = 1/T$. This compact time direction is frequently referred to as the thermal circle. This identification is routinely used in lattice QCD to study the thermal properties of QCD.

We will now focus on pure gluodynamics, that is QCD without light quarks. In this case, the periodicity introduced by thermal physics implies that

$$A_\mu(\tau) = A_\mu(\tau - \beta) \quad (2.195)$$

Similarly, if we consider gauge transformation of the glue field

$$A_\mu^{\mathcal{G}}(\tau) = \mathcal{G}(\tau) A_\mu^{\mathcal{G}}(\tau) \mathcal{G}(\tau)^\dagger + \mathcal{G}(\tau) i \partial_\mu \mathcal{G}^\dagger(\tau) \quad (2.196)$$

a normal gauge transformation implies that the group element $\mathcal{G}(t)$ is also periodic $G(\tau) = G(\tau + i\beta)$. However, there is another possibility as we will discuss now.

Let us consider a particular set of elements of the $SU(N)$ gauge group called the centre of the group. The centre of a group is defined as the set of group elements that commute with all the elements of the group. Since $SU(N)$ is the group of unitary matrices of unit determinant, the centre is given by the multiple of the identity times any of the N -th roots of unity

$$C = Z_i \mathbb{1} \quad \text{with} \quad Z_i^N = 1 \quad (2.197)$$

and the centre of the group is identify with the discrete group \mathcal{Z}_N .

This set of group elements allow us to consider a different set of gauge transformation in the periodic Euclidean time. We may call a centre transformation, \mathcal{G}_c to a gauge transformation that instead of being periodic along the thermal circle it satisfies

$$\mathcal{G}_C(\tau + \beta) = C \mathcal{G}_C(\tau) \quad (2.198)$$

Since C commutes with all the gauge group elements, it is easy to see that under this type of transformations, if A is periodic in euclidean time, its centre transform $A^{\mathcal{G}_C}$ is also periodic. Therefore, centre symmetry is a symmetry of the pure glue Lagrangian in this euclidean space.

Let us now consider another particular type of Wilson line called the Polyakov loop. This is just the Wilson loop of a closed path around the thermal circle.

$$P = \frac{1}{N} \text{tr} \{L\} \quad \text{with} \quad L \equiv \mathcal{T} \exp \left\{ ig \int_0^\beta A_0(\tau, \mathbf{x}) d\tau \right\} \quad (2.199)$$

Because it is loop, this object is invariant under normal gauge transformations $\mathcal{G}(\tau + \beta) = \mathcal{G}(\tau)$. However, under centre transformations, the Polyakov loop changes by a phase

$$Pc = \frac{1}{N} \text{tr} \{ \mathcal{G}_c(\tau + \beta) L \mathcal{G}_c(t) \} = Z_i P \quad (2.200)$$

We may now give a physical interpretation to the Polyakov loop. If we supplement now pure Yang-Mills with an infinite heavy quark, we know from the analysis in section (2.3.2) that the loop L in equation (2.199) corresponds to the propagator of the heavy quark.

If we now add the Heavy quark to the Yang Mills Lagrangian, we can compute the thermal partition function as the partition function of the gauge+heavy quark theory on this periodic time euclidean space

$$\mathcal{Z} = \int \mathcal{D}\phi \mathcal{D}Q e^{-S_{YM} - S_{HQ}} \quad (2.201)$$

Since the HQ Lagrangian is quadratic, it is easy to express it in terms of the Heavy quark propagator and note that we can write

$$\mathcal{Z} = \int \mathcal{D}\phi e^{-S_{YM}} P = \mathcal{Z}_{YM} \langle P \rangle \quad (2.202)$$

with \mathcal{Z}_{YM} the thermal partition function of the pure Yang Mills theory.

Using the statistical mechanics relation between the thermal partition function and the free energy of the system

$$\mathcal{Z} = e^{-\beta F} \quad (2.203)$$

We can identify the free energy associated to the presence of the HQ

$$F_{HQ} = F - F_{YM} \quad (2.204)$$

with the expectation value of the Polyakov Loop

$$\langle P \rangle = e^{-\beta F_{HQ}} \quad (2.205)$$

Therefore, the Polyakov loop is the free energy cost of adding a single heavy quark to pure Yang Mills theory.

2.3.3.1 \mathcal{Z} -symmetry and confinement

After having identified the expectation value of the Polyakov loop with the free energy of a single heavy quark, we can relate this object to confinement. As we have seen if a theory is confining, isolated colour charges cannot exist and the energy cost to introduce a single quark is infinite. Therefore, from equation (2.205) for a confining theory, the expectation value of the Polyakov loop must vanish

$$\langle P \rangle = 0 \quad (2.206)$$

Similarly, if the theory is not confining, or if it becomes non-confining at some temperature, then $\langle P \rangle \neq 0$

We can now relate the transition confinement/deconfinement transition to the breaking of some symmetry. In particular, if the theory is not confining, since $\langle P \rangle$ is not centre-symmetry invariant, since P transforms with a phase under this transformation, equation (2.200). For the theory to be Z_N invariant, $\langle P \rangle = 0$ and the system must be confining. Therefore we may conclude

$$\text{centre symmetry} \rightarrow \langle P \rangle = 0 \rightarrow \text{confinement} \quad (2.207)$$

We may then view the confinement/deconfinement transition as the phase transition associated with the spontaneous breaking of centre symmetry. In this picture $\langle P \rangle$ plays the role of the order parameter: it vanishes in the centre symmetric phase while it takes a non-zero value in the broken phase. This is analogous to the magnetisation in the Ising model in statistical physics. At low energies, when P vanishes, pure Yang Mills is confined and colour charges cannot live in isolation; the dynamical degrees of freedom are glue-balls, colour neutral excitations made out of gauge fields. On the contrary, at high temperature, the symmetry is broken and colour is deconfined, so that the dynamical degrees of freedom become gluons. For $N = 3$ this is a first order phase transition, meaning that the free energy of thermal Yang-Mills is continuous with a discontinuous first derivative at a critical temperature of order $T_c = \Lambda_{YM}$.

2.3.3.2 Dynamical light quarks and confinement

The discussion above nicely connects the deconfinement transition with a breaking of symmetry in the theory. However, all the discussion above has focussed on pure Yang-Mills, without light quarks. The reason for this is that centre-symmetry is only a symmetry of Yang-Mills in euclidean as long as there are no quarks in the Yang-Mills Lagrangian.

Let us consider a quark field in the thermal ensemble. Because fermions are Grassmannian variables, the relation between the fermions at both sides of the thermal circle is different than for bosons, and is necessary to impose anti-periodic boundary conditions. This may be easily seen by considering the two fermion point function. Therefore, the quark fields satisfy

$$q(\tau - \beta) = -q(\tau) \quad (2.208)$$

If we now perform a normal gauge transformation

$$q^{\mathcal{G}}(\tau) = \mathcal{G}(\tau)q(\tau) \quad (2.209)$$

this anti-periodicity is maintained provided $\mathcal{G}(\tau)$ is periodic. However, if we perform a centre transformation

$$q^{\mathcal{G}_c}(\tau - \beta) = C\mathcal{G}(\tau - \beta)q(\tau - \beta) = -Cq(\tau) \quad (2.210)$$

this transformation violates anti-periodic boundary conditions. Therefore, in the presence of dynamical quarks, centre symmetry is explicitly broken.

For sufficiently heavy quarks, with masses much greater than $M \gg \Lambda_{QCD}$ this fact does not alter the existence of a phase transition. Since those quarks are so massive their influence in the region of temperatures where the transition occurs is exponentially suppressed. We may think of these quarks as decoupled from the dynamics at scale T_c and therefore this theory still possesses a first order transition. As the masses of the quarks become smaller, their dynamics start to affect the nature of the transition. For some value of the mass, which is unknown, the transition becomes second order and for even lighter masses there is no transition in strict sense. Lattice studies have shown that for the physical masses of the u, d and s quarks there is indeed no phase transition in the mathematical sense. Nevertheless, the Polyakov loop still shows the effect of confinement, since it takes very small values at zero temperature and rapidly rises to unity around at $T_c = 160$ MeV. This rapid rise goes together with a rapid rise in the energy density of matter about this temperature. The lattice results for these two quantities are shown in figure (2.15). This is the physical realisation of the (cross-over) transition to the quark gluon plasma, a phase where quarks and gluons are liberated and dominate the thermodynamics of QCD.

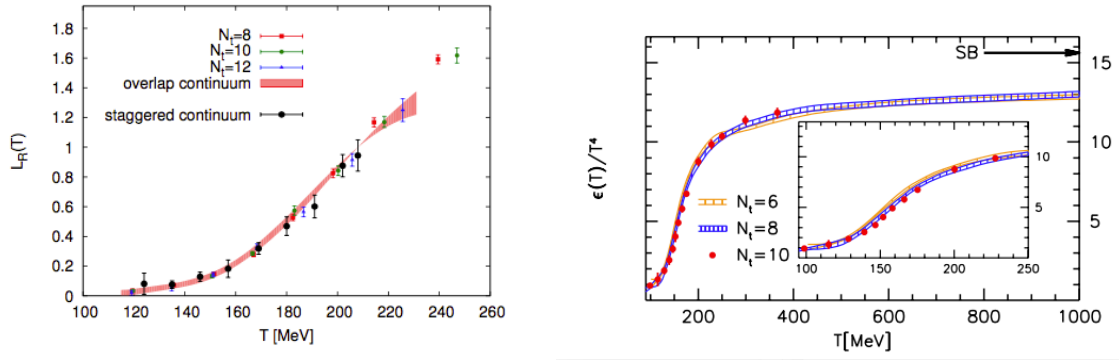


Figure 2.15: Left: Expectation value of the Polyakov loop in QCD as a function of temperature computed via lattice simulations (arXiv:1510.03376). Right: Ratio of the QCD energy density over T^4 as a function of temperature computed on the lattice (arXiv:1007.2580)

Appendix A

Basic facts about SU(N)

Given the importance of the SU(N) group, before discussing the QCD dynamics, we will describe a few of its properties to fix notation and conventions.

The elements of SU(N) may be represented by the exponential map

$$U = \exp \{i\alpha^a t^a\} , \quad (\text{A.1})$$

where α^a are constants and t^a are matrices known as generators of the algebra of the group. The index $a = 1..N^2 - 1$, since the number of independent special and unitary matrices is $N^2 - 1$. In the particular case of $N=3$, the number of generators of the group is $N^2 - 1 = 8$. Defined as in eq. (A.1) the group generators are hermitian

$$(t^a)^\dagger = t^a . \quad (\text{A.2})$$

The explicit expression of the group generators t^a depend on the representation of the group. When the group acts on a N -dimensional complex vector space, *i. e.*, when the group elements are special and unitary matrices, the group is said to be in the *fundamental* representation. These matrices can be chosen such that they satisfy an orthogonality condition given by

$$\text{tr} \{t^a, t^b\} = T_R \delta^{ab} , \quad (\text{A.3})$$

with T_R a normalisation constant, which depends on the representation. For the fundamental representation, it is customary to choose $T_R = 1/2$. For the particular case of $N = 3$ a convenient choice of basis for the group generators, consistent with these conventions, is given by the Gell-Mann matrices,

$$t^a = \frac{1}{2} \lambda^a , \quad (\text{A.4})$$

with

$$\lambda^1 = \begin{pmatrix} 0 & 1 & 0 \\ 1 & 0 & 0 \\ 0 & 0 & 0 \end{pmatrix}, \quad \lambda^2 = \begin{pmatrix} 0 & -i & 0 \\ i & 0 & 0 \\ 0 & 0 & 0 \end{pmatrix}, \quad \lambda^3 = \begin{pmatrix} 1 & 0 & 0 \\ 0 & -1 & 0 \\ 0 & 0 & 0 \end{pmatrix} \quad (\text{A.5})$$

$$\lambda^4 = \begin{pmatrix} 0 & 0 & 1 \\ 0 & 0 & 0 \\ 1 & 0 & 0 \end{pmatrix}, \quad \lambda^5 = \begin{pmatrix} 0 & 0 & -i \\ 0 & 0 & 0 \\ i & 0 & 0 \end{pmatrix}, \quad \lambda^8 = \frac{1}{\sqrt{3}} \begin{pmatrix} 1 & 0 & 0 \\ 0 & 1 & 0 \\ 0 & 0 & -2 \end{pmatrix} \quad (\text{A.6})$$

$$\lambda^6 = \begin{pmatrix} 0 & 0 & 0 \\ 0 & 0 & 1 \\ 0 & 1 & 0 \end{pmatrix}, \quad \lambda^7 = \begin{pmatrix} 0 & 0 & 0 \\ 0 & 0 & -i \\ 0 & i & 0 \end{pmatrix} \quad (\text{A.7})$$

Independently of the representation of the group, the generators form an algebra, which means that their commutator is also a element of the algebra. This means that

$$[t^a, t^b] = i f^{abc} t^c, \quad (\text{A.8})$$

where f^{abc} are a set of (real) numbers called the structure constants of the group. For the particular case of $N = 3$, the commutation relations of the Gell-Mann matrices leads to

$$f^{123} = 1, \quad (\text{A.9})$$

$$f^{147} = -f^{156} = f^{246} = f^{257} = f^{345} = -f^{367} = \frac{1}{2} \quad (\text{A.10})$$

$$f^{458} = f^{678} = \frac{\sqrt{3}}{2} \quad (\text{A.11})$$

In general, the structure constants are anti-symmetric in their indices. In addition, given the commutator identity

$$[t^a, [t^b, t^c]] + [t^b, [t^c, t^a]] + [t^c, [t^a, t^b]] = 0, \quad (\text{A.12})$$

the structure constants satisfy the Jacobi identity

$$f^{ade} f^{bcd} + f^{bde} f^{cad} + f^{cde} f^{abd} = 0. \quad (\text{A.13})$$

This relation shows that if we define the $N^2 - 1$ real $(N^2 - 1) \times (N^2 - 1)$ matrices

$$(T^a)_{bc} \equiv -i f^{abc}, \quad (\text{A.14})$$

these also satisfy the algebra

$$[T^a, T^b] = i f^{abc} T^c. \quad (\text{A.15})$$

We conclude then that these matrices form another representation of the $SU(N)$ group, acting on a real vector space of dimension $N^2 - 1$. This representation is called the fundamental representation. The fundamental and adjoint representations are the two representation we need to construct the QCD Lagrangian.

Another important property of the different representations, that we will use in these lectures, are the values of the Casimir operators. The Casimir operators are defined as

$$T_R^2 = T_R^a \cdot T_R^a, \quad (\text{A.16})$$

where the subindex R denotes de representation. This operator is an invariant of the algebra and its value is constant for each irreducible representation. For the fundamental and adjoint representations these are

$$t_{ij}^a t_{jk}^b = C_F \delta_{ij}, \quad (\text{A.17})$$

$$T_{ab}^d T_{bc}^d = C_A \delta_{ac}, \quad (\text{A.18})$$

where the constants C_F and C_A depend on the rank on the group and are given by

$$C_F = \frac{N^2 - 1}{2N}, \quad (\text{A.19})$$

$$C_A = N. \quad (\text{A.20})$$

The properties of the algebra we have just described appear frequently in perturbative computations.

Appendix B

Feynman Rules

To perform perturbative computation in QCD we need to discuss its Feynman rules. To do so, we must also consider additional terms in the Lagrangian, arising after quantisation. In general, the Lagrangian contains three types of terms

$$\mathcal{L} = \mathcal{L}_{\text{classical}} + \mathcal{L}_{\text{fixing}} + \mathcal{L}_{\text{ghost}} , \quad (\text{B.1})$$

where $\mathcal{L}_{\text{fixing}}$ is the gauge fixing term and $\mathcal{L}_{\text{ghost}}$ is the ghost lagrangian, which depends of the particular gauge fixing conditions. Some of the Feynman rules depend on the gauge fixing condition, while others are independent of the gauge fixing choice. To be concrete, we will show the Feynman rules in covariant gauge, which implies

$$\mathcal{L}_{\text{fixing}} = -\frac{1}{2\lambda} (\partial^\mu A_\mu^a)^2 , \quad (\text{B.2})$$

$$\mathcal{L}_{\text{ghost}} = \partial_\mu C^{a\dagger} D_{ab}^\mu B^b , \quad (\text{B.3})$$

The gauge choice independent Feynman rules are displayed in figure [B.1](#). The fermion propagator is identical to the QED one, up to the trivial colour factor. The coupling of fermions to gauge bosons is analogous as well, with the addition of the colour matrix t^a connecting the colours of the incoming and outgoing quarks. Unlike QED, however, gluons interact among themselves with three and four gluon interactions. This is a consequence of the triple gauge field terms in the non-Abelian field strength.

The gauge dependent Feynman rules are displayed in figure [B.2](#) in the covariant gauge. The gluon propagator depends explicitly of the gauge-fixing parameter λ . This is common to QED in covariant gauge. In addition, there is a trivial colour factor. The other two vertices correspond to the ghost fields, as encoded in $\mathcal{L}_{\text{ghost}}$.

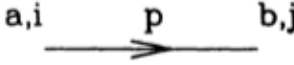
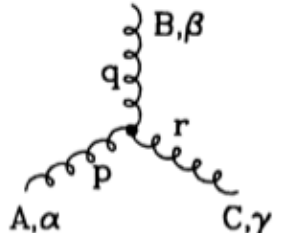
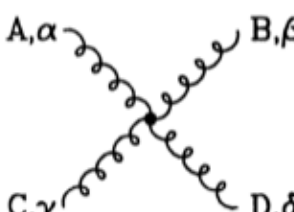
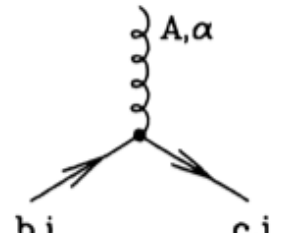
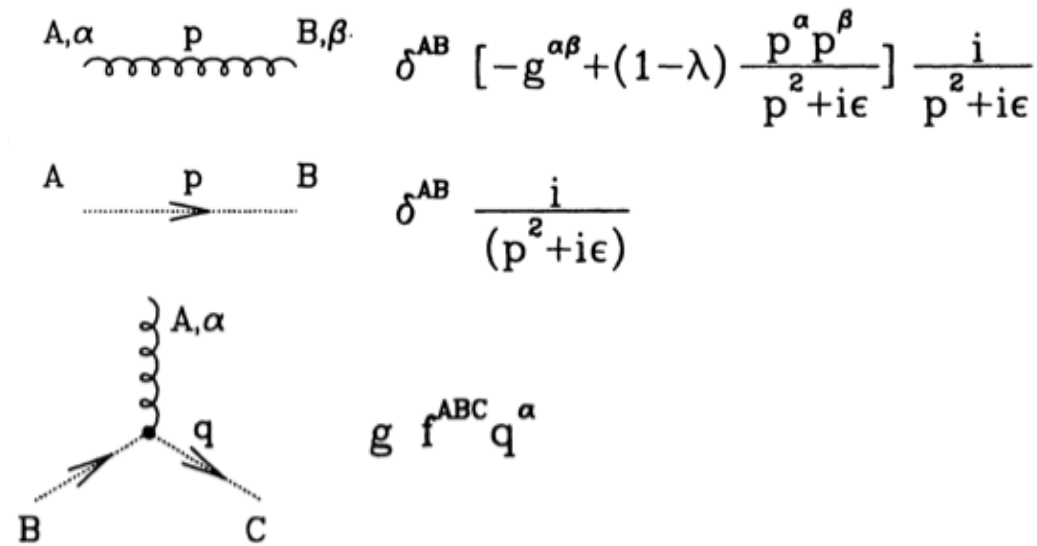
	$\delta^{ab} \frac{i}{(\not{p} - m + i\epsilon)_{ji}}$
	$-g f^{ABC} [(p-q)^\gamma g^{\alpha\beta} + (q-r)^\alpha g^{\beta\gamma} + (r-p)^\beta g^{\gamma\alpha}]$ <p>(all momenta incoming, $p+q+r = 0$)</p>
	$\begin{aligned} & -ig^2 f^{XAC} f^{XBD} [g^{\alpha\beta} g^{\gamma\delta} - g^{\alpha\delta} g^{\beta\gamma}] \\ & -ig^2 f^{XAD} f^{XBC} [g^{\alpha\beta} g^{\gamma\delta} - g^{\alpha\gamma} g^{\beta\delta}] \\ & -ig^2 f^{XAB} f^{XCD} [g^{\alpha\gamma} g^{\beta\delta} - g^{\alpha\delta} g^{\beta\gamma}] \end{aligned}$
	$-ig (t^A)_{cb} (\gamma^a)_{ji}$

Figure B.1: Gauge fixing independent Feynman rules. Figure taken from Ellis, Stirling and Webber.



The figure displays three Feynman diagrams and their associated mathematical expressions:

- Top diagram:** A wavy line representing a gauge boson with momentum p and indices A, α and B, β . The corresponding expression is:

$$\delta^{AB} \left[-g^{\alpha\beta} + (1-\lambda) \frac{p^\alpha p^\beta}{p^2 + i\epsilon} \right] \frac{i}{p^2 + i\epsilon}$$
- Middle diagram:** A horizontal line with a right-pointing arrow, representing a ghost, with endpoints A and B and momentum p . The corresponding expression is:

$$\delta^{AB} \frac{i}{(p^2 + i\epsilon)}$$
- Bottom diagram:** A vertex where a wavy line (gauge boson) with index A, α and momentum q meets two ghost lines (dashed lines with arrows) labeled B and C . The corresponding expression is:

$$g f^{ABC} q^\alpha$$

Figure B.2: Gauge fixing dependent Feynman rules. Figure taken from Ellis, Stirling and Webber.